Graz University of Technology

DOCTORAL THESIS

OPTICAL OXYGEN SENSORS – INDICATORS AND MATERIALS

SYNTHESIS AND APPLICATIONS

Klaus Koren

2012

Zur Erlangung des akademischen Grades

“Doktor der technischen Wissenschaften”

eingereicht an der

Technischen Universität Graz

Supervisor

Univ.-Prof. Dipl.-Chem. Dr.rer.nat. Ingo Klimant

Institute of Analytical Chemistry and Food Chemistry

Graz University of Technology

STATUTORY DECLARATION

I declare that I have authored this thesis independently, that I have not used other than the declared sources / resources, and that I have explicitly marked all material which has been quoted either literally or by content from the used sources.

…… ……..

date (signature)

...PURE VERNUNFT DARF NIEMALS SIEGEN...

(TOCOTRONIC)

DANKSAGUNG

„MAN KANN NIEMANDEN ETWAS LEHREN, MAN KANN IHM NUR HELFEN ES IN SICH SELBST ZU FINDEN“

GALILEO GALILEI

Ich möchte mich bei all jenen bedanken, die ein Stück des Weges mit mir gegangen sind und mich unterstützt haben. Auch wenn mein Name auf dieser Arbeit steht, so hab ich es nicht allein geschafft, ich hätte es auch nie allein schaffen können.

Dass ich den Forscher in mir selbst gefunden habe, liegt wohl hauptsächlich an einer Person und das ist mein Betreuer, Ingo Klimant. Ohne dein Vorbild, deine Motivation, deine Leidenschaft und deine Unterstützung wäre ich wohl nicht so begeistert von der Forschung. Ich danke dir für die Freiräume, die du mir gegeben hast, ohne mich je den Boden unter den Füssen verlieren zu lassen. Wenn man mich fragt, was mir an der Forschung am meisten Spaß macht, so sage ich immer, die Gespräche, das Brainstorming mit Ingo. Ich hoffe ich kann mir diese Freude erhalten und andere anstecken. Danke Ingo!

Sergey…, was soll ich sagen. Auch wenn wir nicht immer einer Meinung waren, so sind wir Freunde geworden und das ist auch gut so. Du hast mir geholfen den „Russen“ in mir zu finden. Du hast mein Herangehen an Probleme und deren Bearbeitung geprägt. Du hast mir geholfen, mich nicht in Details zu verlieren und den Wald hinter all den Bäumen zu sehn. Du hast mich stets unterstützt und bei dem einen oder anderen Bier über Rückschläge hinweg getröstet. Danke Sergey!

Wäre ich drei Jahre lang allein am Institut gewesen, ich wäre längst verrückt und nicht mehr resozialisierbar. Allen Sensoriken und Analytikern sei Dank, dass es nicht so gekommen ist. Ihr alle habt diese drei Jahren zu einigen der besten meines Lebens gemacht, und das obwohl ich erstmals regelmäßig zur Arbeit gehen musste. Ihr alle habt mich in den letzten Jahren begleitet und jeden Tag zu einem Erlebnis gemacht. Ohne eure Freundschaft und Unterstützung wäre diese Arbeit wohl auch fertig geworden, hätte aber nicht so viel Spaß gemacht. Grazie mille Michela für all den Spaß im Büro. Danke: Lisi für deinen ansteckenden Optimismus; Daniel für deinen „synthetischen“ und menschlichen Support; Tobi für geteiltes Leid und die fotographische Dokumentation; Birgit für deine Empathie; Christoph für all deinen technischen Support; Philipp für die beste Barcelona Rundfahrt. Danke, Babsi E. für deinen erfrischenden Blickwinkel; Babsi N. für den oft rettenden Schluck Milch; Spela für Badminton Lehrstunden; Susi für Schokolade und das Kind in dir; Tijana für deine Ehrlichkeit; Gerda für das Einführen der Ordnung. Danke Martin, Norbert und Peter für frisches Blut und neue Ideen. Danke Torsten für deine Unterstützung. Danke Eveline für jede einzelne Bestellung, das Rücken frei halten und dein stets offenes Ohr. Danke Tobi B., Herbert, Erika, Chrisi und Iris für eure Unterstützung und das lösen so einiger Probleme. Danke allen Lebensmittelchemikerinnen für guten Kaffee und die Versuchsküche und allen Spurenanalytikern für die eine oder andere Messung oder Einschulung.

Eine Gruppe bzw. ein Institut ist mehr als die Summe der einzelnen Teile. Ich bin froh ein Teil dieser Gruppe gewesen zu sein und werde das wohl nie vergessen.

Ich hatte das Vergnügen einigen dabei zu „helfen es in sich selbst zu finden“. Es war für mich eine der schönsten Erfahrungen und liebsten Aufgaben zu lehren und ich habe dadurch so viel zurückbekommen. Luki, ich glaube ich habe von dir sicher gleich viel gelernt, wie du von mir. Du warst sicher der selbstständigste Diplomand den es gibt und ich bin sehr froh, dass ich mit dir arbeiten durfte. Bewahre dir das Kind in dir und deine liebenswürdige Art, dann wird es dir nie schlecht gehen. Ich hatte das Vergnügen einige Bachelor Studierende zu betreuen. Evi, Berni, Stefan, Peter und Rahel ich möchte euch allen danken, für eure Motivation und euren erfrischenden Zugang. Ob ihr es glaubt oder nicht ich habe von euch und mit euch sehr viel gelernt. Ich würde mir wünschen, dass ihr euer Potenzial weiter ausschöpft und die Zeit mit mir in guter Erinnerung behaltet.

Auch möchte ich meinen Kooperationspartnern und -partnerinnen danken. Ohne eure Expertise und Bereitschaft wäre vieles nicht möglich gewesen. Danke Dmitri, Ruslan, Robert, Kathrin, Babsi, Andi, Jana,…

Ich möchte mich bei all meinen Freunden bedanken. Danke: Gamsi, Fini, Gerri, Hanna, Peter, Martin, Simone, Marie, Christine, Thomas, Patrick, Lissi, Johnny, Simon & Uli, Flautz & Helena, Vanessa, Uwe; all @ TUBOKU; Wolfi, Bernhard, Reini und alle anderen im 9er;… Ein Leben ohne Freunde ist wie ein Wald ohne Bäume! Danke euch allen!

Auch wenn man Erwachsen ist, so ist es schön einen sicheren Hafen zu haben in den man jeder Zeit zurück kann. Danke Mama, Papa, Opa, Oma^2 und allen andern. Es ist schön ein Fangnetz zu haben, das einem Sicherheit gibt. Ich weiß, es fällt euch nicht immer leicht mich los zu lassen umso mehr schätze ich es, dass ihr es tut und mich immer unterstützt. Danke Katrin, es ist schön, dass wir so ein Selbstverständnis haben und immer für einander da sind. Ich bin froh und stolz, dein Bruder zu sein.

Die letzten Zeilen meiner Danksagung gehören einem sehr besonderen Menschen, meiner Kati. Auch wenn du es mir nicht immer glaubst, so hast du mich in den letzten Jahren so viel unterstützt wie niemand anderer. Deine Liebe und Zuneigung haben mir Kraft gegeben. Du hast meine Launen ertragen und mich bestärkt. Du bist für mich „zuhause“, der Mensch bei dem alles gut ist. Ich kann dir nicht oft genug danken, ich kann nur sagen, dass ich sehr glücklich bin, dich zu haben. Du bist mein „Kati-(i)on“ die positive Energie die ich so sehr liebe!

KURZFASSUNG

Optische Sauerstoffsensoren sind wichtige Analysengeräte im wissenschaftlichen und industriellen Kontext. In dieser Arbeit würden neue Indikatoren und Materialien für die optische Sauerstoffmessung entwickelt. As erstes wurde eine neue Klasse an Indikatoren synthetisiert, die sogenannten Iridium(III) porphyrine. Diese Indikatoren ermöglichen schnelle und effektive Funktionalisierung via Liganden-Austausch. Die Möglichkeit des Liganden-Austausches wurde genutzt um zellpermeable Indikator-Peptide Komplexe zu erzeugen. Zellulärer Sauerstoff konnte mit diesen Komplexen in einer Vielzahl von Zelllinien gemessen werden. Zusätzlich wurde die Stabilität optischer Sauerstoffsensoren durch kovalentes Binden des Indikators zur Sensormatrix erhöht. Dieser synthetische Schritt unterbindet das Migrieren und Auswaschen des Indikators. Das Click-chemische Konzept wurde auf eine Vielzahl an Materialen und Anwendungen übertragen. Zu guter Letzt wurde der Einfluss der Sensormatrix auf die Performanz des Sensors evaluiert und ein Set an neuen Sensormaterialien hegestellt und untersucht.

ABSTRACT

Optical oxygen sensors are important analysis tools in academia and industry alike. In this thesis new materials and indicators for optical oxygen sensors were developed. At first a new class of indicator dyes were synthetized, the so-called iridium(III) porphyrins. Those indicators enable fast and efficient functionalization via ligand exchange reactions. This feature was used to prepare cell penetrating indicator-peptide conjugates. The conjugates enable sensing of cellular oxygen in a variety of cell lines. Additionally the stability of sensor materials was improved by covalently coupling the indicator dye to the sensor matrix. This click-chemistry based linkage eliminated dye migration and leaching. The presented concept was adapted and used for a variety of materials or applications. Finally the influence of the sensor matrix on sensor performance was evaluated and a set of new materials was prepared and tested.

CONTENT

INTRODUCTION

Oxygen is more than 20% of the air that we breathe; it is simply one of the most important molecules on earth. Nearly all living organisms on this planet need oxygen to survive. Therefore, it is obvious that this particular molecule is of great importance. Measuring the oxygen concentration is essential in a huge variety of systems and in everyday life.

This PhD thesis and the research that led to this thesis focus on oxygen as an analyte and on optical methods to measure oxygen. In particular this thesis deals with the synthesis of new oxygen indicators, their application in biological samples and with the development and improvement of oxygen sensors.

This thesis is written in a cumulative manner, meaning that it includes research papers that were produced during the work that led to this thesis. First, a theoretical background on oxygen and oxygen sensors will be given. This will guide to the practical work that was performed during this PhD thesis, either finished or on-going.

PART I
THEORETICAL BACKGROUND

OXYGEN

The eighth element of the periodic table is the most abundant element on earth and is called oxygen [1]. In its elemental form it mainly appears as dioxygen (O_2). Dioxygen or molecular oxygen is the most stable form of elemental oxygen and is often referred to as oxygen. At ambient conditions oxygen is a colorless and odorless gas that makes up nearly 21% of the atmosphere of this planet. Oxygen is a non-polar compound with a moderate and highly temperature and pressure dependent solubility in water. At 0 °C 14.16 mg of oxygen are soluble in water. With increasing temperature the solubility decreases.

As the ground state of oxygen has a triplet configuration ($^3\Sigma_g^-$), oxygen is a paramagnetic substance. This explains the diradical character of O_2. Apart from the ground state two short-lived excited singlet states exist ($^1\Delta_g$ and $^1\Sigma_g^+$). The energy differences between those two singlet states and the triplet ground state are 94.72 and 157.85 kJ/mol, respectively [1].

A SHORT HISTROY

Nowadays nearly 21% of the atmosphere consists of oxygen, but this was not always the case. Actually at the beginning of the earth the atmosphere was anoxic, meaning that oxygen was only present in trace amounts. Scientists estimate that molecular oxygen (O_2) reached significant levels on this planet around 2.5 billion years ago [2]. At that time the evolution of organisms that were able to transfer solar energy into chemical energy began; the process of photosynthesis started. Within this process carbon dioxide and water are converted into glucose [3]. A side product of photosynthesis is oxygen. As the number of organisms capable of photosynthesis increased, also the oxygen concentration increased. This led to a significant change in the atmosphere and consequently changed life on this planet [4].

In more detail the development of oxygen on this planet can be divided into five stages [2] as seen in figure 1. In the first period the concentration of oxygen was below a few parts per million. At that time oxygen was mainly produced by splitting water due to UV irradiation. The question mark in figure 1 points out, that scientists have some evidence that even at this early stage oxygen may have been produced via photosynthesis. Nevertheless, oxygen levels did not increase as most of the oxygen produced was used to oxidize inorganic material. This changed at

the great oxidation event around 2.5 billion years ago. At that time in stage two the oxygen partial pressure reached levels probably a bit higher than 0.02 atm. During stage three this virtually did not change. This indicates that the production and consumption of oxygen were in equilibrium. In the fourth stage the oxygen levels again increased. In the last stage a maximum was passed before returning to current levels. Figure 1 shows the different stages for the atmosphere, shallow oceans and the deep oceans. It is believed that the oxygen concentration on this planet affected life throughout the history. The first organisms that lived on this planet survived in an oxygen free atmosphere. This means that they used fermentation or anaerobic respiration using alternative electron acceptors like metal ions or sulfur. After oxygen became available most of those species were extinguished or suppressed to anoxic regions. Nowadays only in very extreme and oxygen free conditions like the deep oceans organisms using anaerobic respiration can be found. Fermentation, on the other hand, is still often used by a variety of organisms in the absence of oxygen to produce energy via glycolysis.

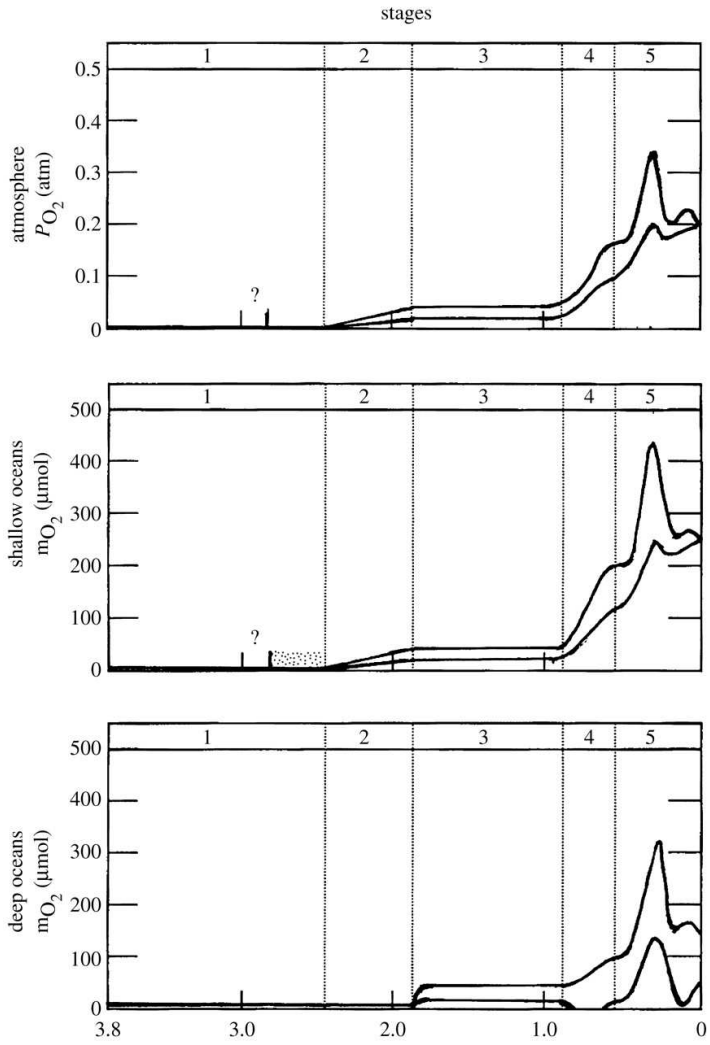

FIGURE 1: ESTIMATED EVOLUTION OF THE OXYGEN LEVELS FROM 3.8 BILLION YEARS AGO UP TO NOW; OXYGEN PARTIAL PRESSURE IN THE ATMOSPHERE AND OXYGEN CONCENTRATION IN THE SHALLOW AND DEEP OCEANS.[1]

Roughly 1 billion years after oxygen became important, the first eukaryotic organisms containing mitochondria appeared. By oxidizing glucose to carbon dioxide and water inside the mitochondria those microorganisms closed the energy circle. While oxygen was first produced as a byproduct, it is now essential to generate energy or to be more specific adenosine

[1] Picture taken from H.D. Holland, The Oxygenation of the Atmosphere and Oceans, Phil. Trans. R. Soc. B. 361 (2006) 903–915 with permission of the Royal Society

triphosphate (ATP). The appearance of metazoan organisms can be seen as a further landmark that happened just 0.5 billion years ago. Those more complex organisms found ways to transport oxygen to every cell to ensure that enough energy is produced, as those multicellular organisms needed large amounts of energy. Up to now we have found no better or more effective way and still rely on those mechanisms. As the oxygen levels changed over time, it is believed that oxygen was also responsible for the creation of species nowadays extinguished [4]. Except for water, probably no other small molecule had such an impact on life on this planet.

With a few exceptions all living species on this planet rely on oxygen as their main source of energy. Without this very simple molecule our planet would look totally different.

SOME BIOLOGICALY RELEVANT REACTIONS INVOLVING OXYGEN

In this chapter the biological relevance of oxygen will be outlined. The goal of this section is to show that oxygen is a key molecule for all kinds of organisms by discussing a few reactions involving this molecule. There are lots of additional reactions that involve oxygen; so this is just a short selection. The information in this chapter is mainly extracted from a classical biochemistry text book [5].

PHOTOSYNTHESIS

All relevant reactions involving oxygen started with photosynthesis. At the great oxidation event the oxygen levels in the atmosphere reached significant levels. This happened roughly 2.5 billion years ago[6]. Although this date is a very important event in earth history, it is well believed that photosynthesis as a reaction and energy source started earlier [7]. Probably the first produced oxygen reacted with inorganic material and so it took quite some time before oxygen accumulated in the atmosphere.

The word photosynthesis combines the two Greek words photon (light) and synthesis (putting together). In fact, this already gives a good impression of photosynthesis because light as an energy source forms organic compounds (carbohydrates).

In the presence of light, plants and cyanobacteria consume carbon dioxide and water and produce carbohydrates via a complex reaction scheme. The fundamental photosynthetic reaction can be written as followed;

$$CO_2 + H_2O + light \rightarrow (CH_2O) + O_2$$

The compartments inside eukaryotic cells where photosynthesis takes place are called chloroplasts. The photoreceptors are located inside those inner- and outer-membrane containing organelles. In plants the two most important pigments are *Chlorophyll a* (*Chl a*) and *Chlorophyll b* (*Chl b*) (figure 2). In cyanobacteria the corresponding pigments have a slightly altered structure resulting in changed absorption spectra. In plants, for example, *Chl a* and *Chl b* effectively absorb the blue and red part of the spectrum, but not the green part. This of course yields the green color of plants or leaves.

In fact, the photosynthetic reaction can be divided into two steps, the light reaction and the dark reaction [5]. During the light reaction a pigment interacts with light and gets oxidized. A chain of electron transfer reactions, later a proton gradient builds up across the membrane that can be used to produce ATP. Additionally, NADPH (reduced nicotinamide adenine dinucleotide phosphate) is created. The oxidized pigment gets reduced by water and creates oxygen as a byproduct. In the dark reaction the high energy products ATP and NADPH that were produced form carbohydrates from CO_2. It is important to note that both reactions happen in light, but only the first is light dependent.

Several chlorophyll molecules and sometimes even other pigments are needed to collect enough light energy which is needed for photosynthesis. This is accomplished by so called light harvesting complexes. Energy transfer from the antenna molecules towards the reactive center occurs with a high efficiency in less than 10^{-10} seconds. This energy transfer triggers an electron transfer and a subsequent buildup of a proton gradient that can be used for the biosynthesis of carbohydrates. At this point there is no need to go into too much detail regarding the protein complexes and enzymes involved in this process.

Briefly, photosynthesis is a light driven reaction cascade that is essential for the creation of biomass as well as oxygen. Photosynthesis is the only relevant process that can build up oxygen.

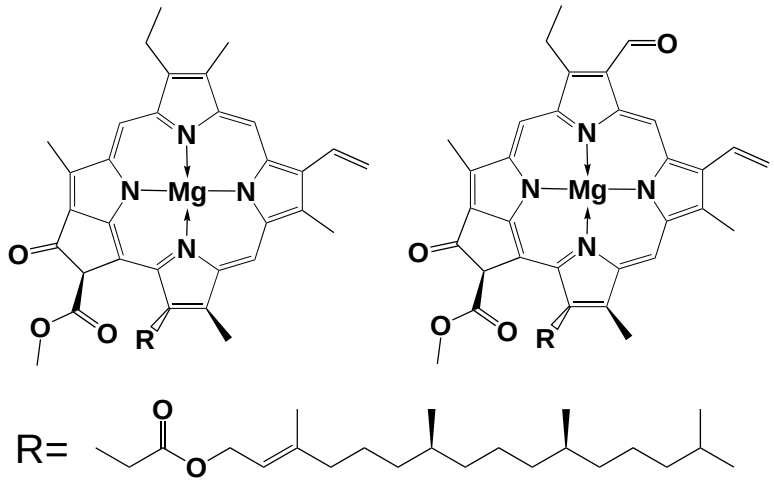

FIGURE 2: STRUCTURES OF *CHLOROPHYLL A* (LEFT) AND *CHLOROPHYLL B* (RIGHT).

ELECTRON TRANSPORT CHAIN AND OXIDATIVE PHOSPHORYLATION

In aerobic organisms the glucose that is produced during photosynthesis gets fully oxidized and serves as an energy source. Inside eukaryotic cells this oxidation happens inside the mitochondria, the so-called power plants of the cell. Mitochondria have lots in common with prokaryotes and are believed to originate from small prokaryotes that lived in eukaryotic cells. Like the chloroplasts the mitochondria consist of an inner and an outer membrane [5].

The oxidation of glucose can be divided in two reaction steps. In the first step, the carbon atoms of glucose are oxidized. This happens during glycolysis and within the citric acid cycle. In the second step, oxygen gets reduced and thereby consumed. The first step is essentially the same used in fermentation and is not dependent on oxygen.

Within glycolysis and the citric acid cycle 10 molecules of NADH and two molecules of $FADH_2$ (reduced form of flavin adenine dinucleotide) are produced. They carry the 12 electron pairs that were produced during the reactions involved in either glycolysis or the citric acid cycle. It is not the aim of this work to fully explain the biological reactions involved. For now it is enough to know that the NADH and $FADH_2$ molecules transfer the electrons to other compounds and get reoxidized to NAD+ and FAD. Before the electrons are used to reduce oxygen, they get transferred by subsequent redox reactions involving four enzyme complexes. During this

electron transfer a proton gradient is built up across the mitochondrial membrane. This gradient can then be used for the synthesis of ATP via the oxidative phosphorylation.

This way of energy production has several consequences. First, aerobic metabolism has a huge advantage over anaerobic metabolism. While anaerobic glycolysis can only produce two molecules of ATP per glucose molecule, aerobic metabolism yields 32 ATP molecules per glucose molecule. This means that aerobic metabolism is 16 times more efficient. This is of course highly important for multicellular organisms that have a high energy demand. On the other hand, organisms and tissues rely on oxygen as glycolysis cannot provide the energy needed. Additionally, the oxygen based metabolism goes hand in hand with the creation of reactive oxygen species (ROS). Although ROS are only created in small quantities, they can lead to cell damage [8]. Several degenerative diseases like Parkinson's disease or Alzheimer's disease are related to oxidative destruction of mitochondria. In 1969 the enzyme Superoxide dismutase was discovered by Irwin Fridovich [9]. This enzyme is the first defense line within nearly all cells against ROS. Superoxide dismutase catalyzes the transformation of the highly reactive superoxide into oxygen and hydrogen peroxide. Additionally, antioxidants from plant origin could help protecting cells from ROS.

To sum up it can be said that aerobic metabolism is a complex, but highly efficient energy source. One molecule of glucose and six molecules of oxygen can be used to produce 32 molecules of ATP. This of course leads to a huge dependence of organisms on nutrition and oxygen. Besides a high energy output aerobic metabolism also leads to problems associated with reactive oxygen species.

OXYGEN SUPPLY

As seen above the supply of oxygen is essential for single cells as well as for complex multicellular organisms. Cells and tissues are generally supplied by oxygen in a passive way, meaning via diffusion of oxygen. In more complex and bigger organisms this is no longer possible and an active transport system needs to be implemented, like the vascular system. The vascular system consists of a circulating “liquid phase” (e.g. blood). Special proteins are needed in order to increase the solubility of oxygen in the liquid. Those proteins contain oxygen binding heme groups. The heme group is an iron containing porphyrin that can reversibly bind oxygen.

This group is located inside the protein. Some examples for oxygen binding proteins are myoglobin (a small intracellular protein, for example in muscles) and hemoglobin (oxygen transporter in blood). Oxygen binding introduces a structural change in the heme group that affects the entire protein and can be used to trigger storage and release of oxygen.

Using specialized oxygen transport mechanisms higher organisms can ensure that enough oxygen is available and can be delivered to every cell. This is crucial for the survival of the whole organism.

HYPOXIA-INDUCILE FACTOR

Oxygen supply is essential for cells as well as multicellular organisms. In the ideal normoxic situation the oxygen supply is sufficient and respiration works efficient. If the cellular oxygen concentration increases (hyperoxia) or decreases (hypoxia), the concentration of reactive oxygen species (ROS) increases [10]. This indicates that the oxygen concentration has to be maintained in a narrow concentration range to ensure efficient respiration and to avoid cell damage. The transcription factor hypoxia-inducible factor 1 (HIF-1) plays a vital role in keeping the cellular oxygen levels constant [3].

HIF 1 consists of two subunits, the oxygen regulated HIF-1α and the constitutively expressed HIF-1β [11]. HIF-1α is produced and degraded continuously under normoxic conditions. In hypoxic condition degradation is inhibited. This leads to an accumulation of HIF-1α and consequently to a dimerization with HIF-1β. The dimer of HIF-1α and HIF-1β binds to hypoxia-response elements in the target genes and increases transcription.

The effects of HIF-1 can be seen in the simple organism *Caenorhabditis elegans*. This organism consists of less than thousand cells and all cells obtain oxygen via diffusion. In case of oxygen depletion HIF-1 induces the production of enzymes needed for glycolysis [12] to ensure the production of ATP. Similar strategies can be seen in mammalian cells where HIF-1 affects the production of a lot of enzymes [11]. Even the development and function of the oxygen delivery systems (vascular systems) are influenced by HIF-1.

Briefly, it can be said that HIF-1 is a main regulator in all cells that responds to the oxygen concentration and induces the needed consequences. This means that oxygen can control the

production of certain enzymes or molecules. So the dependence on oxygen is even encoded on our genes.

MEASURING OXYGEN

As oxygen is such extremely important molecule [13], measuring oxygen is of course essential. Over time several methods were introduced. In this chapter some of the common approaches will be discussed. At first a titration based method will be presented. Of course this method is an offline method that needs sampling prior to the analysis. The two following methods rely on chemical sensors and enable online and real-time measurements. One of the methods is based on electrochemistry, while the second one uses optical signal transduction. The optical method will be discussed in more detail, as this thesis focuses on this approach.

AN EXAMPLE FOR AN OFFLINE METHODE - WINKLER TITRATION

In an offline method a sample has to be taken prior to the analysis. This means that there is a certain time delay between the sampling and the analysis result. During this time delay the studied system, e.g. a river or water treatment plant, is not monitored. Consequently, it is only possible to react to changes in the system after a certain time. Nevertheless, offline systems are routine methods in all kinds of fields, as they unlike online measurements enable sample preparation prior to analysis.

As an example for an offline oxygen measurement method the so called Winkler Titration will be presented. This method was developed by Winkler as early as 1888 [14]. First, the oxygen present in the water sample is fixed by oxidizing Mn(II) to Mn(III) in an alkaline environment. After changing to an acidic pH the now soluble Mn^{3+} can oxidize iodide to I_2. The amount of elemental iodine is proportional to the amount of initially dissolved oxygen. Finally the iodine concentration can be determined by titration with sodium thiosulfate ($Na_2S_2O_3$). This method only needs a few beakers, standard chemicals and a burette. In contrast to many other methods the Winkler titration measures oxygen concentrations. Although the method is simple, it is the

standard reference method to all existing technologies. As the measurement still needs a certain time and cannot be automated, new approaches try to overcome this problem.

When continuous measurements of an analyte concentration are needed, this method is not the right choice. In this case an online system needs to be used that can be automated and does not consume the analyte or needs sample preparation. For such purposes chemical sensors are required.

CHEMICAL SENSORS

To enable online measurements in a variety of applications chemical sensors are used, but what is a chemical sensor? According to the IUPAC "*A chemical sensor is a device that transforms chemical information, ranging from the concentration of a specific sample component to total composition analysis, into an analytically useful signal. The chemical information, mentioned above, may originate from a chemical reaction of the analyte or from a physical property of the system investigated.*" [15]. This definition can be extended when demanding that chemical sensors should work continuously and reversible like done by Wolfbeis and others [16,17]. Additionally, often the possibility of miniaturization is mentioned as a criterion.

In general a chemical sensor consists of the following essential parts: a receptor that interacts, in the best case, specifically with the analyte and the transducer that converts the interaction of the analyte with the receptor into a measurable signal. Chemical sensors and biosensors can be distinguished Based on the receptor, as the receptor in a biosensor should be of biological origin, e.g. enzyme or antibody.

Chemical sensors are normally classified regarding the transducer [18]. The following classification is according to the IUPAC[15]:

(1) **Optical devices** use changes in optical phenomena due to analyte interaction for signal transduction. These can be absorption, luminescence, reflectance, scattering and so on.
(2) **Electrochemical devices** use electrochemical effects for signal transduction. These effects can be spontaneous or stimulated. Different operating principles can be used including potentiometry and voltammetry.

(3) **Electrical devices** do not use electrochemical reactions, but rather changes in electrical properties due to interactions with the analyte.
(4) **Mass sensitive devices** measure a change in the mass due to binding and accumulation of the analyte.
(5) **Thermometric devices** measure a change in heat after a reaction or interaction of the analyte with the sensor.
(6) **Magnetic devices** use changes in the magnetic properties for detection purposes.
(7) Additionally other types of **radiation**, e.g. radioactivity, or physical property can be used, as long as they are used for the detection of an analyte.

This classification is just one of the possible; alternatively chemical sensors can be classified regarding the analyte or the field of application. In the following, an electrochemical oxygen sensor will be described and, in more detail, optical oxygen sensors will be presented.

ELECTROCHEMICAL OXYGEN SENSORS

As an example for an electrochemical oxygen sensor the so-called Clark electrode [19] will be presented. This electrochemical sensor was developed by Prof. Leland Clark [20]. The sensor relies on the reduction of oxygen on a cathode. As this process is not selective to oxygen, a gas permeable membrane is needed to separate the sample from the electrode. Normally, a Teflon membrane is used that allows oxygen to diffuse towards the electrode while blocking nongaseous parts of the sample. Further parts of the sensor are a reference electrode, an electrolyte and a power supply. During the electrochemical reaction oxygen is reduced to OH^-, this means that the analyte is consumed during the measurement. Consequently, continuous stirring is needed to maintain equilibrium with the environment of the sensor.

The development of the Clark electrode was extremely important for the field of chemical sensors as it enabled online measurements of oxygen and triggered a variety of further developments in this field [21]. This led to the first blood gas analyzer [22] and to the first biosensor when Clark used an enzyme layer in combination with his electrode [23]. Those electrodes also had a huge impact on understanding biochemical reactions and oxygen dependence of cells and tissues [24].

Although electrochemical oxygen sensors were further developed and miniaturized, they are being replaced especially in biological applications by optical oxygen sensors. While electrochemical sensors always need to be in electrical contact with the measurement device, optical sensors can be read out without direct contact using light. This enables intracellular measurements in cells using microscopy techniques or similar.

OPTICAL OXYGEN SENSORS

The probably first evidence that oxygen concentrations could be measured optically was obtained around 1930. At that time Kautsky and Hirsch reported that the room-temperature luminescence of several dyes absorbed on silica gel can be quenched by molecular oxygen [25]. It was not until 1974 that Hesse patented the first fiber optical oxygen sensor. Shortly afterwards, Opitz and Lübbers reported the first optical sensor system to simultaneously measure oxygen and carbon dioxide [26]. In the 1980s and 1990s several improvements were made in this field, including the use of phosphorescent dyes and the realization of decay time measurements [27]. Those developments pioneered the development of micro- [28] and nanometer sized sensors [29] for biological applications.

Nowadays, nearly all reversible optical oxygen sensors rely on quenching the luminescence of an indicator dye. This process involves the collision of oxygen with an excited state of the indicator. During this collision the energy is transferred from the indicator to the oxygen molecule resulting in a radiationless deactivation of the indicator. As a consequence, the luminescence intensity and the decay time are both reduced. To better understand this mechanism the following chapter will deal with luminescence and quenching.

"Luminescence is an emission of ultraviolet, visible or infrared photons from an electrically excited species."[30] There are multiple ways that can lead towards this excited species. Luminescence can be classified depending on the kind of excitation used. When the excited state is reached by absorbing a photon, the luminescence is referred to as photoluminescence.

Within the group of photoluminescence two different types of emission can be distinguished, namely fluorescence and phosphorescence. The different processes that lead to either of the both mentioned emissions can be best understood when looking at the Jablonski diagram (figure 3).

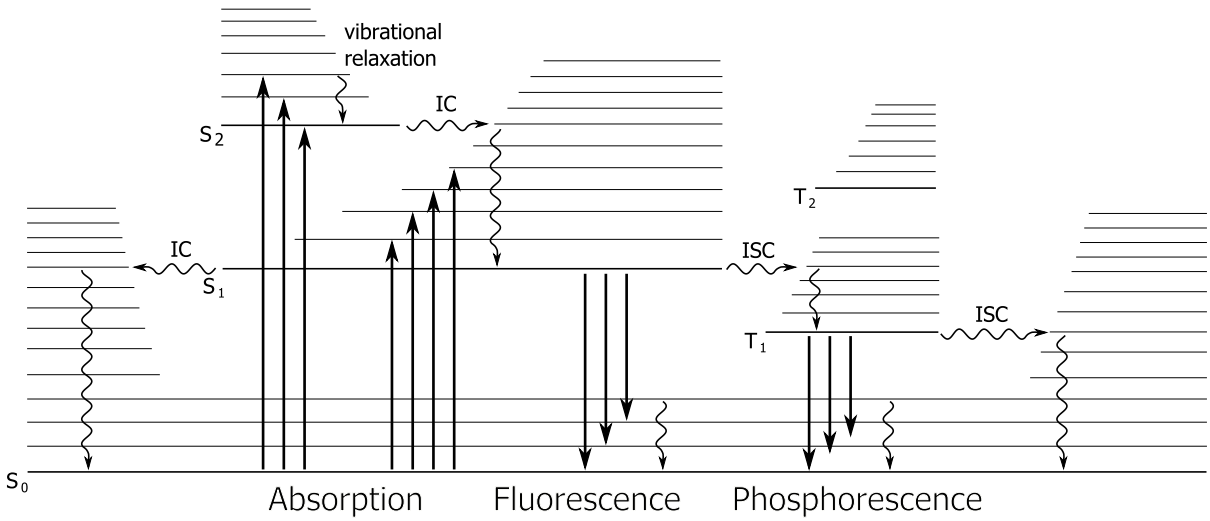

FIGURE 3: JABLONSKI DIAGRAM.

After absorbing a photon the molecule reaches an electronically excited state. After vibrational relaxation the molecule has several possibilities to return to the ground state; the non-radiative process of internal conversion, or fluorescence and phosphorescence which both involve the emission of a photon. Fluorescence occurs from an excited singlet state and the photon is emitted within a few nanoseconds after absorption. Prior to phosphorescence the molecule has to transfer from the singlet excited state into a triplet excited state via inter-system crossing. This process is quantum mechanically forbidden, but can be made possible by spin-orbit

coupling. This effect is promoted by the presence of heavy atoms. As inter-system crossing is a forbidden process, the molecule remains longer in this excited state (µsec to sec) prior to the emission of a photon.

All those processes have specific rate constants. The non-radiative processes of internal conversion and inter-system crossing can be summarized in a non-radiative rate constant (k_{nr}), while the radiative processes are represented by the constant k_r. Of course these processes occur for both excited electronic states (S_1 and T_1). With those different rate constants the decay time (τ) can be derived.

$$\tau = \frac{1}{k_{nr} + k_r}$$

The decay time is the time after a pulse excitation when the intensity has decreased to $1/e$ of the initial value. As reaching S_0 from T_1 by inter-system crossing is a slow process, phosphorescence has a significantly longer decay time (µs to sec) than fluorescence (≈ ns).

Besides the decay time the quantum yield (Φ) is a very important parameter. The quantum yield is the fraction of excited molecules that by returning to the ground state emit a photon [30]. In terms of rate constants this can be expressed as followed.

$$\Phi = \frac{k_r}{k_r + k_{nr}} = \tau \times k_r$$

If the non-radiative process is much slower than the radiative, the maximum quantum yield of 1 can be obtained, meaning that every excited molecule will emit a photon.

The processes mentioned so far and rate constants only include one molecule, the indicator dye or luminophore itself. When an additional species is present, the processes involved can become a bit more complex. The additional species can interact either with the ground state or excited state of the luminophore. When this interaction yields in a decrease in photon emission, the processes involved are called quenching. In this case the additional species is a quencher of the luminophore emission. If the quencher interacts with the excited state of the luminophore, this process is called dynamic quenching. Oxygen for example is a typical dynamic quencher of phosphorescence. In the Jablonski diagram the quencher can be included; this additional process also has a rate constant (k_q).

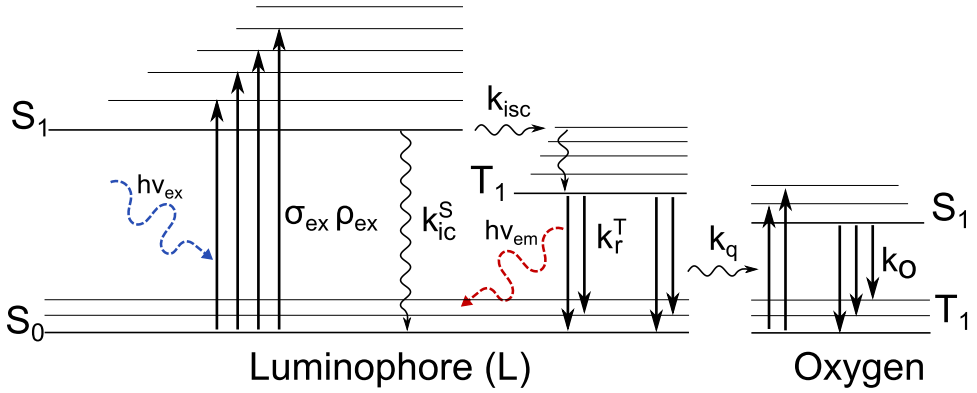

FIGURE 4: JABLONSKI DIAGRAM WITH OXYGEN AS QUENCHER

As the quenching process is an energy transfer from the luminophore to the quencher (in this case oxygen), this process is non-radiative. This rate constant (k_q) can be combined with the other non-radiative rate constants. This means that upon quenching the decay time, quantum yield and luminescence intensity decrease. The quencher concentration influences those parameters according to the Stern-Volmer kinetics. Following this approach the decrease is measured in comparison to the unquenched situation. In the absence of a quencher the measured decay time is the unquenched decay time (τ_0). The same applies for the quantum yield and intensity. By increasing the quencher concentration [Q] the measured parameters decrease. This leads to the Stern-Volmer equation. The product of k_q and τ_0 is often called the Stern-Volmer constant (K_{SV}).

$$\frac{\tau_0}{\tau} = \frac{\Phi_0}{\Phi} = \frac{I_0}{I} = 1 + k_q \tau_0 [Q]$$

The luminescence quenching of oxygen is the basis of (nearly) every optical oxygen sensor. This means in detail that an excited indicator (luminophore) transfers its energy to oxygen. This process involves the collision of oxygen with the excited indicator. Therefore, the longer the indicator remains in its excited state, the higher the probability of an effective collision. As optical oxygen sensors rely on dynamic quenching, they are affected by temperature. With increasing temperature the diffusion of oxygen increases, while at the same time the decay time of the indicator decreases due to thermal quenching. In general it can be said, the higher the temperature the more effective the quenching process.

In contrast to dynamic quenching static quenching involves the ground state of the luminophore. Consequently, the decay time is not affected, while quantum yield and intensity are. In this case also the temperature effect is different as the quencher luminophore interaction is weakened with increasing temperature.

While intensity measurements are easily affected by, for example, changes in the excitation intensity or the detector, the decay time can be used as an intrinsically referenced signal. The decay time can be measured using two different methods (figure 5). In the first method the sample is excited using a short light pulse and the emission of photons over time is measured. Such an experiment gives the so-called decay curve and enables measuring the decay time at $I=I_0/e$. The second approach uses a sinusoidally modulated light source with a specific frequency (f) to excite the luminophore. The measured luminescence is consequently also sinusoidally modulated, but delayed in phase. This phase shift (φ) can be used to obtain the decay time using the following equation.

$$\tau = \frac{\tan(\varphi)}{2\pi f}$$

Both approaches can be used to obtain the decay time. While the first approach is based in the time-domain, the second one is frequency based. For optical oxygen sensors both can be used in theory. From a practical point of view mainly phase-modulation fluorometry is used, as for phosphorescence measurements such instruments are easier to miniaturize and measurements are faster.

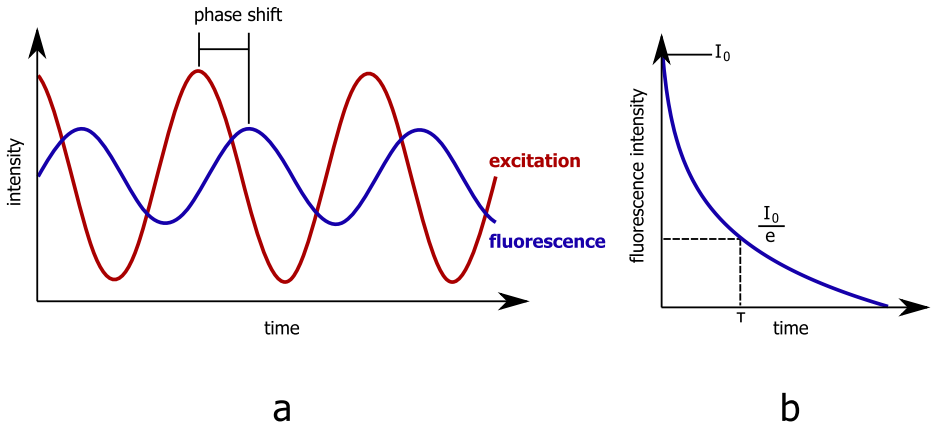

FIGURE 5: A: PHASE-MODULATION FLUOROMETRY: EXCITATION AND EMISSION ARE SINUSOIDALLY MODULATED, THE PHASE SHIFT CAN BE USED TO OBTAIN THE DECAY TIME. B: PULSE FLUOROMETRY: AFTER A SHORT EXCITATION PULSE THE PHOTON EMISSION IS MEASURED OVER TIME.

The luminescence of an indicator can be quenched by oxygen as the energy of the excited luminophore can be transferred to oxygen. This reduces the luminescence intensity, decay time and quantum yield of the luminophore. At the same time oxygen is excited to a singlet state. So the quenching process produces a highly reactive oxygen species as byproduct. Singlet oxygen can then return to its ground state either radiationless or by emitting a photon (λ= 1270 nm) itself.

This basic process of collision induced energy transfer is the essence in every oxygen sensor. Depending on the luminophore used, the matrix and the environment the sensor has a different characteristic. In the next chapters the different strategies towards oxygen sensors will be described.

MATERIALS USED IN O_2 SENSORS

At this point the difference between a probe and a sensor should be explained. Although often used as synonyms for each other, there is an inherent difference between them. A sensor is the entire device consisting of the indicator immobilized in a matrix, the needed optic components (fibers, filters etc.) and a data processing unit. A probe is in this sense just a part of the sensor. This could be the indicator alone or the indicator embedded in a polymer (like in nanoparticles [31,32]) or even modified dyes that enable special applications [33]. Often also the term “sensing material” is used as a synonym to probe. As pointed out by Wolfbeis, only the whole setup should be called sensor, because you also do not call your hard drive computer [17,34].

The key component of an oxygen sensor is anyway the indicator dye. The photophysical parameters of the indicator influence the final sensor. Namely the decay time influences the sensitivity, the photostability influences the operating time, the absorption and emission characteristics influence the needed light source and filters, and the quantum yield in combination with the molar absorption coefficient (ε) determine the brightness of the sensor. The first indicators used were polycyclic aromatic hydrocarbons [35,36], those materials show oxygen dependent fluorescence.

Later organometallic compounds replaced the fluorescent indicators (figure 6). This is because those compounds show bright and long lived phosphorescence [37]. Within this group the first prominent indicators were polypyridyl complexes of the transition metals Ru^{2+}, Os^{3+} and Ir^{3+}.

The most commonly used complexes were based on Ru^{2+} [38,39]. As an example, $Ru(dpp)_3^{2+}$ should be mentioned [40]. This dye can be excited using blue light and shows emission in the orange-red part of the spectrum with a decay time of typically 4 to 6 µsec. Recently, iridium(III) cumarine complexes were synthesized showing bright luminescence and good solubility in organic solvents and are willingly used [41]. Cyclometallated complexes of platinum(II) and iridium(III) are an additional alternative.

The second important class of transition metal complexes uses porphyrin-macrocycles as ligands. Among the metals used Pt^{2+} and Pd^{2+} are by far the most important. A short summary of the materials used can be found in [42]. Generally, the decay time of the palladium(II) complex is around ten times longer than for the corresponding platinum(II) complex. This means the Pd^{2+}-porphyrin based sensors are around ten times more sensitive. Octaethylporphyrin was among the first used ligands [43]. Unfortunately, they are not extremely photostable. The photostability problem was overcome when tetra(pentafluorophenyl)porphine ligands were used [44]. Up to now complexes of this ligand are among the most widely used and photostable indicators [34]. Complexes of both of those ligands emit in the red spectral region after absorbing green (Q-band) or violet-blue (Soret-band) photons. Additional porphyrin based indicators include ketopophyrines complexes. Lately π-extended porphyrins became popular as they absorb red photons and emit in the near infrared region [45–48]. This enables subcutaneous measurements and reduces the background luminescence. A further trend goes towards functional indicators and new combinations of indicators and biomolecules [49,50].

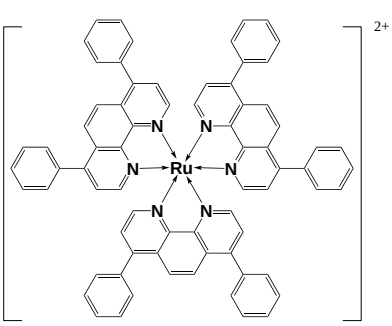

Ru(II) polypyridyl complexes
λ_{max}(abs) = 450-470 nm
ε = 20,000-30,000 $M^{-1}cm^{-1}$

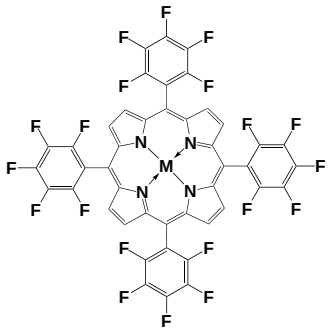

Pt(II) and Pd(II) tetra(pentafluorophenyl)porphine
λ_{max}(abs) = 380-430 nm (Soret);
500-550 nm (Q-bands)
ε =150,000-300,000 $M^{-1}cm^{-1}$ (Soret);
15,000-25,000 $M^{-1}cm^{-1}$ (Q-bands)

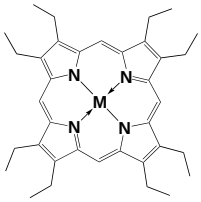

Pt(II) and Pd(II) octaethylporphyrin
λ_{max}(abs) = 380-430 nm (Soret);
500-550 nm (Q-bands)
ε =150,000-300,000 $M^{-1}cm^{-1}$ (Soret);
15,000-25,000 $M^{-1}cm^{-1}$ (Q-bands)

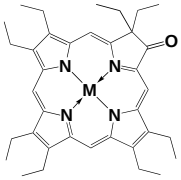

Pt(II) and Pd(II) ketoporphyrin complexes
λ_{max}(abs) = 390-410 nm (Soret);
590-605 nm (Q-bands)
ε ~ 90,000 $M^{-1}cm^{-1}$ (Soret);
~ 55,000 $M^{-1}cm^{-1}$ (Q-bands)

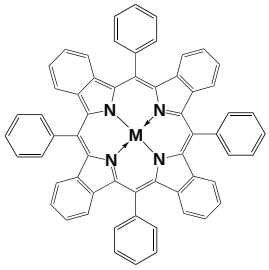

Pt(II) and Pd(II) tetrabenzoporphyrin complexes
λ_{max}(abs) = 420-450 nm (Soret);
600-635 nm (Q-bands)
ε =200,000-400,000 $M^{-1}cm^{-1}$ (Soret);
130,000-180,000 $M^{-1}cm^{-1}$ (Q-bands)

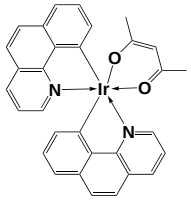

cyclometallated Ir(III) complexes
λ_{max}(abs) = 400-500 nm
ε ~ 5,000 $M^{-1}cm^{-1}$

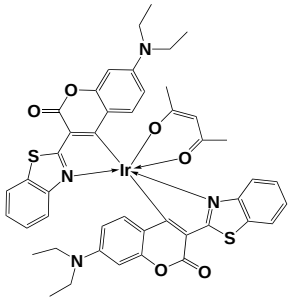

Ir(III) coumarin complexes
λ_{max}(abs) = 450-490 nm
ε ~ 90,000 $M^{-1}cm^{-1}$

FIGURE 6: LUMINESCENT OXYGEN INDICATORS WITH CORRESPONDING ABSORPTION AND EMISSION PROPERTIES.

Besides the indicator the sensor matrix is the second essential component of an optical oxygen sensor. While for the indicator the photophysics play a major role, other parameters determine the usability of the matrix. In detail, the matrix has to be permeable to oxygen, a suitable environment for the indicator used, chemically stable and in at best commercially available. Lots of polymers were used as matrix material [37]. Among the polymers the main difference arises from the changed oxygen permeability. High permeability was observed in silicones and also fluorinated polymers [51]. In typical glassy polymers like polystyrene, poly(methyl methacrylate) or poly(vinyl chloride) the permeability is lower, but the mechanical stability of

the sensor film or coating is higher. Also other materials like cellulose based polymers [52] or other polymers [53] can be used. As an alternative to polymers materials like organically modified silica (ORMOSILS) [54–56] or silica gel [57] can be applied. All those materials enable different applications and enable tuning the sensitivity as well as the stability.

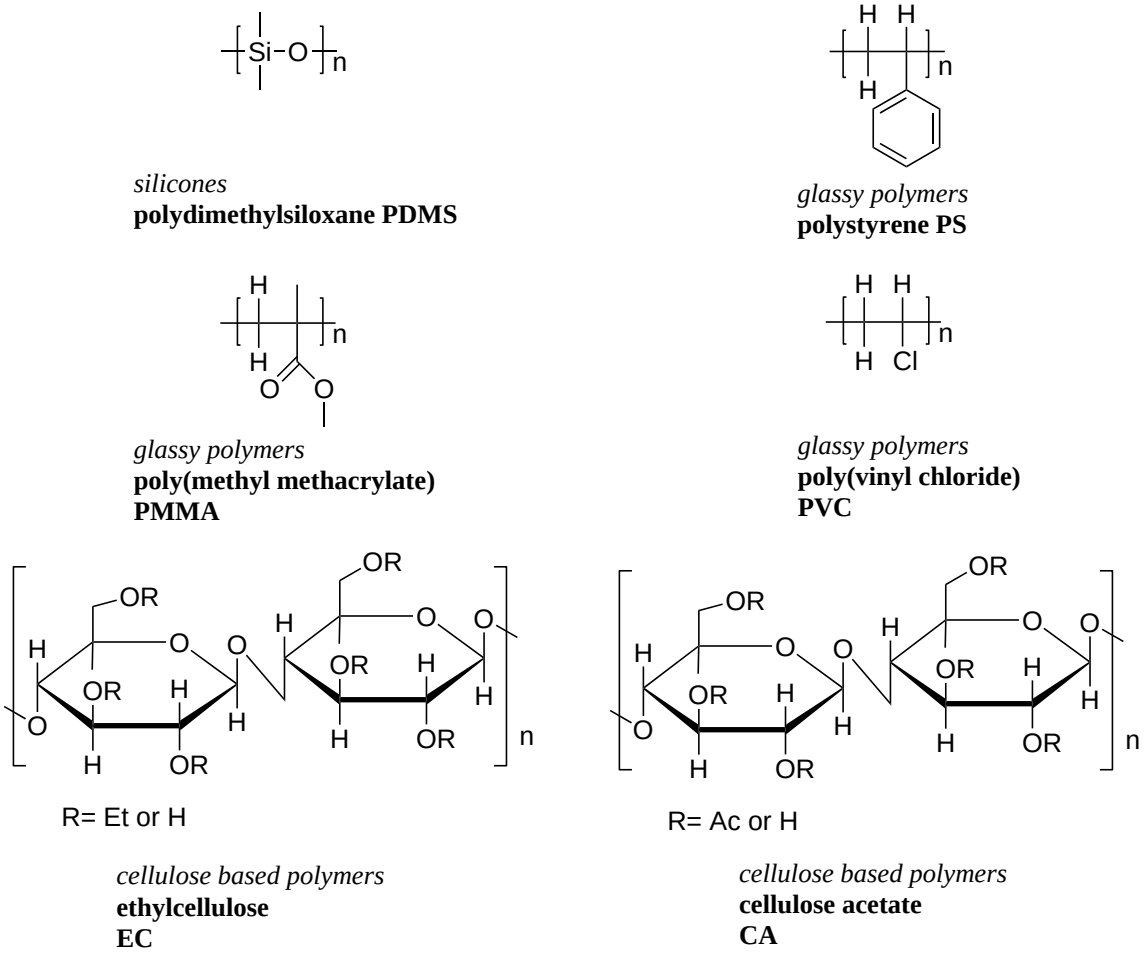

FIGURE 7: POLYMERS USED IN OPTICAL OXYGEN SENSORS.

In an optical oxygen sensor the indicator dye is immobilized in a polymer and fixed on the sensor support. The support can be an optical fiber, a planar polymer or glass or micro/nanostructured materials including particles. Depending on the platform the obtained sensors may also be classified [58]. For oxygen probes further strategies are common, including

dendrimers [59], nanoparticles [32,60,61], and dye-conjugates with peptides or other biological species [33,62,63].

Additionally to the chemical components an optical oxygen sensor also consists of optical components and electrical parts. The main optical components are fibers, either made from glass or plastic, filters and lenses [18]. The electrical parts consist of an excitation source, nowadays mainly LEDs, a detector unit, PMT or photodiode, and a control module. For time resolved measurements the controller has to either pulse the light source or modulate the light. A variety of different setups exist and many of them are commercialized.

APPLICATIONS OF OPTICAL O_2 SENSORS AND PROBES

The field of application of optical oxygen sensors is as big and diverse as life itself. Oxygen probes [64] and nanoparticles [65] are widely applied for oxygen measurements inside cells and tissues. For cell penetrating probes the cells are first incubated with the probes and can then be analyzed using plate readers or microscopes. Generally simple intensity measurements are possible, but time resolved or ratio-metric methods are favored especially in biological samples. Besides probes also microsensors may be used for spatially resolved oxygen measurements in tissues or sediments [66]. Other biological applications include the monitoring of water quality, photosynthesis studies [67], enzymatic activity and many more.

Medical applications include the measurement of blood gas, breath analysis, glucose measurements (in combination with an enzyme layer) and so on.

Aside from biological measurements optical oxygen sensors are also used in industrial processes [68]. Some applications include online measurements in breweries, bioprocess monitoring or measurements of air quality in mines. Several companies produce specialized sensor solutions for those applications.

Another interesting application field are so-called pressure sensitive paints [69]. For this method oxygen sensitive films are applied on models of airplanes, cars or similar and placed in a wind tunnel. As the luminescence is affected by the local pressure this technique can be used to measure the pressure [70].

Food quality and safety are also topics where optical oxygen sensors can be used. In this field also irreversible sensors are used [71]. For the integration into food packaging the sensors need to be very stable and of course very cheap.

Oxygen sensors are needed in a variety of fields and have not even reached their full potential yet. As long as oxygen will be the main source of energy on this planet optical, oxygen sensors will be valuable tools.

REFERENCES:

[1] A.F. Holleman, E. Wiberg, Lehrbuch der Anorganischen Chemie, 101., verb. u. stark erw. A., Gruyter, 1995.

[2] H.D. Holland, The Oxygenation of the Atmosphere and Oceans, Phil. Trans. R. Soc. B. 361 (2006) 903–915.

[3] G.L. Semenza, Life with Oxygen, Science. 318 (2007) 62–64.

[4] N. Lane, Oxygen: The Molecule that Made the World, Oxford University Press, USA, 2004.

[5] D.J. Voet, J.G. Voet, C.W. Pratt, Lehrbuch der Biochemie, 2. Aufl., Wiley-VCH Verlag GmbH & Co. KGaA, 2002.

[6] R.E. Kopp, J.L. Kirschvink, I.A. Hilburn, C.Z. Nash, The Paleoproterozoic snowball Earth: a climate disaster triggered by the evolution of oxygenic photosynthesis, Proc. Natl. Acad. Sci. U.S.A. 102 (2005) 11131–11136.

[7] R. Buick, When Did Oxygenic Photosynthesis Evolve?, Phil. Trans. R. Soc. B. 363 (2008) 2731–2743.

[8] V. Yankovskaya, R. Horsefield, S. Törnroth, C. Luna-Chavez, H. Miyoshi, C. Léger, u. a., Architecture of Succinate Dehydrogenase and Reactive Oxygen Species Generation, Science. 299 (2003) 700–704.

[9] J.M. McCord, I. Fridovich, Superoxide dismutase: The first twenty years (1968–1988), Free Radical Biology and Medicine. 5 (1988) 363–369.

[10] R.D. Guzy, P.T. Schumacker, Oxygen Sensing by Mitochondria at Complex III: The Paradox of Increased Reactive Oxygen Species During Hypoxia, Exp Physiol. 91 (2006) 807–819.

[11] M. Tomita, G.L. Semenza, C. Michiels, T. Matsuda, J.-N. Uchihara, T. Okudaira, u. a., Activation of hypoxia-inducible factor 1 in human T-cell leukaemia virus type 1-infected cell lines and primary adult T-cell leukaemia cells, Biochem J. 406 (2007) 317–323.

[12] A.C. Epstein, J.M. Gleadle, L.A. McNeill, K.S. Hewitson, J. O'Rourke, D.R. Mole, u. a., C. elegans EGL-9 and mammalian homologs define a family of dioxygenases that regulate HIF by prolyl hydroxylation, Cell. 107 (2001) 43–54.

[13] J.W. Severinghaus, Fire-air and dephlogistication. Revisionisms of oxygen's discovery, Adv. Exp. Med. Biol. 543 (2003) 7–19.

[14] L.W. Winkler, Die Bestimmung des im Wasser gelösten Sauerstoffes,, Berichte der deutschen chemischen Gesellschaft,. 21 (1888) 2843–2854.

[15] A. Hulanicki, S. Glab, F. Ingman, Chemical sensors: definitions and classification, Pure and Applied Chemistry. 63 (1991) 1247–1250.

[16] O.S. Wolfbeis, B.M. Weidgans, FIBER OPTIC CHEMICAL SENSORS AND BIOSENSORS: A VIEW BACK, in: F. Baldini, A.N. Chester, J. Homola, S. Martellucci (Hrsg.), Optical Chemical Sensors, Springer Netherlands, 2006: S. 17–44.

[17] O.S. Wolfbeis, Chemical sensors — survey and trends, Fresenius' Journal of Analytical Chemistry. 337 (1990) 522–527.

[18] P. Gründler, Chemische Sensoren: Eine Einführung für Naturwissenschaftler und Ingenieure, 1. Aufl., Springer Berlin Heidelberg, 2004.

[19] J. Severinghaus, P. Astrup, History of blood gas analysis. IV. Leland Clark's oxygen electrode, Journal of Clinical Monitoring and Computing. 2 (1986) 125–139.

[20] L.C. CLARK Jr., R. WOLF, D. GRANGER, Z. TAYLOR, Continuous recording of blood oxygen tensions by polarography., Journal of applied physiology. 6 (1953) 189–193.

[21] L. Nei, Some Milestones in the 50-year History of Electrochemical Oxygen Sensor Development, ECS Transactions. 2 (2007) 33–38.

[22] J.W. Severinghaus, The invention and development of blood gas analysis apparatus, Anesthesiology. 97 (2002) 253–256.

[23] L.C. Clark Jr., C. Lyons, Electrode system for continuous monitoring in cardiovascular surgery, Annals of the New York Academy of Sciences. 102 (1962) 29–45.

[24] W.J. Whalen, P. Nair, R.A. Ganfield, Measurements of oxygen tension in tissues with a micro oxygen electrode, Microvascular Research. 5 (1973) 254–262.

[25] H. Kautsky, A. Hirsch, Nachweis geringster Sauerstoffmengen durch Phosphoreszenztilgung, Zeitschrift für anorganische und allgemeine Chemie. 222 (1935) 126–134.

[26] D.W. Lübbers, N. Opitz, The pCO2-/pO2-optode: a new probe for measurement of pCO2 or pO2 in fluids and gases, Z. Naturforsch., C, Biosci. 30 (1975) 532–533.

[27] F. Baldini, A.N. Chester, J. Homola, S. Martellucci, hrsg., Optical Chemical Sensors, o. J.

[28] Klimant, V. Meyer, M. Kühl, Fiber optic oxygen microsensors: a new tool in aquatic biology, 40 (1995) 1159–1165.

[29] B.M. Cullum, T. Vo-Dinh, The development of optical nanosensors for biological measurements, Trends Biotechnol. 18 (2000) 388–393.

[30] B. Valeur, Molecular Fluorescence: Principles and Applications, 1. Aufl., Wiley-VCH, 2001.

[31] S.M. Borisov, T. Mayr, G. Mistlberger, K. Waich, K. Koren, P. Chojnacki, u. a., Precipitation as a simple and versatile method for preparation of optical nanochemosensors., Talanta. 79 (2009) 1322–1330.

[32] S.M. Borisov, I. Klimant, Optical nanosensors—smart tools in bioanalytics, Analyst. 133 (2008) 1302–1307.

[33] R.I. Dmitriev, A.V. Zhdanov, G.V. Ponomarev, D.V. Yashunski, D.B. Papkovsky, Intracellular oxygen-sensitive phosphorescent probes based on cell-penetrating peptides, Analytical Biochemistry. 398 (2010) 24–33.

[34] O.S. Wolfbeis, Materials for fluorescence-based optical chemical sensors., J. Mater. Chem. 15 (2005) 2657–2669.

[35] I. Bergman, Rapid-response Atmospheric Oxygen Monitor based on Fluorescence Quenching, Nature. 218 (1968) 396–396.

[36] O.S. Wolfbeis, H. Offenbacher, H. Kroneis, H. Marsoner, A fast responding fluorescence sensor for oxygen, Microchimica Acta. 82 (1984) 153–158.

[37] Y. Amao, Probes and Polymers for Optical Sensing of Oxygen, Microchimica Acta. 143 (2003) 1–12.

[38] J.G. Vos, J.M. Kelly, Ruthenium polypyridyl chemistry; from basic research to applications and back again, Dalton Trans. (2006) 4869–4883.

[39] K. Kalyanasundaram, Photochemistry of Polypyridine and Porphyrin Complexes, Academic Press, 1992.

[40] E.R. Carraway, J.N. Demas, B.A. DeGraff, J.R. Bacon, Photophysics and photochemistry of oxygen sensors based on luminescent transition-metal complexes., Analytical Chemistry. 63 (1991) 337–42.

[41] S.M. Borisov, I. Klimant, Ultrabright Oxygen Optodes Based on Cyclometalated Iridium(III) Coumarin Complexes, Analytical Chemistry. 79 (2007) 7501–7509.

[42] M. Schäferling, The Art of Fluorescence Imaging with Chemical Sensors,, Angewandte Chemie International Edition. 51 (2012) 3532–3554.

[43] D.B. Papkovsky, J. Olah, I.V. Troyanovsky, N.A. Sadovsky, V.D. Rumyantseva, A.F. Mironov, u. a., Phosphorescent polymer films for optical oxygen sensors, Biosensors and Bioelectronics. 7 (1992) 199–206.

[44] G. Khalil, M. Gouterman, S. Ching, C. Costin, L. Coyle, S. Gouin, u. a., Synthesis and spectroscopic characterization of Ni, Zn, Pd and Pt tetra(pentafluorophenyl)porpholactone with comparisons to Mg, Zn, Y, Pd and Pt metal complexes of tetra(pentafluorophenyl)porphine, Journal of Porphyrins and Phthalocyanines. 06 (2002) 135.

[45] O.S. Finikova, A.V. Cheprakov, S.A. Vinogradov, Synthesis and Luminescence of Soluble meso-Unsubstituted Tetrabenzo- and Tetranaphtho[2,3]porphyrins, The Journal of Organic Chemistry. 70 (2005) 9562–9572.

[46] S.M. Borisov, G. Nuss, I. Klimant, Red Light-Excitable Oxygen Sensing Materials Based on Platinum(II) and Palladium(II) Benzoporphyrins, Analytical Chemistry. 80 (2008) 9435–9442.

[47] F. Niedermair, S.M. Borisov, G. Zenkl, O.T. Hofmann, H. Weber, R. Saf, u. a., Tunable phosphorescent NIR oxygen indicators based on mixed benzo- and naphthoporphyrin complexes, Inorg Chem. 49 (2010) 9333–9342.

[48] S.M. Borisov, G. Zenkl, I. Klimant, Phosphorescent platinum(II) and palladium(II) complexes with azatetrabenzoporphyrins-new red laser diode-compatible indicators for optical oxygen sensing, ACS Appl Mater Interfaces. 2 (2010) 366–374.

[49] K. Koren, S.M. Borisov, R. Saf, I. Klimant, Strongly Phosphorescent Iridium(III)-Porphyrins - New Oxygen Indicators with Tuneable Photophysical Properties and Functionalities, Eur. J. Inorg. Chem. 2011 (2011) 1531–1534.

[50] S. Silva, P.M.R. Pereira, P. Silva, F.A.A. Paz, M.A.F. Faustino, J.A.S. Cavaleiro, u. a., Porphyrin and phthalocyanine glycodendritic conjugates: synthesis, photophysical and photochemical properties, Chem. Commun. 48 (o. J.) 3608–3610.

[51] Y. Amao, T. Miyashita, I. Okura, Novel optical oxygen sensing material: Platinum octaethylporphyrin immobilized in a copolymer film of isobutyl methacrylate and tetrafluoropropyl methacrylate, Reactive and Functional Polymers. 47 (2001) 49–54.

[52] A. Mills, A. Lepre, Controlling the Response Characteristics of Luminescent Porphyrin Plastic Film Sensors for Oxygen, Anal. Chem. 69 (1997) 4653–4659.

[53] K. Stubenrauch, M. Sandholzer, F. Niedermair, K. Waich, T. Mayr, I. Klimant, u. a., Poly(norbornene)s as matrix materials for platinum tetrakis(pentafluorophenyl)porphyrin based optical oxygen sensors, European Polymer Journal. 44 (2008) 2558–2566.

[54] I. Klimant, F. Ruckruh, G. Liebsch, A. Stangelmayer, O.S. Wolfbeis, Fast response oxygen micro-optodes based on novel soluble ormosil glasses, Mikrochimica Acta. 131 (1999) 35–46.

[55] V.S. Tripathi, G. Lakshminarayana, M. Nogami, Optical oxygen sensors based on platinum porphyrin dyes encapsulated in ORMOSILS, Sensors and Actuators B: Chemical. 147 (2010) 741–747.

[56] R.M. Bukowski, R. Ciriminna, M. Pagliaro, F.V. Bright, High-Performance Quenchometric Oxygen Sensors Based on Fluorinated Xerogels Doped with [Ru(dpp)3]2+, Anal. Chem. 77 (2005) 2670–2672.

[57] S.M. Borisov, P. Lehner, I. Klimant, Novel optical trace oxygen sensors based on platinum(II) and palladium(II) complexes with 5,10,15,20-meso-tetrakis-(2,3,4,5,6-pentafluorphenyl)-porphyrin covalently immobilized on silica-gel particles, Analytica Chimica Acta. 690 (2011) 108–115.

[58] C. McDonagh, C.S. Burke, B.D. MacCraith, Optical Chemical Sensors, Chemical Reviews. 108 (2008) 400–422.

[59] A.Y. Lebedev, A.V. Cheprakov, S. Sakadzić, D.A. Boas, D.F. Wilson, S.A. Vinogradov, Dendritic phosphorescent probes for oxygen imaging in biological systems, ACS Appl Mater Interfaces. 1 (2009) 1292–1304.

[60] S.M. Buck, Y.-E.L. Koo, E. Park, H. Xu, M.A. Philbert, M.A. Brasuel, u. a., Optochemical nanosensor PEBBLEs: photonic explorers for bioanalysis with biologically localized embedding, Curr Opin Chem Biol. 8 (2004) 540–546.

[61] S.M. Borisov, T. Mayr, G. Mistlberger, I. Klimant, Dye-Doped Polymeric Particles for Sensing and Imaging, in: A.P. Demchenko (Hrsg.), Advanced Fluorescence Reporters in Chemistry and Biology II, Berlin, Heidelberg, Springer Berlin Heidelberg, 2010: S. 193–228.

[62] A. Fercher, G. Ponomarev, D. Yashunski, D. Papkovsky, Evaluation of the derivates of phosphorescent Pt-coproporphyrin as intracellular oxygen-sensitive probes, Analytical and Bioanalytical Chemistry. 396 (2010) 1793–1803.

[63] R.I. Dmitriev, H.M. Ropiak, D.V. Yashunsky, G.V. Ponomarev, A.V. Zhdanov, D.B. Papkovsky, Bactenecin 7 peptide fragment as a tool for intracellular delivery of a phosphorescent oxygen sensor, FEBS J. 277 (2010) 4651–4661.

[64] R. Dmitriev, D. Papkovsky, Optical probes and techniques for O2 measurement in live cells and tissue, Cellular and Molecular Life Sciences. (o. J.) 1–15.

[65] Y.-E.K. Lee, R. Kopelman, R. Smith, Nanoparticle PEBBLE sensors in live cells and in vivo, Annu Rev Anal Chem (Palo Alto Calif). 2 (2009) 57–76.

[66] I. Klimant, G. Holst, M. KÃ¼hl, A simple fiberoptic sensor to detect the penetration of microsensors into sediments and other biogeochemical systems, Limnology and Oceanography. 42 (1997) 1638–1643.

[67] T. Takeuchi, K. Yokoyama, K. Kobayashi, M. Suzuki, E. Tamiya, I. Karube, u. a., Photosynthetic activity sensor for microalgae based on an oxygen electrode integrated with optical fibres, Analytica Chimica Acta. 276 (1993) 65–68.

[68] R. Narayanaswamy, O.S. Wolfbeis, Optical Sensors: Industrial, Environmental and Diagnostic Applications, Springer, 2004.

[69] G.E. Khalil, C. Costin, J. Crafton, G. Jones, S. Grenoble, M. Gouterman, u. a., Dual-luminophor pressure-sensitive paint: I. Ratio of reference to sensor giving a small temperature dependency, Sensors and Actuators B: Chemical. 97 (2004) 13–21.

[70] J.H. Bell, E.T. Schairer, L.A. Hand, R.D. Mehta, Surface Pressure Measurements Using Luminescent Coatings1, Annual Review of Fluid Mechanics. 33 (2001) 155–206.

[71] A. Mills, Oxygen indicators and intelligent inks for packaging food, Chem. Soc. Rev. 34 (2005) 1003.

PART II
PUBLICATIONS IN PEER REVIEWED JOURNALS

OUTLOOK

In this section the publications in peer reviewed journals that orginated during this thesis are collected. Prior to the publication the concept or idea behind the corresponding publication is described. After some chapters additional projects that are based on the research within those chapters are presented. The additional projects are currently under development and will not be dissucsed extensively.

According to the title “Optical Oxygen Sensors – Indicators and Materials - Synthesis and Applications” the work within this thesis gives a good overview on oxygen sensors.

The main components of an optical oxygen sensor is the indicator dye. The molecule that interacts with oxygen; the molecule that emits the light that can be measured; the molecule that can be quenched by oxygen. In the first publication a new class of indicators is presented; so-called iridium(III) porphyrins. Those dyes consist of a porphyrin macrocycle with an Ir(III) as center atom. As Ir(III) has two additional axial binding domaines, those can be used to attach ligands that alter the photophysical properties and can then, also be used to enable coupling.

The second paper uses those indicators and combines them with peptides. The so prepared probes prepared this way can penatrate trough the cell membrane and enable intracellular oxygen measurements in a variety of mammalian cells. The straight forward synthesis and good photophysical properties make them interesting candidates for metabolic studies.

Besides the indicator an optical oxygen sensor consists of a matrix. The matrix has the purpose of fixing the indicator on a substrate (e.g. fibre) and influences the sensitivity and stability of the indicator. The last two publications deal with this component of the sensor. In one case a strategy is presented that enables covalent coupling of the indicator to the matrix. This is a convenient way to eliminate migration and leaching of the indicator, two factors limiting sensor stability. In the last paper the effects of the sensor matrix on sensitivity and sensor stability are discussed. A set of chemically similar polymers are presented that enable the fine-tuning of the sensitivity.

All in all it can be said that this thesis covers the full range of chemistry that is needed to produce an optical oxygen sensor or probe. Synthesis of indicators and matrix materials are described, as well as their effects on sensor characteristics were studied.

The oxygen sensitive dye is the heart of every optical oxygen sensor. Throughout the years a variety of indicators were synthetized and used. Probably the most prominent representatives are porphyrin complexes of platinum(II) and palladium (II). Similar to *Chlorophyll* and *heme* those indicators consist of a porphyrin macrocycle and a complexed central atom, in this case Pt(II) or Pd(II). Porphyrins themselves are a heterocyclic macrocycle, which is composed of four pyrrole subunits that are interconnected via methine bridges (=CH-) [1]. The simplest porphyrin is called porphine; substituted porphines are called porphyrins. When bearing a metal as central atom the structures are called metalloporphyrins.

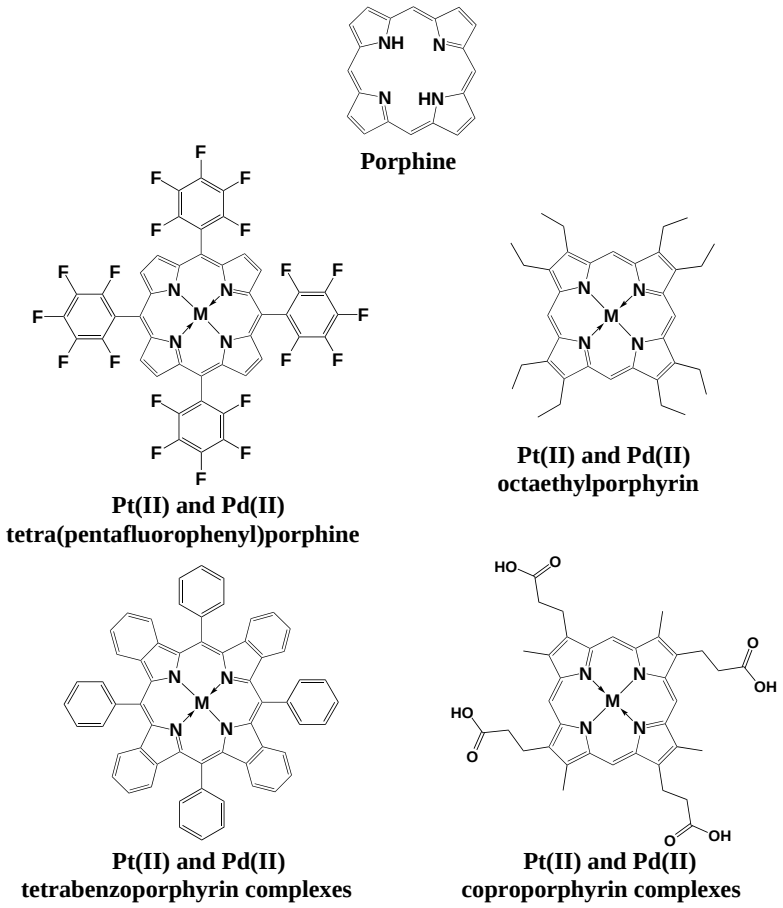

FIGURE 1: PORPHINE STRUCTURE AND SOME DERIVED PORPHYRINS. ALL THE METALLOPORPHYRINS SHOWN SHOW STRONG PHOSPHORESCENCE AND CAN BE USED AS OXYGEN INDICATORS.

Porphyrins and also metallopophyrins show strong absorptions in the visible range of the spectrum. Some porphyrins have luminescence properties. Especially the strong phosphorescence of Pt(II) and Pd(II) porphyrins is used in optical oxygen sensors. The photophysical properties can be changed depending on the structure of the substituents on the macrocycle [2]. Synthetic modifications of the macrocycle are possible, but often they turn out to be quite laborious and challenging.

Besides porphyrins also cyclometallated complexes of Ir(III) or Pt(II) are used as oxygen indicators. Complexes of Ir(III) are especially interesting as Ir(III) offers six coordination sites [3]. Ir(III) complexes normally show absorptions in the near UV or the blue part of the spectrum. Those complexes often show a charge-transfer character and an intense phosphorescence in the orange part of the spectrum.

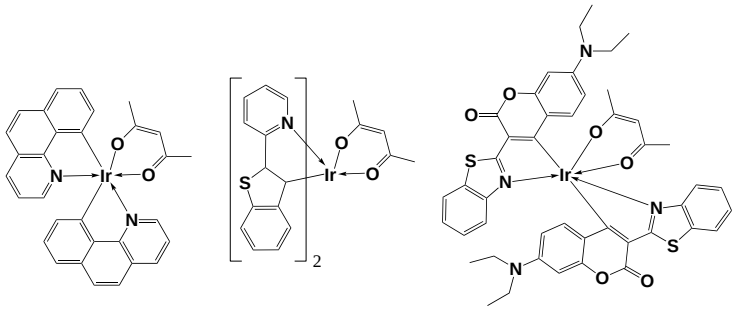

FIGURE 2: CYCLOMETALLATED IR(III) COMPLESES.

Both classes of indicators were used in oxygen sensors previously. Surprisingly the combination of Ir(III) and porphyrins is rare. Only a few older papers were found that reported the synthesis of such Ir(III)-metalloporphyrins [4,5]. No reports on luminescence properties of such complexes could be found. Due to the fact that unlike platinum(II) and palladium(II) iridium(III) offers two additional binding sites , the synthesis seems to be more challenging. On the other hand, the axial ligands may be used for further reactions.

So the following question arises: *do Ir(III) porphyrins show any kind of luminescence and could they be used for optical oxygen sensors? And if so, could the axial ligands be used to change the properties of the potential indicator?* Those questions will be answered in the first publication.

REFERENCES

[1] K.M. Kadish, The porphyrin handbook, Elsevier, 2000.

[2] K. Kalyanasundaram, Photochemistry of Polypyridine and Porphyrin Complexes, Academic Press, 1992.

[3] M.C. DeRosa, D.J. Hodgson, G.D. Enright, B. Dawson, C.E.B. Evans, R.J. Crutchley, Iridium Luminophore Complexes for Unimolecular Oxygen Sensors, Journal of the American Chemical Society. 126 (2004) 7619–7626.

[4] H. Ogoshi, J.-I. Setsune, Z.-I. Yoshida, Syntheses and reactions of iridium complexes of octaethylporphyrin, Journal of Organometallic Chemistry. 159 (1978) 317–328.

[5] K.M. Kadish, Y.J. Deng, J.D. Korp, Synthesis, x-ray structure, and characterization of [bis(diphenylphosphino)ethane]dichlorobis(octaethylporphyrinato)diiridium, Inorganic Chemistry. 29 (1990) 1036–1042.

STRONGLY PHOSPHORESCENT IRIDIUM(III) PORPHYRINS – NOVEL OXYGEN INDICATORS WITH TUNABLE PHOTOPHYSICAL PROPERTIES AND FUNCTIONALITIES

THIS CAPTER WAS PUBLISHED AS SHORT COMMUNICATION IN

EUROPEAN JOURNAL OF INORGANIC CHEMISTRY 2011 ISSUE 10, 1531-34

DOI: 10.1002/EJIC.201100089

AUTHORS: KLAUS KOREN, SERGEY M. BORISOV*, ROBERT SAF AND INGO KLIMANT

ABSTRACT:

Synthesis and characterization of four iridium(III)-octaethylporphyrins and a π-extended iridium(III)-benzoporphyrin is presented. Strong room temperature phosphorescence was observed for all the complexes with quantum yields up to 30%. Axial ligands were introduced to tune the photophysical properties and the solubility. Complexes bearing lipophilic ligands such as pyridine or N-(n-butyl)imidazole were incorporated into polystyrene yielding optical oxygen sensors. Covalent coupling of the dye is possible by introducing ligands with binding domains (1-imidazoleacetic acid). This enabled preparation of a water-soluble oxygen probe (via staining of Bovine Serum Albumine) and a trace oxygen sensor (via coupling to aminomodified silica-gel).

INTRODUCTION

Strongly luminescent metal complexes are applied as indicators in optical sensors[1], as emitters in OLEDs[2] and as labels.[3] Consequently they attract much attention of scientific community. Among others metalloporphyrins (especially Pt^{II}- and Pd^{II}-porphyrins), Ru^{II}-polypyridyl complexes[4] and Ir^{III}-cyclometallated compounds[5] are extensively studied representatives. Phosphorescent complexes based on porphyrins and their derivatives (porphyrin-ketones, porphyrin-lactones, π-extended porphyrins) are very versatile since different modifications of

the porphyrin macrocycle are possible.[6] Complexes based on Ir^{III}-cyclometallated compounds usually possess high luminescence quantum yields but often low absorption coefficients.[7,8]

To the best of our knowledge, nothing is known about phosphorescent Ir^{III}-porphyrins. This is not surprising considering that the synthesis and chemistry of such complexes are more difficult than for corresponding Pt^{II}- and Pd^{II}-metallopophyrins, which are known to be strongly phosphorescent at r.t. The question arises if Ir^{III}-porphyrins show any kind of luminescence at r.t. In fact, the combination of Ir^{III} as central metal and porphyrins as ligands is relatively rare in literature[9-13] and mainly catalytic properties of such complexes have been studied.[14-16] Recently barely luminescent (quantum yield from 0.03 to 1.2%) Ir^{III}-corrols have been reported.[17]

Besides potentially interesting photophysical properties, the combination of six-coordinating Ir^{III} and porphyrins also creates new synthetic possibilities. In contrast to the square planar Pt^{II}- and Pd^{II}-porphyrins, two additional ligands are introduced in the Ir^{III}-porphyrin system. The axial ligands may influence photophysical properties and affect solubility. Introducing ligands with binding domains or groups suitable for covalent linkage would also be of great interest. In this work several different Ir^{III}-porphyrins were synthesized and characterized.

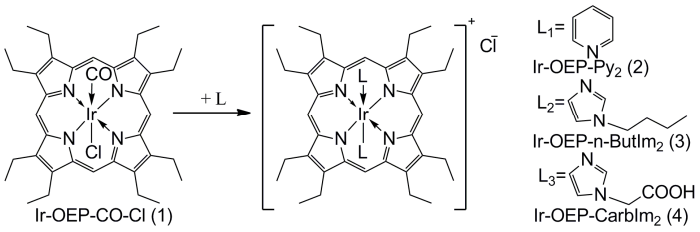

SCHEME 1. CHEMICAL STRUCTURES OF THE FOUR IR^{III}-OCTAETHYLPORPHYRIN COMPLEXES

RESULTS AND DISCUSSION

At first the complexes were studied based on an octaethylporphyrin macrocycle with varying axial ligands (Scheme 1 and Table 1). The carbonyl complex (Ir-OEP-CO-Cl[9]) was employed for preparation of the other complexes using rather simple and fast ligand exchange reactions. High phosphorescence quantum yields (QY up to 21%) were obtained for all the complexes making them good candidates for oxygen sensing. Photophysical properties were affected by the axial ligands. The positively charged complexes with two identical ligands show quite similar properties in contrast to neutral Ir-OEP-CO-Cl. In fact, despite slightly lower luminescence QY Ir-

OEP-CO-Cl has a significantly longer decay time (τ_0 = 97 µs). Also, the absorption and emission bands are bathochromically shifted (Figure 1 and Table 1). In contrast to the well-known Pt^{II}-octaethylporphyrin (Pt-OEP), the absorption peaks of all Ir^{III}-porphyrins are slightly broader (by about 5 nm at FWHM of the Soret band) and bathochromically shifted. This enables excitation via the strongly absorbing Soret band with visible light (400 to 405 nm) for all Ir^{III}-octaethylporphyrins.

TABLE 1. PHOTOPHYSICAL PROPERTIES OF IR^{III}-OCTAETHYLPORPHYRINS

	λ_{max} (abs) [nm] (ε [$10^{-3}cm^{-1}M^{-1}$])[b]	λ_{max} (em) [nm][a]	τ_0 [µs]	Φ [%][a]
Ir-OEP-CO-Cl	404 (165), 518 (15), 550 (31)	672	97[a] (108)[e]	14
Ir-OEP-Py_2	389 (148), 509 (11), 539 (26.6)	655	40[a] (52) [e]	19.5
Ir-OEP-*n*-$ButIm_2$	390 (150), 508 (9.7), 541 (15)	655	27[a] (35) [e]	20
Ir-OEP-$CarbIm_2$	388 (142), 507 (10), 538 (18)[c]	652[c]	37[c] 26[d]	21[c] 8[d]
Pt-OEP	382 (214), 503 (9.5), 536 (42.5)	649	75[a] (86)[e]	41.5
Pd-OEP	395 (127), 513 (9), 547 (32)	669	(1217)[e]	≈19

Diluted solutions of [a] toluene, [b] $CHCl_3$, [c] EtOH, [d] aqueous buffer (pH 7.3) at r.t.; [e] in PS at 25°C

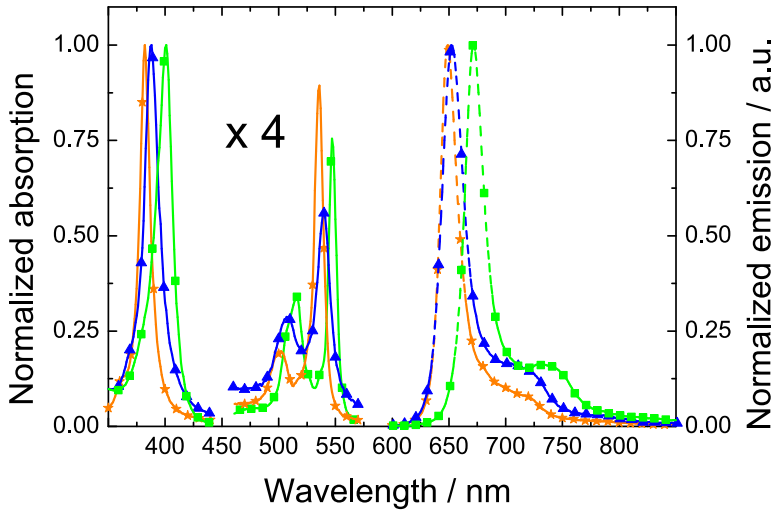

FIGURE 1. ABSORPTION (SOLID LINE) AND EMISSION SPECTRA (DASHED LINE) OF IR-OEP-CO-CL (LIGHT GRAY SQUARES), IR-OEP-CARBIM$_2$ (GRAY TRIANGLES) AND PT-OEP (BALCK STARS) AS REFERENCE

Axial ligands can also be used to change solubility or to introduce binding groups. Similarly to Ir-OEP-CO-Cl, the complexes bearing pyridine or *N*-(*n*-butyl)imidazole as axial ligands are well-soluble in organic solvents such as acetone, chloroform and toluene. Therefore, these complexes can be incorporated into polystyrene or other polymers yielding oxygen sensors. Stern-Volmer plots for the oxygen sensing materials based on the above indicators in PS are shown in Figure 2a. They are compared to the established Pt-OEP in the same matrix.

Quenching behaviour in polymeric films is usually described by the so called "two site model",[18] which suggests that some dye molecules are less quenchable by the analyte than others, leading to non-linear calibration curves.

It is noticeable that the Stern-Volmer plots for presented Ir^{III}-porphyrins show higher linearity than the Pt^{II} analogue (Figure 2a). Surprisingly, in case of Ir-OEP-CO-Cl a linear Stern-Volmer plot (R^2=0.997) from 0 to 100% air saturation was obtained. Interestingly, the size of the axial ligands seems to affect the second order rate quenching constant ($k_q=K_{SV}/\tau_0$). In fact, k_q increases when the size of the axial ligands increases (k_q= 361, 500 and 529 [$hPa^{-1}s^{-1}$] for Ir-OEP-CO-Cl, Ir-OEP-Py$_2$ and Ir-OEP-n-ButIm$_2$, respectively). This could possibly be explained by the participation of the axial ligands in the energy transfer reaction.

Axial ligands can also be used to introduce polar groups or binding moieties. For example, imidazole bearing a carboxylic group renders the porphyrin soluble in polar solvents such as ethanol, methanol and even in aqueous buffer (physiological pH).

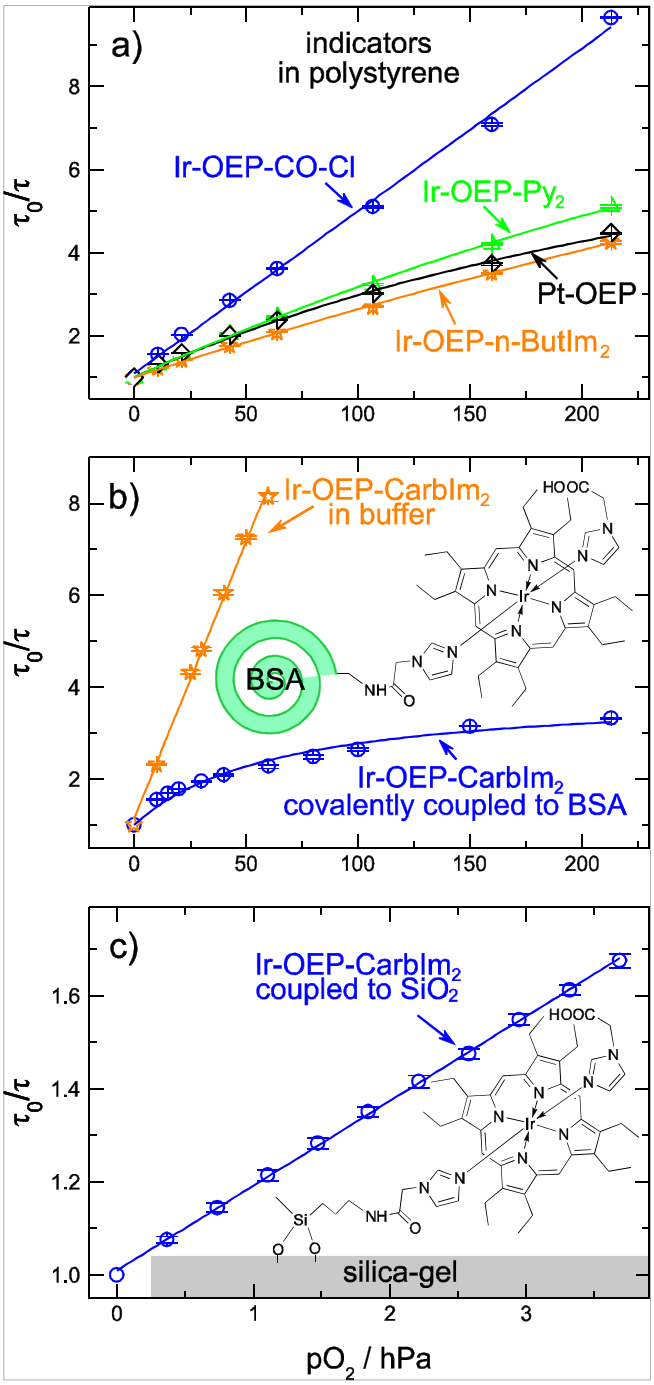

FIGURE 2. STERN-VOLMER PLOTS FOR THE SENSING MATERIALS BASED ON IR^{III}-PORPHYRINS; PT-OEP IS USED AS A REFERENCE.

The solubility in polar media and the presence of the carboxylic group enable coupling to biomolecules such as proteins, antibodies or lipids. To demonstrate its binding capability Ir-OEP-CarbIm$_2$ was coupled to bovine serum albumin, BSA, (τ_0 = 24 µs). As expected, the quenching efficiency decreases upon binding to BSA since the dye is better shielded from oxygen (Figure 2b). The highly non-linear calibration plot can be explained by linking to the protein in various positions having different oxygen accessibility. Protein- or peptide-bound oxygen-sensitive dyes are interesting tools to measure e.g. cell respiration,[19] particularly due to their small size and good solubility in biological media.

Evidently, covalent coupling is not only attractive for biomolecules but also for polymers or functionalized surfaces. Previously, we demonstrated that trace oxygen sensors can be designed by covalently immobilizing Pt^{II}- and Pd^{II}-pophyrin complexes on the surface of amino-modified silica-gel.[20] For the first time Ir-OEP-CarbIm$_2$ enables coupling to silica-gel via the axial ligand (τ_0 = 26µs) instead of modifying the porphyrin macrocycle. The obtained sensor is sensitive to small oxygen concentrations (Figure 2c) and shows a highly linear calibration plot (R^2=0.999).

Finally, the combination of Ir^{III} and an π-extended benzoporphyrin was investigated. Pt^{II}- and Pd^{II}- benzoporphyrins are known to emit in the near infrared (NIR) part of the spectrum.[21,22] NIR emitting complexes are particularly interesting as they enable subcutaneous measurements. In this work we combined Ir^{III} with teraphenyltetrabenzoporphyrin and chose *N*-(*n*-butyl)imidazole as axial ligand (Ir-TPTBP-*n*-ButIm$_2$). Unfortunately, bonding of the axial ligands seems to be weaker in case of the benzoporphyrin and they can be partly replaced e.g. by solvent molecules during the purification. Nevertheless, the results presented confirm that Ir^{III} was complexed by the porphyrin (Figure 3). Strong NIR phosphorescence was observed (quantum yield ≈ 30%, τ_0 ≈ 23µs) for Ir-TPTBP-n-ButIm$_2$. Thus, the Ir^{III}-porphyrin complexes represent significantly stronger emitters than the Ir^{III}-corrols (QY < 1.2%)[17]. Since the position of the phosphorescence maxima of the Ir^{III}-benzoporphyrin and the Ir^{III}-corrols is similar such a huge difference in the QY cannot be explained by the lower energy gap between the triplet excited state and the ground state in case of the corrols (λ_{max} ~ 790 nm).[17] A smaller size of the cavity in case of corrols may result in non-planarity of the Ir^{III} corrols which may promote non-radiative deactivation.

CONCLUSION

It can be concluded that Ir^{III}-porphyrin complexes are strong RT emitters. In contrast to the well-known Pt^{II}- and Pd^{II}-porphyrins the Ir^{III} complexes bear axial ligands which have pronounced effects on photophysical properties and solubility of the dyes. They can also be used to introduce functional groups to enable e.g. covalent coupling. The new dyes are particularly promising as indicators for oxygen sensors with tailor-made sensitivity.

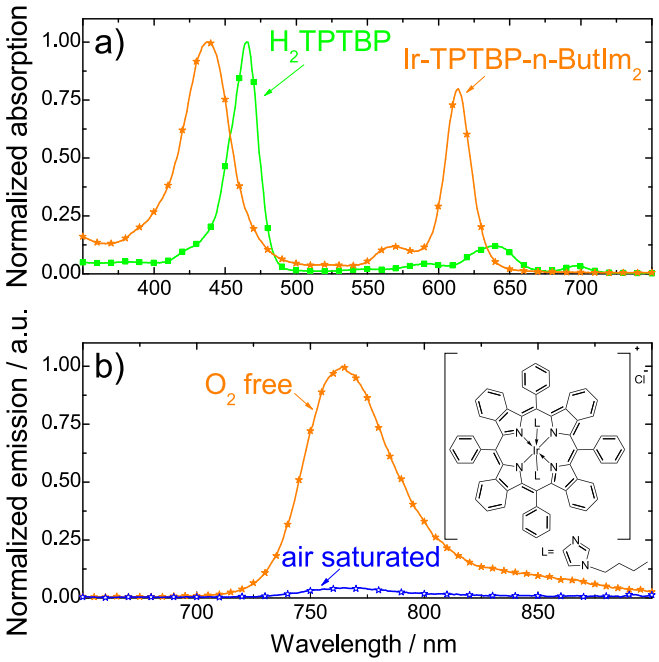

FIGURE 3. A) ABSORPTION SPECTRA OF THE FREE LIGAND H_2TPTBP AND IR-TPTBP-N-BUTIM$_2$; B) EMISSION SPECTRA OF IR-TPTBP-N-BUTIM$_2$ IN TOLUENE SOLUTION

EXPERIMENTAL SECTION

Ir-OEP-Cl-CO (**1**) was synthesized as described in the literature[9]. Complexes (**2**), (**3**) and (**4**) were obtained by ligand exchange reactions. Ligand exchange was accelerated by using large excess of the ligands. Ir-TPTBP-n-ButIm$_2$ was synthesized by metallating the free porphyrin (H_2TPTBP[23]) and subsequent replacement of the axial ligands. Ir-OEP-CarIm$_2$ was coupled to aminomodified silica gel particles as well as to BSA via an amide bound using EDC and NHS as coupling reagents.

ACKNOWLEDGMENTS

The authors would like to thank K. Greimel and T. Reiter from the Institute of Environmental Biotechnology at the Graz University of Technology for technical support. Financial support by the Austrian ScienceFund (FWF; Research Project No. P21192-N17) is gratefully acknowledged.

REFERENCES

[1] O. S. Wolfbeis, J. Mater. Chem. ***2005****, 15, 2657-2669.*

[2] R. Evans, P. Douglas, C. Winscom, Coord. Chem. Rev. ***2006****, 250, 2093-2126*

[3] D. B. Papkovsky, T. C. O'Riordan, J. Fluoresc. ***2005****, 15, 569-584.*

[4] J. G. Vos, J. M. Kelly, Dalton Trans. ***2006****, 4869-4883.*

[5] M. C. DeRosa, D. J. Hodgson, G. D. Enright, B. Dawson, C. E. B. Evans, R. J. Crutchley, J. Am. Chem. Soc. ***2004****, 126, 7619-7626.*

[6] The Porphyrin Handbook, (Eds.: K.M. Kadish, K.M. Smith and R. Guilard), Academic, San Diego, ***2000***

[7] C. Ulbricht, B. Beyer, C. Friebe, A. Winter, U. S. Schubert, Adv. Mater. ***2009****, 21, 4418-4441.*

[8] S. Lamansky, P. Djurovich, D. Murphy, F. Abdel-Razzaq, R. Kwong, I. Tsyba, M. Bortz, B. Mui, R. Bau, M. E. Thompson, Inorg. Chem. ***2001****, 40, 1704-1711.*

[9] H. Ogoshi, J. Setsune, Z. Yoshida, J. Organomet. Chem. ***1978****, 159, 317-328.*

[10] N. Sadasivan, E. B. Fleischer, J. Inorg. Nucl. Chem. ***1968****, 30, 591-601.*

[11] K. M. Kadish, Y. J. Deng, J. D. Korp, Inorg. Chem. ***1990****, 29, 1036-1042.*

[12] C. Swistak, J. L. Cornillon, J. E. Anderson, K. M. Kadish, Organometallics ***1987****, 6, 2146-2150.*

[13] H. Kanemitsu, R. Harada, S. Ogo, Chem. Commun. ***2010****, 46, 3083.*

[14] C. W. Cheung, K. S. Chan, Organometallics ***2008****, 27, 3043-3055.*

[15] C. Cheung, H. Fung, S. Lee, Y. Qian, Y. Chan, K. Chan, Organometallics ***2010****, 29, 1343-1354.*

[16] X. Song, K. S. Chan, Organometallics ***2007****, 26, 965-970.*

[17] J. H. Palmer, A. C. Durrell, Z. Gross, J. R. Winkler, H. B. Gray, J. Am. Chem. Soc. ***2010****, 132, 9230-9231.*

[18] E. R. Carraway, J. N. Demas, B. A. DeGraff, J. R. Bacon, Anal. Chem. ***1991****, 63, 337-42.*

[19] D. B. Papkovsky, J. Hynes, Y. Will, Expert Opin. Drug Metab. Toxicol. ***2006****, 2, 313-323.*

[20] S. M. Borisov, P. Lehner, I. Klimant, Anal. Chim. Acta submitted

[21] O. S. Finikova, A. V. Cheprakov, S. A. Vinogradov, J. Org. Chem. ***2005****, 70, 9562-9572.*

[22] S. M. Borisov, G. Nuss, I. Klimant, Anal. Chem. ***2008****, 80, 9435-9442.*

[23] S. M. Borisov, I. Klimant, Dyes and Pigm. ***2009****, 83, 312-316.*

SUPPORTING INFORMATION

STRONGLY PHOSPHORESCENT IRIDIUM(III)-PORPHYRINS – NOVEL OXYGEN INDICATORS WITH TUNABLE PHOTOPHYSICAL PROPERTIES AND FUNCTIONALITIES

KLAUS KOREN, SERGEY M. BORISOV, ROBERT SAF AND INGO KLIMANT*

EXPERIMENTAL SECTION

MATERIALS:

1,5-Cyclooctadien, pyridin, 2-ethoxyethanol and diphenylether were purchased from Aldrich (www.sigmaaldrich.com); N-hydroxysuccidinimide (NHS) from Fluka ; N-(n-butyl)imidazole and iridium trichloride hydrate from ABCR (www.abcr.de); 1-imidazoleacetic acid and 1-ethyl-3(3-dimethylaminopropy) carbodiimide hydrochloride (EDC) from TCI (www.tcieurope.eu); polystyrene (MW. 250000) from Fisher Scientific (www.fishersci.com); poly(ethylene glycol terephthalate) support (Mylar®) from Goodfellow (www.goodfellow.com); platinum(II) octaethylporphyrin (Pt-OEP), palladium(II) octaethylporphyrin (Pd-OEP) and octaethylporphyrine ($OEPH_2$) from Frontier Scientific (www.frontiersci.com); bovine serum albumin (BSA) from Roth (www.carl-roth.de). $[Ir(COD)(\mu\text{-}Cl)]_2$ was synthesized as described in the literature[1]. Silica-gel 60 (0.063-0.200 mm) was purchased from Merck (www.merck.de) and neutral aluminum oxide (50-200 µm) was purchased from Acros Organics (www.acros.com). All other solvents were from Roth (www.carl-roth.de) and used without further purification. Throughout this work deionized water was used.

METHODS:

Mass spectrometry was performed on a Micromass TofSpec 2E Time-of-Flight Mass Spectrometer. The instrument is equipped with a nitrogen laser (337nm wavelength, operated at a frequency of 5 Hz), and a time lag focusing unit. Ions were generated by irradiation just

above the threshold laser power. Positive ion spectra were recorded in reflectron mode applying an accelerating voltage of 20 kV and externally calibrated with a suitable mixture of poly(ethyleneglycol)s (PEG). The spectra of 100–150 shots were averaged to improve the signal-to-noise ratio. Analysis of data was done with MassLynx-Software V3.5 (Micromass/Waters, Manchester, UK). Samples were dissolved in THF (C = 0.1mgmL^{-1}), dithranol or α-Cyanocinnamic acid was used as matrix (C=10mgmL−1 in THF), respectively. The solutions were mixed in the cap of a microtube in the ratio of 1μL:10μL. Then, 0.5μL of the resulting mixture were deposited on the sample plate (stainless steel) and allowed to dry under air. LDI mass spectrometry was performed on the same instrument.

Absorption spectra were measured at a Cary 50 UV–VIS spectrophotometer (www.lzs-concept.com). Emission spectra were acquired on a Hitachi F-7000 fluorescence spectrometer (www.inula.at) equipped with a red-sensitive photo-multiplier R 928 from Hamamatsu (www.hamamatsu.com). The emission spectra were corrected for the sensitivity of the PMT which was calibrated using a halogen lamp. Relative luminescence quantum yields were determined using a solution of Pt-OEP in toluene as a standard (quantum yield = 41.5%). The solutions of the dyes were thoroughly deoxygenated by bubbling nitrogen through.

Luminescence phase shifts for the dyes in solutions were measured with a two-phase lock-inamplifier (SR830, Stanford Research Inc., www.thinksrs.com). Excitation was performed with the light of a 405 nm (for OEP complexes) or a 450 nm (for benzoporphyrin complexes) LED which was sinusoidally modulated at frequencies of 2.5, 5 and 8 kHz. A bifurcated fiber bundle was used to guide the excitation-light to the cuvette and to guide back the luminescence after passing the OG630 (Schott), for OEP complexes, or RG 9 (Schott), for benzoporphyrin complexes, glass filter. The luminescence was detected with a photo-multiplier tube (H5701-02, Hamamatsu, www.sales.hamamatsu.com). Temperature was controlled by a cryostat ThermoHaake DC50. Gas calibration mixtures were obtained using a gas mixing device (MKS, www.mksinst.com). Trace oxygen concentrations were measured as reported elsewhere[2]

Synthesis of Chloro-(octaethylporphyrinato)-carbonyliridium(III) (Ir-OEP-Cl-CO) (1)

Ir-OEP-Cl-CO (1) was synthesized as described in the literature[3]. In brief, 200 mg of $OEPH_2$ (0.374 mmol) and 300 mg of $[Ir(COD)(\mu\text{-}Cl)]_2$ (0.482 mmol) were refluxed in 200 mL of p-xylene for about 8 hours. Reaction progress was monitored via UV-Vis absorption. After solvent removal silica gel chromatography was performed. Starting material and byproducts were eluted using toluene. The product was eluted with toluene:acetone (95 : 5). yield: 105 mg (35%)

UV-Vis: (toulene), λ/nm (relative intensity): 404 (1.00), 518 (0.09), 550 (0.19); ^1H NMR (300 MHz, $CDCl_3$), ppm: 10.31 (s; 4H), 4.15 (q; 16H), 2.02 (t; 24H)

FIGURE S 1: ^1H NMR IR-OEP-CO-CL IN $CDCL_3$

FIGURE S 2: $^{1}H^{1}H$ COSY NMR IR-OEP-CO-CL IN $CDCL_3$

Synthesis of bis-pyridino-octaethylporphyrinatoiridium(III) chloride (Ir-OEP-Py2) (2)

47 mg of Ir-OEP-CO-Cl (0,059 mmol) was refluxed in 5 mL of pyridine for 24 hours. The product was precipitated with 50 mL of H_2O and 10 mL of saturated NaCl solution. The precipitate was washed 3 times with water, dried and purified on silica gel. Byproducts were removed using CH_2Cl_2 and CH_2Cl_2:acetone (1:1). The product eluted using acetone:MeOH (95:5). 34 mg (yield: 65%) of Ir-OEP-Py_2 were obtained.

UV-Vis: ($CHCl_3$), λ/nm (relative intensity): 389 (1.00), 509 (0.075), 539 (0.18)

HRMS (MALDI): m/z $[M]^+$ calc. 881.4016 , found 881.4037

^{1}H NMR (300 MHz, $CDCl_3$), ppm: 10.19 (s; 4 H), 6.03 (t; 2H), 4.94 (t; 4H), 4.10 (q; 16H), 1.91 (t; 24H), 0.23 (d; 4H)

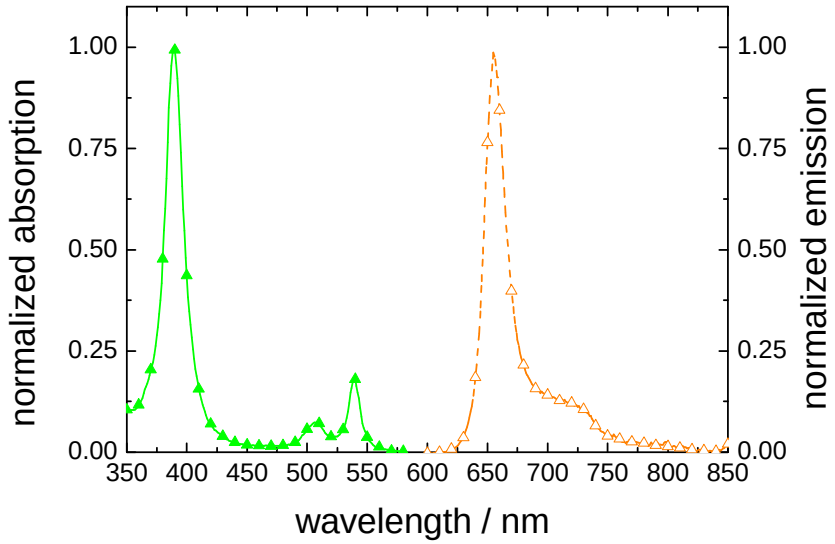

FIGURE S 3: NORMALIZED ABSORPTION (FULL LINE) AND EMISSION (DASHED LINE) SPECTRA OF IR-OEP-PY$_2$

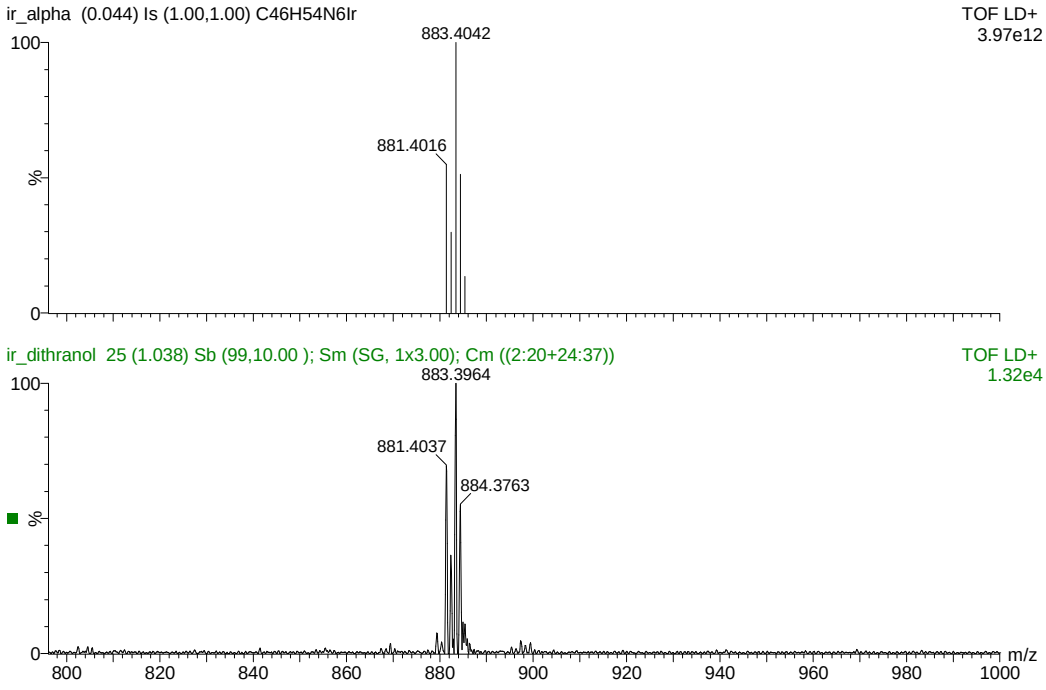

FIGURE S 4: TOP: CALCULATED ISOTOPE PATTERN FOR $C_{46}H_{54}N_6IR$; BOTTOM: MEASURED ISOTOPE PATTERN FOR IR-OEP-PY$_2$

FIGURE S 5: ^{1}H NMR IR-OEP-PY_2 IN $CDCL_3$

FIGURE S 6: $^{1}H^{1}H$ COSY NMR IR-OEP-PY_2 IN $CDCL_3$

Synthesis of bis-(N-(n-Butyl)imidazolo)-octaethylporphyrinatoiridium(III) chloride (Ir-OEP-n-ButIm2) (3)

80 mg of Ir-OEP-CO-Cl (0.10 mmol) was dissolved in 5 mL of N-(n-Butyl)imidazole and stirred at 120° C for one hour. The mixture was precipitated with 50 mL of H_2O and 10 mL of saturated NaCl solution. The precipitate was washed 3 times with water, dried and purified on Al_2O_3. Starting material was removed using CH_2Cl_2:acetone (1:1), the product eluted using acetone:MeOH (95:5). 58 mg of Ir-OEP-n-ButIm$_2$ (yield: 60%) were isolated.

UV-Vis: ($CHCl_3$), λ/nm (relative intensity): 390 (1.00), 508 (0.065), 541 (0.10)

HRMS (MALDI): m/z $[M]^+$ calc. 971.5173 , found 971.5223

^{1}H NMR (300 MHz, $CDCl_3$), ppm: 10.08 (s; 4 H), 4.59 (broad s; 2H), 4.08 (q; 16H), 2.22 (t; 4H), 1.90 (t; 24H), 0.45 (broad s; 2H), 0.28 – 0.15 (m; 10H), 0.13 (s; 2H), -0.16 (hex; 4H).

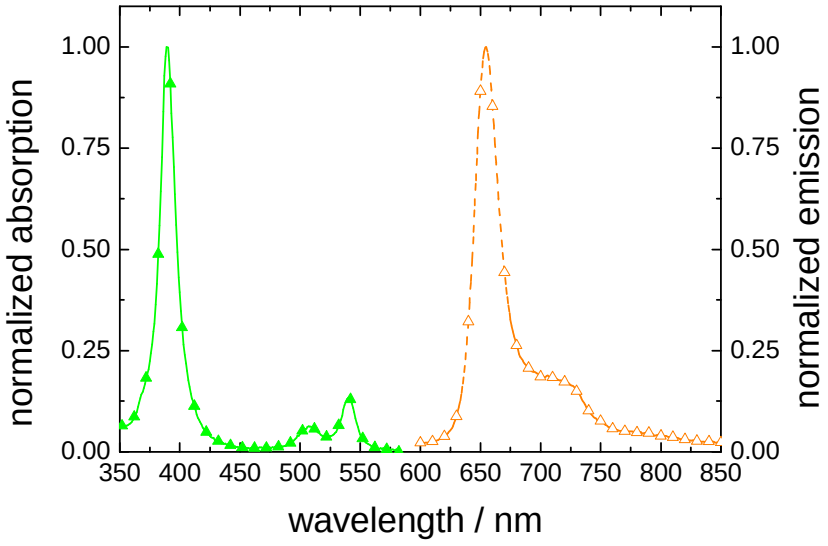

FIGURE S 7: NORMALIZED ABSORPTION (FULL LINE) AND EMISSION (DASHED LINE) SPECTRA OF IR-OEP-N-BUTIM$_2$

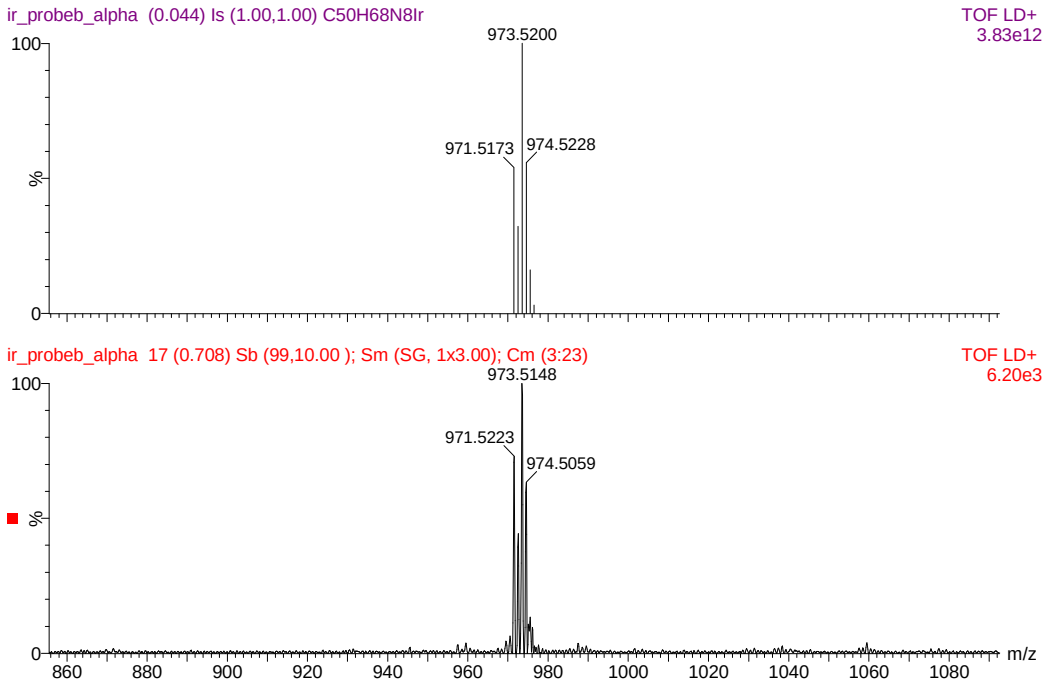

FIGURE S 8: TOP: CALCULATED ISOTOPE PATTERN FOR $C_{50}H_{68}N_8IR$; BOTTOM: MEASURED ISOTOPE PATTERN FOR IR-OEP-N-BUTIM$_2$

FIGURE S 9: ^{1}H NMR IR-OEP-N-BUTIM$_2$ IN $CDCL_3$

FIGURE S 10: $^{1}H^{1}H$ COSY NMR IR-OEP-N-BUTIM$_2$ IN CDCL$_3$

Synthesis of octaethylporphyrinatoiridium(III) bis-1-Imidazoleacetic acid (Ir-OEP-CarbIm2) (4)

103 mg of Ir-OEP-CO-Cl (0.138 mmol) and 500 mg of 1-Imidazoleacetic acid (3.96 mmol) were dissolved in 20 mL of 2-ethoxyethanol. The solution was refluxed for 1 hour. After cooling to room temperature the solution was poured into a mixture of H_2O and saturated NaCl solution (1:1, 100 mL in total). After stirring for several minutes the precipitated product was separated via centrifugation and washed three times with dest H_2O and dried. 40 mL of water and 2 mL of 1 M NaOH were added to the obtained solid. After ultrasonification for 30 minutes the soluble and insoluble fraction were separated via centrifugation. The soluble fraction was collected. After adding 4 mL of 1 M HCl the product precipitated and was collected via centrifugation and washed three times. After drying 35 mg (yield: 26%) of Ir-OEP-CarbIm$_2$ were obtained.

UV-Vis: (EtOH), λ/nm (relative intensity): 388 (1.00), 509 (0.07), 540 (0.14)

IR (KBr): 1625 cm^{-1} (C=O carboxylic group)

HRMS (MALDI): m/z [M]⁺ calc. 975.4031 , found 975.4072

^{1}H NMR (300 MHz, d_4-MeOD), ppm: 10.22 (s; 4 H), 4.65 (broad s; 2H), 4.13 (q; 16H), 2.90 (s; 4H), 1.94 (t; 24H), 0.11 (broad s; 2H), 0.01 (s; 2H).

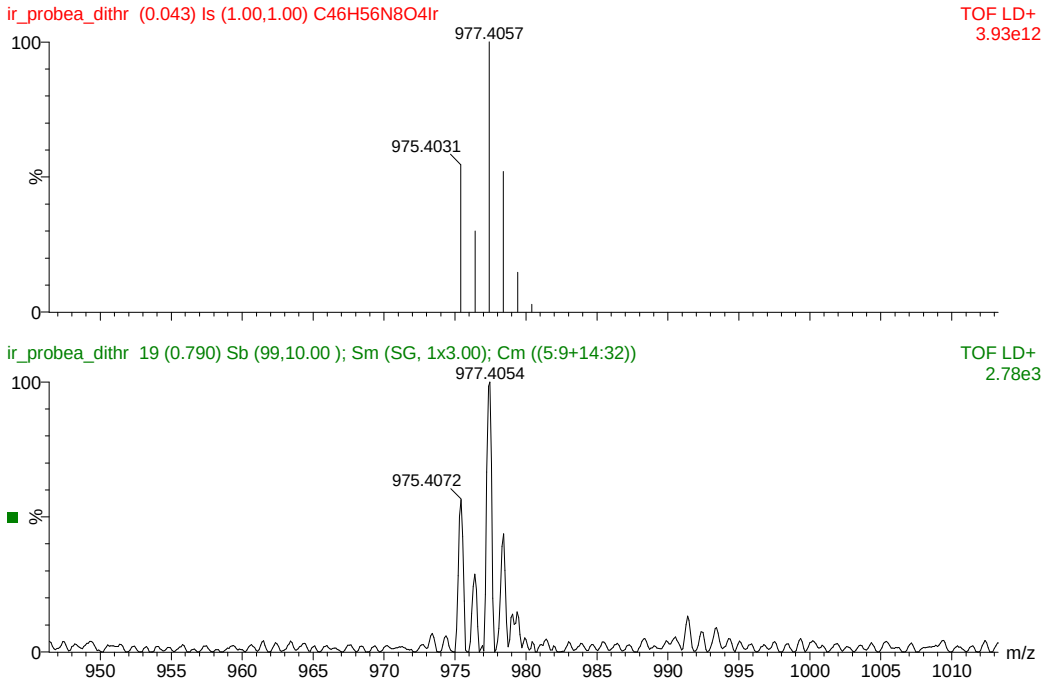

FIGURE S 11: TOP: CALCULATED ISOTOPE PATTERN FOR $C_{45}H_{56}N_8O_4IR$; BOTTOM: MEASURED ISOTOPE PATTERN FOR IR-OEP-CARBIM$_2$

FIGURE S 12: ^{1}H NMR IR-OEP-CARBIM$_2$ IN D_4-MEOD

FIGURE S 13: $^{1}H^{1}H$ COSY NMR IR-OEP-CARBIM$_2$ IN D_4-MEOD

SYNTHESIS OF BIS- (N-(N-BUTYL)IMIDAZOLO)-TETRAPHENYLTETRABENZOPORPHYRINATOIRIDIUM(III) CHLORIDE (IR-TPTBP-N-BUTIM2) (5)

Tetraphenyltetrabenzoporphyrin (H_2TPTBP) was synthesized as reported earlier[4]. Side reactions in the reported synthesis lead to benzyl adducts (C_7H_6 groups are fused to the porphyrin) that contaminate the porphyrin, but do not influence the photophysical properties of the ligand.

100 mg of H_2TPTBP (0.123 mmol) and 125 mg of $[Ir(COD)(\mu\text{-}Cl)]_2$ (0.186 mmol) were dissolved in 80 mL of ethylene glycol and stirred at 170° C for 6 hours. Reaction progress was monitored via UV-Vis absorption. The solution was precipitated using 100 mL of water. The precipitate was separated via centrifugation and washed twice with water. After drying the crude product was used for the subsequent step without further purification.

5 mL of N-(n-Butyl)imidazole were added to the crude product. The solution was stirred at 50° C for 30 minutes. After precipitation with water and subsequent washing the dried product was purified by column chromatography on Al_2O_3 (removal of starting material, eluent: toluene-acetone (1:1); elution of metalated porphyrins, eluent: acetone-MeOH (95:5). After reprecipitation from CH_2Cl_2 with hexane 30 mg of Ir-TPTBP-n-ButIm_2 (5) and byproducts (missing one or two of the axial ligands) were obtained.

^{1}H NMR (300 MHz, CDCl3), ppm: 8.31 (d; 8.1H), 8.2 (d; 8.3H), 7.87 (m; 12.5H), 7.13 (m; 9.1H), 7.0 (m; 8H) 4.72 (broad s; 1H), 3.86 (s; 0.3H benzyl adducts), 3.65 (s; 1.03H) 2.30 (t; 1.84H), 0.35 – 0.18 (m; 7.8H), -0.11 (m; 1.98H), -1.39 (broad s; 1.2H).

UV-Vis: ($CHCl_3$), λ/nm (relative intensity): 438 (1.00), 568 (0.12), 614 (0.8)

HRMS (LDI): m/z $[M]^+$ calc. 1253.458 , found 1253.448

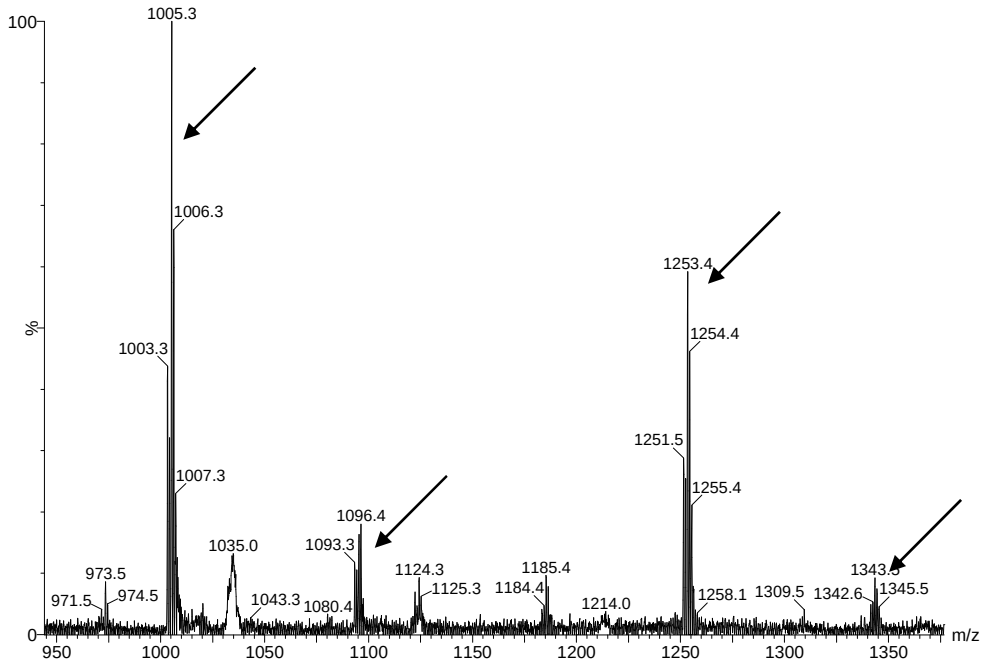

FIGURE S 14: LDI MASS SPECTRUM: IR-TPTBP WITHOUT FURTHER LIGANDS WAS EITHER CREATED DURING THE IONIZATION BUT MAY ALSO BE PRESENT INITIALLY. THE ADDITIONAL C7H6 IS DUE TO SIDE REACTIONS DURING THE PORPHYRIN SYNTHESIS [4]. THE IR(III)-PORPHYRIN WITH BOTH OF THE INTRODUCED LIGANDS (IR-TPTBP-N-BUTIM2) WAS ALSO FOUND.

FIGURE S 15: TOP: CALCULATED ISOTOPE PATTERN FOR $C_{74}H_{60}N_8IR$; BOTTOM: MEASURED ISOTOPE PATTERN FOR IR-TPTBP-N-BUTIM$_2$

Coupling of Ir-OEP-CarbIm2 to BSA

3.8 mg of EDC (dissolved in 250 µL of phosphate buffer pH 7.3 200 mM), 6 mg of NHS (dissolved in 250 µL of phosphate buffer pH 7.3 200 mM) and 4 mg of Ir-OEP-CarbIm$_2$ (dissolved in 1 mL of EtOH) were combined and mixed at room temperature for 15 minutes. Afterwards 12.4 mg of Bovine Serum Albumin (BSA) (dissolved in 1 mL of phosphate buffer pH 7.3 200 mM) were added. The reaction was carried out at room temperate under continuous stirring for 18 hours.

Protein was purified via size exclusion chromatography with an Amersham pharmacia biotech ÄKTA purifier 900.

Coupling of Ir-OEP-CarbIm2 to aminomodified silica gel particles

Aminomodified silica gel particles (ASP) were obtained as described in the literature[2]. 24 mg ASP (dispersed in 1 mL of phosphate buffer pH 7.3 200mM), 6 mg of EDC (dissolved in 1 mL of phosphate buffer pH 7.3 200 mM), 8 mg of NHS (dissolved in 1 mL of phosphate buffer pH 7.3 200mM) and 2 mg of Ir-OEP-CarbIm$_2$ (dissolved in 1 mL of EtOH) were combined and mixed for 4 hours at room temperature. As a control reaction (blank) the same reaction was carried out without EDC and NHS.

In both cases the particles were separated via centrifugation and washed three times with EtOH and three times with H_2O. While the coupling reaction yielded red colored particles, the control reaction produced virtually uncolored particles.

Preparation of sensor films

The „cocktails“ for coating were prepared by dissolving 1 mg of an indicator and 200 mg of polystyrene in 1800 mg of $CHCl_3$. The cocktails were knife-coated on Mylar support to give, after solvent evaporation, phosphorescent sensor films of ~2.5 µm thickness.

Sensor film containing indicator (4) coupled to silica gel was prepared as followed. 20 mg of the particles were dispersed in 50 mg silicon E4 (www.wacker.com) and 150 mg hexane. The

mixture was knife-coated on a glass slide and dried overnight. Finally the sensor film was dried in a vacuum drying chamber for 45 minutes.

References:

[1] R. Walter, S. Kirchner, R. Franz, U.S. Patent 6,399,804, 2002

[2] S. M. Borisov, P. Lehner, I. Klimant, Anal. Chim. Acta submitted

[3] H. Ogoshi, J. Setsune, Z. Yoshida, Journal of Organometallic Chemistry 1978, 159, 317-328.

[4] S. M. Borisov, I. Klimant, Dyes and Pigments 2009, 83, 312-316.

CONCEPT - BIO CONJUGATION FOR CELLULAR OXYGEN PROBES

As seen in the previous publication Ir(III) porphyrins can have several axial ligands including imidazole. Based on these results the next question was self-evident. *Could Ir(III) porphyrins be linked to biological material especially peptides via the structurally similar amino acid histidine?*. Due to the structural similarity between histidine and imidazole we were quite optimistic. Additionally, we already had a method on our hands that allowed us to react the unpolar Ir-OEP-CO-Cl with polar compounds (e.g. 1-imidazoleacetic acid).

In cooperation with Dmitri B. Papkovsky's lab from the University College Cork special peptide sequences were designed. As Dmitri B. Papkovsky and his team are experts in the field of intracellular oxygen measurements, the goal was to modify the Ir(III) porphyrins in a manner that would allow us to generate cell penetrating oxygen probes.

As oxygen is of such importance to all cellular functions, measuring the oxygenation of individual cells can be used to evaluate the bioenergetics status of the cells. Optical oxygen probes for cellular respiration had been pioneered by Wilson et al. [1]. After that a variety of methods were developed [2] and are currently used.

In contrast to many probes nowadays used Ir(III) porphyrins could enable straight-forward and direct coupling to the biomolecule by simply using an amino acid.

REFERENCES

[1] W.L. Rumsey, J.M. Vanderkooi, D.F. Wilson, Imaging of Phosphorescence: A Novel Method for Measuring Oxygen Distribution in Perfused Tissue, Science. 241 (1988) 1649–1651.

[2] R. Dmitriev, D. Papkovsky, Optical probes and techniques for O2 measurement in live cells and tissue, Cellular and Molecular Life Sciences. (2012) 1–15.

COMPLEXES OF IR(III)-OCTAETHYLPORPHYRIN WITH PEPTIDES AS PROBES FOR SENSING CELLULAR O_2

THIS CHAPTER WAS PUBLISHED AS FULL PAPER IN

CHEMBIOCHEM 2012 VOLUME 13, ISSUE 8, 1184–1190

DOI: 10.1002/CBIC.201200083

AUTHORS: KLAUS KOREN, RUSLAN I. DMITRIEV, SERGEY M. BORISOV, DMITRI B. PAPKOVSKY AND INGO KLIMANT

ABSTRACT

Ir(III)-porphyrins is a relatively new group of phosphorescent dyes which have potential for oxygen sensing and labeling of biomolecules. The requirement of two axial ligands for the Ir(III) ion permits simple linkage of biomolecules by one-step ligand exchange reaction, for example using precursor carbonyl chloride complexes and peptides containing histidine residue(s). Using this approach, we produced three complexes of Ir(III)-octaethylporphyrin with cell- penetrating (Ir1 and Ir2) and tumor-targeting (Ir3) peptides and studied their photophysical properties. All the complexes were stable and possessed bright, long-decay (unquenched lifetimes exceeding 45 μs) phosphorescence at around 650 nm, and moderate sensitivity to oxygen. The Ir1 and Ir2 complexes showed positive staining of a number of mammalian cell types, demonstrating localization similar to endoplasmic reticulum and ATP-and temperature independent intracellular accumulation (direct translocation mechanism). Their low photo- and cytotoxicity allows probing of intracellular oxygen.

INTRODUCTION

Molecular oxygen (O_2) is one of the key metabolites and functional parameters of live cells and tissues reflecting their respiration activity, mitochondrial function and oxygenation state [1, 2]. Numerous methods for direct and indirect assessment of O_2 in the cell and tissue were proposed, which include Clark (micro)electrodes [3, 4], electron paramagnetic resonance (EPR) [5, 6], optical

sensing [4, 7, 8] and special 'hypoxia' probes (HIF constructs, nitroimidazoles, etc) [9]. In recent years, new methods for minimally invasive sensing of intracellular O_2 (icO2) were introduced which use nitroxyl and esterified trityl (triarylmethyl) radicals [5, 6, 10, 11], O_2-sensitive genetically encoded GFP constructs [12], endogenous mitochondrial protoporphyrin IX [13, 14], BTP, Ru-polypirydyl, Pt- and Pd-porphyrin probes based on cell-penetrating peptide(s) or nanoparticles [15-27].

Planar Pt(II) and Pd(II)-complexes of porphyrin dyes exhibit strong phosphorescence at room temperature which is readily quenched by O_2 [28]. Characteristic spectral properties of such compounds allow their use in different O_2 sensing materials and detection modalities, including as time-resolved fluorescence/phosphorescence [29], phosphorescence quenching microscopy/ FLIM [30-32] or ratiometric detection[22, 33]. With the development of cell targeting vectors [34-36] and nanoparticle technology [37, 38], intracellular delivery of such sensors became possible. Thus, PtCP conjugates with oligoarginine or bactenecin 7 peptides, PtTFPP and PtOEP dyes embedded in positively charged nanoparticles, with or without additional cell-penetrating coating were found useful for biological and physiological studies[17-21, 24]. At the same time, mechanisms of their transport into the cell and control of intracellular localization and fate remain poorly understood and require further investigation of structure-activity relationships.

Ir(III)-porphyrins represent a relatively new group of phosphorescent dyes [39] which so far have not been explored in details. The six coordination geometry of Ir(III) central atom makes these dyes attractive for synthesis of new supramolecular structures. The tetrapyrrole macrocycle occupies four coordination sites, while the remaining two axial sites can be used to introduce nitrogen-containing heterocycles such as pyridine and imidazole [39]. This can be used to design new indicator dyes and supramolecular structures with attractive features and spectral properties similar to those of Pt-porphyrins.

In this study we further develop this synthetic approach, by attaching to the Ir-octaethylporphyrin (Ir-OEP) short peptide sequences via histidine residues (structural analogs of imidazoles). These complexes are characterized spectroscopically and tested on a number of different cell lines, with the aim of producing new phosphorescent probes with cell permeating and/or binding capabilities.

SYNTHESIS OF THE CONJUGATES

Previously, several complexes with nitrogen containing heterocycles were prepared, using Ir-OEP-CO-Cl precursor dye and simple ligand exchange reactions (Fig. 1) in 2-ethoxyethanol, which at elevated temperature dissolves both the hydrophobic dye and polar ligands (e.g. carboxyimidazole) [39]. A similar strategy was applied to couple the Ir-OEP-CO-Cl with short peptide sequences via their histidine residues. This method also allows for synthesis of mono- and hetero-substituted Ir(III)-porphyrins, however in present study we mainly focused on symmetric di-substituted Ir-OEP derivatives.

TABLE 1. PHOTOPHYSICAL PROPERTIES FOR THE SYNTHESIZED CONJUGATES.

Conjugate	Mw / g/mol	Charge	λmax Abs / nm	λmax Em / nm	Q.Y.	τ_0 / μs
Ir1	2282.8	+9	386; 506; 540	654	0.13[a]; 0.16[b]	58
Ir2	2154.7	+3	388; 508; 539	652	0.08[a]; 010[b]	69
Ir3	1804.1	+1	386; 507; 540	654	0.13[a]; 0.15[b]	47

a in PBS; b in PBS with 10%FBS

Based on our recent studies with peptide conjugates of coproporphyrin dyes (PtCP, PdCP, CPK) [17, 18], we decided to prepare Ir-OEP complexes with two peptide structures which are expected to provide cell-penetrating ability for the resulting complexes: i) histidine-tetraarginine, HR_4 (Ir1), and ii) truncated fragment of cell-penetrating bactenecin 7 peptide, PRPLP (Ir2). In addition, a complex containing RGD sequence (known for its ability to bind to tumor cell membranes [40]) was prepared (Ir3). Structures of these complexes are presented in Fig. 1. Notably, all the peptides were amidated at the C-terminus in order to retain the positive charge of the complexes and they were soluble in 2-ethoxyethanol.

The ligand exchange reaction performed at elevated temperature produced a characteristic hypsochromic shift in the porphyrin absorption spectrum [39], which indicated formation of the complexes, the latter were then purified by RP-HPLC. Confirmation of purity and molecular structure of the complexes by ^{1}H NMR, HPLC and MS can be found in Supporting Information (Figs. S1, S2). After purification the conjugates were stored in DMSO or water in the dark at 4 °C,

being stable for several months. Conversely, when a peptide without histidine residue (R_4) was used, no changes in absorption of Ir-OEP-CO-Cl and no complex formation were seen, even after prolonged 48 h incubation (results not shown).

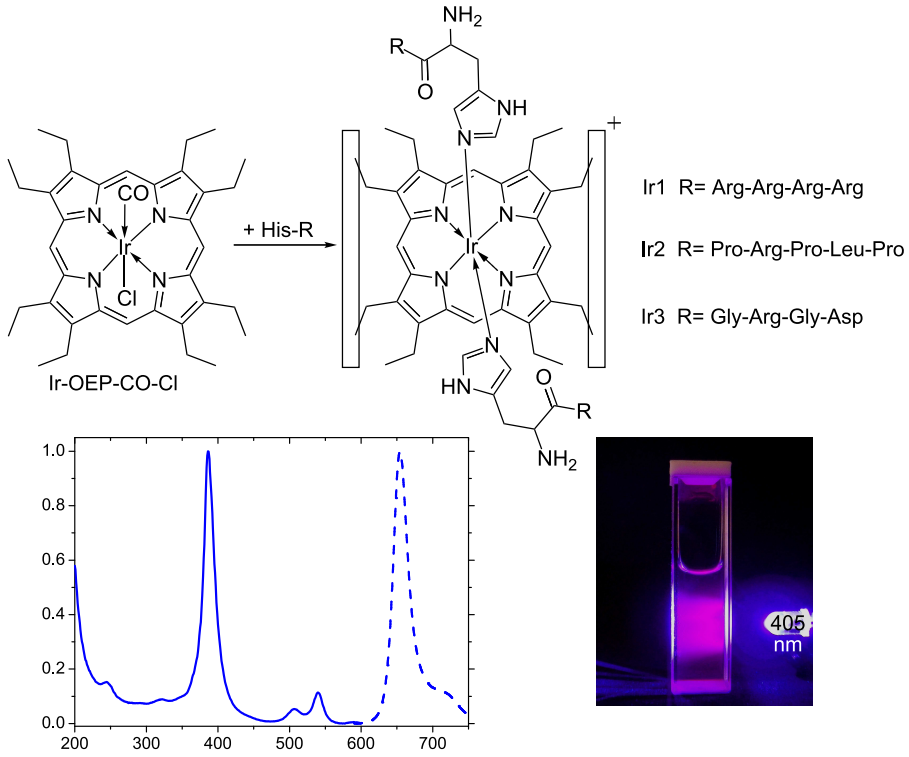

FIG. 1. STRUCTURES AND ELECTRONIC SPECTRA OF THE NEW IR-OEP COMPLEXES. STARTING FROM IR-OEP-CO-CL, THE COMPLEXES WERE OBTAINED BY THE REACTION WITH HISTIDINE CONTAINING PEPTIDES (TOP PANEL). ABSORPTION AND EMISSION SPECTRA OF IR1AND A PHOTOGRAPHIC IMAGE OF THE BRIGHT RED EMISSION IN DEOXYGENATED SOLUTION UNDER 405 NM LED EXCITATION.

SPECTRAL PROPERTIES AND O_2 SENSITIVITY OF CONJUGATES

Absorption and emission spectra of the three peptide conjugates were found to be similar (Figure 1). High resemblance with Pt-porphyrins can be seen [18], with the Soret band at around 386 nm and Q-bands at 506 and 540 nm, and peptide absorption in the UV region. The conjugates were readily soluble in aqueous solutions; their phosphorescence was not affected by the common media, serum and additives used in cell culture (Table 1) and quantum yields in deoxygenated solutions ranged from 8 to 16%. Red, long-decay emission of these complexes

allows their sensitive detection by time-resolved fluorometry (Fig. S3). Thus, on a standard microplate TR-F reader Victor2 the conjugate Ir1 was detectable down to 1 nM concentration in both deoxygenated and as oxygenated solutions (Fig. S4). Quenched lifetimes for the complexes in air-saturated solutions were at the lower end of instrument time resolution (limited by Xe-flash lamp having pulse duration of about >10 microseconds). However, reliable sensing of O_2 on such instruments using rapid lifetime determination (RLD) method [41] was still possible over the O_2 range 0-250 μM (0-21% atmospheric O_2) (Fig. S3B). Interestingly, Ir2 showed the longest decay time (69 μs), but the lowest quantum yield.

Stability of Ir1 was assessed by exposing it to competing ligand in aqueous solution. When Ir1 was incubated in PBS with 10-fold molar excess of free histidine for 24 h at 37 °C, no changes on HPLC chromatogram (no additional peaks) were seen (not shown). This data prove that under physiological conditions dissociation or substitution of the peptide ligands in such complexes is insignificant.

CELL STAINING PROPERTIES OF THE IR CONJUGATES

Cell penetrating ability of Ir1 and Ir2 probes was tested using MEF cells as a model. At concentrations 1-10 μM and incubation times 6-16 h both probes demonstrated efficient staining of the cells, accumulating in perinuclear regions and partially co-localizing with the marker of endoplasmic reticulum, ER Tracker Green (Fig. 2). Such intracellular localization differs from that of the similar peptides conjugated to PtCP dye via its peripheral propionic acid residues [17-19]. Notably, Ir2 demonstrated small degree of aggregation on the cell surface.

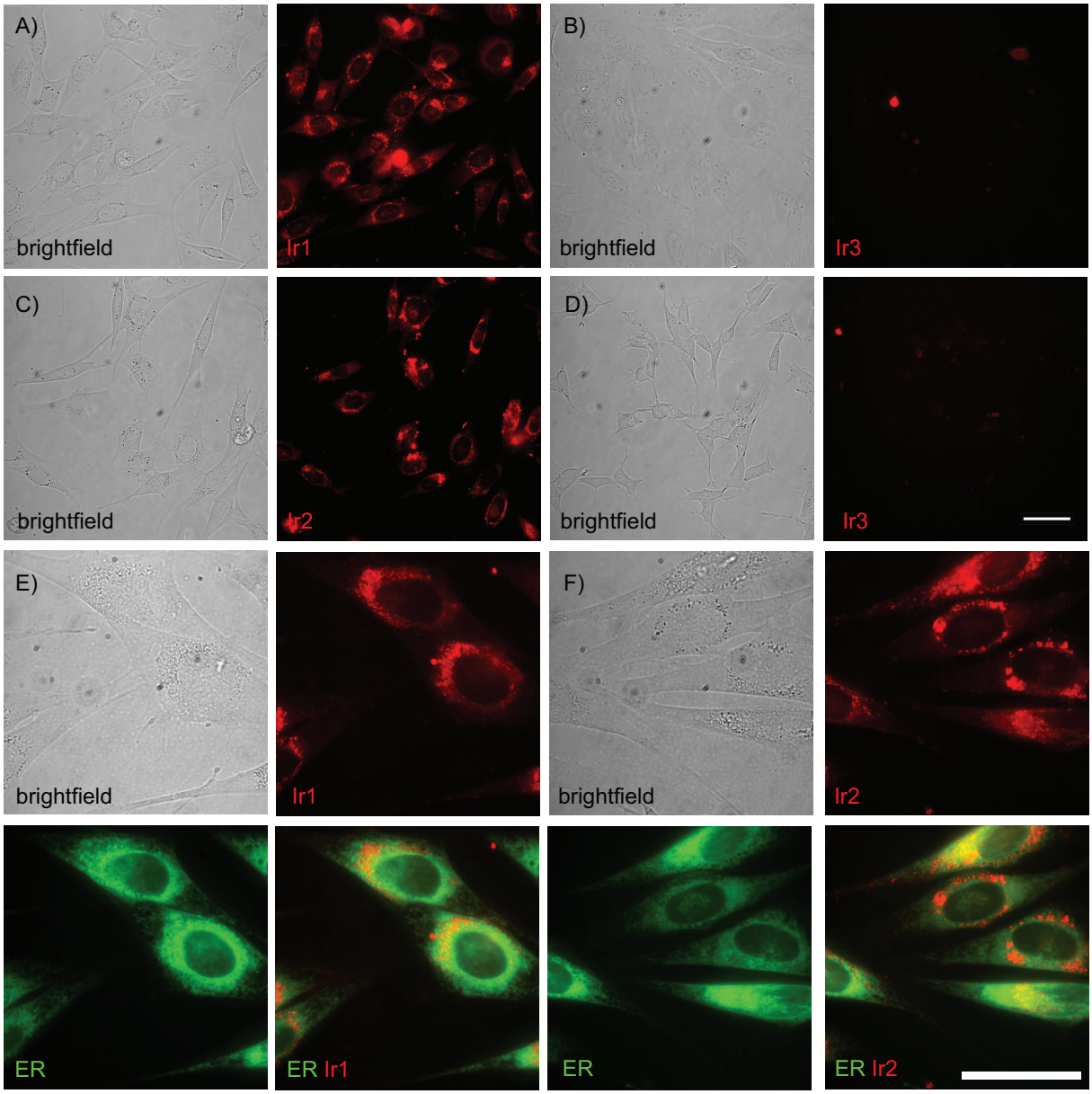

FIG. 2. STAINING OF CELLS WITH IR1, IR2 AND IR3 PROBES. A, C, E, F REPRESENT BRIGHTFIELD AND FLUORESCENT IMAGES OF MEF, B – HELA AND D – SH-SY5Y CELLS. IR-OEP PHOSPHORESCENCE (RED) WAS RECORDED USING 390NM EXCITATION AND 650NM EMISSION FILTER SET, AND ER TRACKER GREEN FLUORESCENCE (GREEN) - USING 490NM EXCITATION AND 530NM EMISSION FILTERS. SCALE BARS CORRESPOND TO 50 μM.

Conjugates Ir1 and Ir2 were further tested with COS-7, HeLa, SH-SY5Y, PC12 cell lines and with mixed cultures of primary neurons and astrocytes. For all these cells positive cytoplasmic staining was observed (Fig. S5). Such cell-specificity of Ir1 and Ir2 probes is significantly better than for the other O_2 probes, for which staining of SH-SY5Y and primary neuronal cells was low

(RID, unpublished data). This also suggests that Ir1 and Ir2 employ different mechanisms of endocytosis or, perhaps, direct translocation through plasma membrane (temperature and ATP-independent [35, 42-44]).

To evaluate the cell entry mechanism as possible direct translocation, additional experiments were carried out. First, monitoring of kinetics of intracellular accumulation demonstrated that probe internalization was completed in about 3-6 h (see Ir1 data in Fig. 3). This makes possible analysis of cell loading at low temperature or upon ATP depletion. ATP depletion was induced by removing glucose from the medium and adding oligomycin (thus blocking both glycolysis and oxidative phosphorylation [2]). Under these conditions we still saw efficient cell staining with Ir1 and Ir2, although cell appearance changed significantly (Fig. S6). At low temperature (4 instead of 37 ^{o}C) when endocytosis in slowed down [45] we also observed faint intracellular staining with Ir1 and Ir2 (Fig. S6). Based on these results and considering that probe diffusion is also decreased at low temperature, we concluded that Ir1 and Ir2 utilize direct translocation mechanism. Endocytosis-dependent cellular uptake is common reported mechanism for oligoarginine and Pro-rich peptide structures [44, 46-48]. In this case internalized conjugate must undergo endosomal escape to reach the cytoplasm or other cellular organelles [49]. We investigated cell loading in the presence of concanamycin A, an inhibitor of V-ATPase and lysosomal function, and observed a minor effect on Ir1 localization and more profound on Ir2 (Fig. S6). This data indicate that, even if these probes use endocytosis mechanism of cell entry, their escape from the endosomes is insignificant.

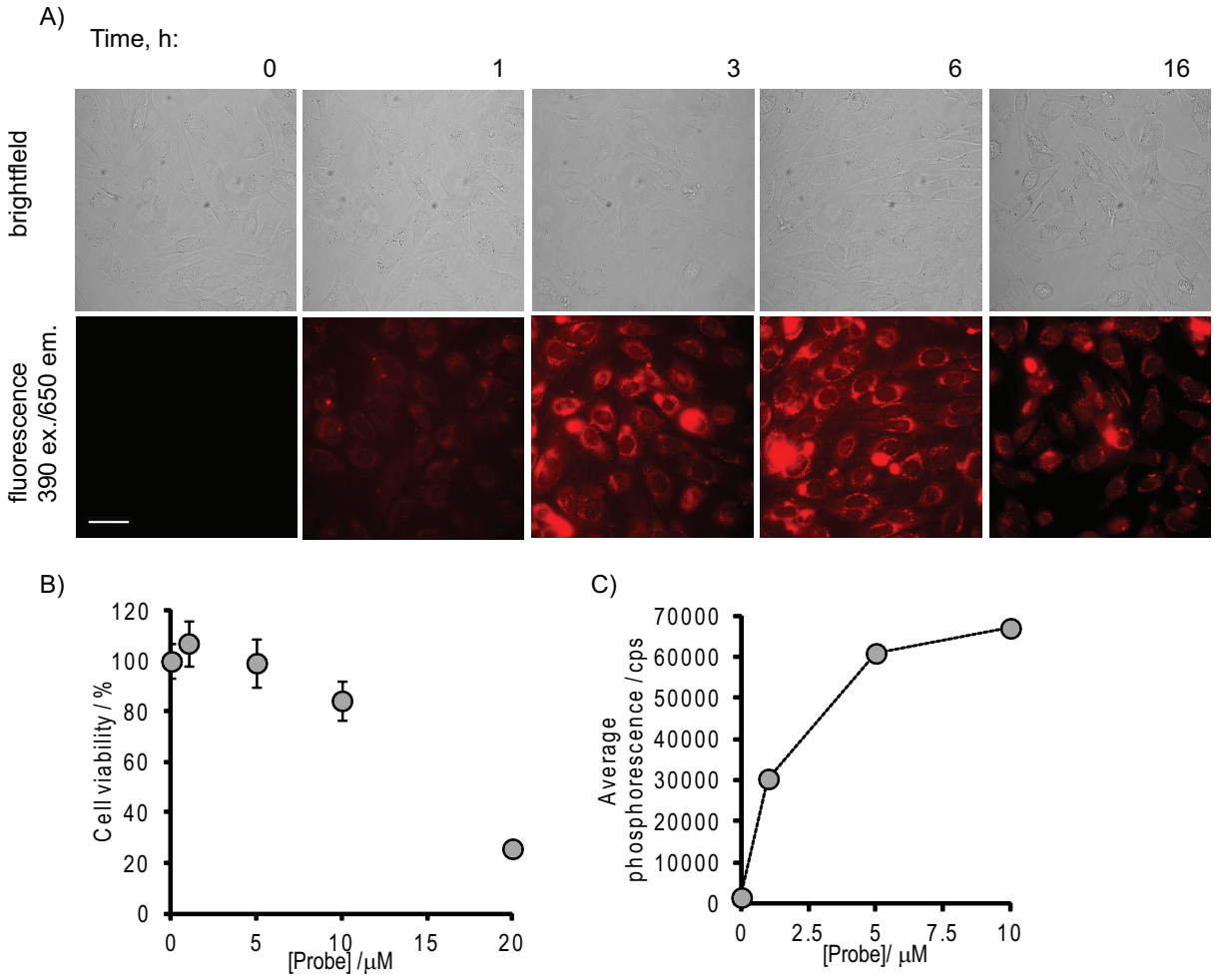

FIG. 3. TIME AND CONCENTRATION-DEPENDENCE OF CELL STAINING AND CHANGES IN CELL VIABILITY FOR IR1 COMPLEX WITH MEF CELLS. A: CELLS WERE INCUBATED WITH THE COMPLEX (10 μM) FOR INDICATED TIME, WASHED AND ANALYZED BY MICROSCOPY (BRIGHTFIELD AND FLUORESCENT IMAGES). SCALE BAR 50 μM. B: CHANGES IN VIABILITY (TOTAL CELLULAR ATP) MEASURED AFTER EXPOSING THE CELLS TO 0 – 20 μM OF IR1 FOR 16 H. C: AVERAGE PHOSPHORESCENCE INTENSITY SIGNALS FROM THE CELLS STAINED WITH 0-10 μM OF IR1.

The Ir3 probe which contains tumor cell targeting vector (RGD peptide) was tested for interaction with two cancer cell lines, HeLa and SH-SY5Y. After 1 h incubation with 5 μM of Ir3, we observed no detectable staining of the cells (Fig. 2). This lack of binding functionality of the RGD sequences attached to the Ir-OEP moiety can be due to a number of factors, including sterical factors, positive charge on the adjacent Ir(III) ion or hydrophobicity of the porphyrin core. On the other hand, the absence of cell staining by Ir3 confirms the essential role of cell-penetrating peptide moieties in intracellular delivery of the Ir1 and Ir2 probes.

Efficient uptake of Ir1 and Ir2 by the cells allows their use for sensing of intracellular O_2 (icO_2). Photostability of these IrOEP based probes is moderate and similar to PtCP conjugates. Unlike the highly photostable PtPFPP based probes [20], they are not very suitable for luminescence microscopy and FLIM applications but look promising for icO_2 sensing experiments in RLD mode performed on TR-F readers similarly to other O_2 probes [17, 19, 50, 51].

We first tested the Ir1 probe for possible toxic effects on MEF cells after 16 h of loading, and found that at 20 μM its toxicity was high, but at 10 μM and below it was minimal (Fig. 3B). Fig. 3C shows that 5-10 μM probe concentrations produce high phosphorescent signals with cells (50,000-60,000 cps at delay time 30 μs). Then Ir1 probe was calibrated with non-respiring MEF cells (at 10 μM staining concentration) at dissolved O_2 ranging 0-200 μM (Fig. 4C). The calibration data points (lifetimes ranging from ~ 18 μs to 40 μs) were fitted with the following analytical function (R^2 0.9865):

$$[O_2] = 60018.16*\exp(-\tau/3.01643), \qquad (1)$$

where O_2 is expressed in μM and τ in μs. The Stern-Volmer plots showing clear non-linearity (Fig. 4B) were fitted with the 2-site-model (see [52] and equation 2), from which model parameters were determined as follows: F = 0.6; K_{SV1} = 0.074; K_{SV2} = 0.00027 ($r^2 > 0.999$). Generally, K_{SV2} is significantly smaller than K_{SV1} ($K_{SV1} > K_{SV2}*100$) indicating that one fraction of the probe is easier accessible by oxygen than the other. For biological samples such a behavior is not unusual [8, 53].

$$\frac{\tau}{\tau_0} = \frac{F}{1+K_{SV1}*pO_2} + \frac{1-F}{1+K_{SV2}*pO_2} \qquad (2)$$

Using the calibration Eqn. 1, relative deoxygenation of cells at different levels of external (atmospheric) hypoxia was calculated (Fig. 4C). One can see, that when dissolved O_2 is ≤50 μM the cells are almost completely (>90%) deoxygenated. Compared to the data obtained by Fercher et al with PtPFPP-RL100 probe (undefined intracellular location) [20], our data show lower cell deoxygenation at similar concentrations of dissolved O_2. This may be explained by different character of intracellular localization of the Ir1 and PtPFPP-RL100 probes (i.e. PtPFPP

is located closer to mitochondria) and possible existence of intracellular O_2 gradient or, by lower respiration activity in MEF cells, stained with Ir1 conjugate. Indeed, with moderate toxicity at 10 μM concentration, the activity of oxidative phosphorylation may be compromised.

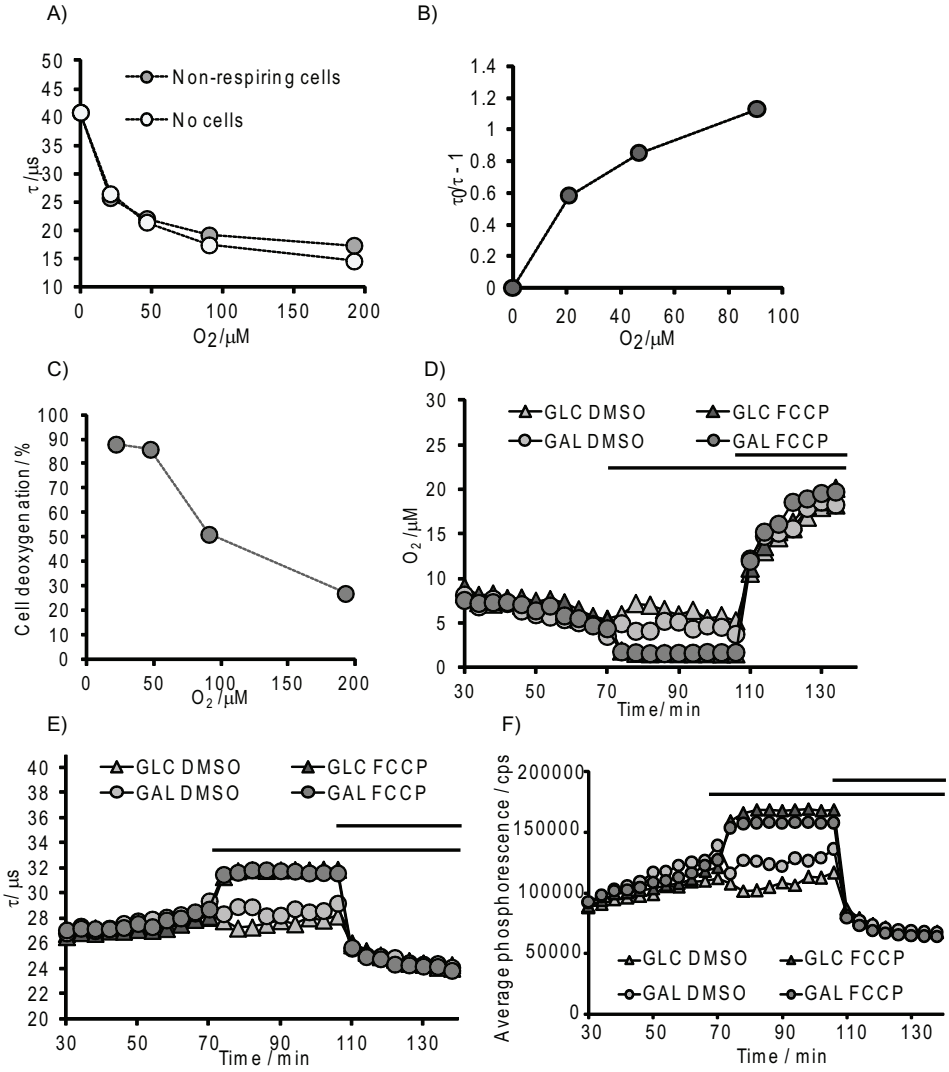

FIG. 4. SENSING OF ICO_2 IN MEF CELLS WITH IR1 PROBE. A: PHOSPHORESCENCE LIFETIME (τ) CALIBRATIONS IN NON-RESPIRING MEF CELLS (PROBE IN SOLUTION WITHOUT CELLS IS ALSO SHOWN; 21% O_2 CORRESPOND TO 200 μM OF DISSOLVED O_2). B: STERN-VOLMER PLOT FOR IR1 WITH NON-RESPIRING MEF CELLS. C: RELATIVE DEOXYGENATION OF THE RESPIRING CELLS IN SAMPLES EXPOSED TO VARIOUS LEVELS OF EXTERNAL PO_2. D: PROFILES OF ICO_2 IN MEF CELLS STAINED WITH IR1 AT REST AND UPON METABOLIC STIMULATION. E, F: RAW PHOSPHORESCENCE LIFETIME (τ) AND INTENSITY RESPIRATION PROFILES OF D. THE LONG BAR SHOWS THE FIRST TREATMENT WITH FCCP OR DMSO, THE SHORT BAR – SECOND TREATMENT WITH ANTA.

We also monitored O_2 in MEF cells loaded with 5 μM of Ir1 in glucose(-)/galactose(+) medium exposed to hypoxic conditions (8% ambient O_2) and stimulated with 2 μM FCCP (uncoupler) and 10 μM AntA (ETC inhibitor) (Fig. 4D). In this case, basal O_2 in resting cells of about 8-5 μM was reduced to ~ 0.5 μM upon FCCP stimulation and then upon AntA treatment increased to 20 μM (reoxygenation due to stopped respiration). The addition of DMSO (carrier) produced practically no response. Raw oxygenation profiles (in phosphorescence lifetime and intensity scales) corresponding to cellular respiration are shown in Fig. 4E,F.

CONCLUSION

Overall, this study demonstrated that stable 1:2 complexes of Ir-porphyrins with peptides bearing histidine residues can be prepared by the simple and flexible ligand exchange procedure. With the examples of two cell-penetrating and one tumor-targeting peptides, we showed the flexibility of this methodology, which can be extended to other biologically relevant structures. The resulting complexes displayed good solubility in aqueous media, showing bright phosphorescence and unquenched lifetimes of above 40 μs. The Ir1 and Ir2 probes showed cell-penetration ability which involves direct translocation mechanism, broad cell specificity and efficient staining of different cell lines. Their intracellular distribution was close to endoplasmic reticulum. Such probes represent useful tools for O_2 sensing and particularly for real-time monitoring of icO_2 which can be realized on existing commercial TR-F readers or, with additional modifications, in ratiometric intensity-based detection formats.

EXPERIMENTAL SECTION

MATERIALS

Luminescent cell viability kit CellTiter-Glo was from Promega (Madison, WI, USA), fluorescent probe ER Tracker Green was from from Invitrogen (Bio Sciences, Dun Laoghaire, Ireland). Standard cell culture 96 well and white (for CellTiter Glo Kit) 96 well plates from Greiner Bio-One (Frickenhausen, Germany). Glass-bottom mutliwell inserts were from Ibidi (Martinsried, Germany). All the other reagents were from Sigma-Aldrich Ltd. (Dublin, Ireland). The peptides

with C-terminal amidation and confirmed structure (MS) and purity (HPLC) were from GenScript (Piscataway, NJ, USA).

SYNTHESIS AND CHARACTERIZATION OF CONJUGATES IR1, IR2 AND IR3

To a screw-cap glass vial, Ir-OEP-CO-Cl (2-3 μmol; produced as described in [39, 54]) and the peptide (4-5 equivalents) were added, dissolved in 2-ethoxyethanol (2 ml) by incubation at 75 °C for 1 h, and then left to react overnight at 60 °C. After the absorption band of Ir-OEP-CO-Cl at 550 nm was no longer visible, the reaction was stopped and solvent removed. Then water (2 ml) was added to dry red residue, sonicated for 15 min followed by removal of the insoluble fraction by centrifugation. The water-soluble fraction was purified by HPLC (Agilent 1100 Series) on a semi-preparative column VP 250/10 Nucleodur 100-5 RP-C18 using 0.1% aqueous acetic acid – methanol gradient. Typical product yield after purification was 30% ±5%. ^{1}H-NMR spectra were recorded in D_2O on a 300 MHz spectrometer from Brucker. Mass spectrometric analysis was carried out on a triple quadrupole API 2000 mass spectrometer (Applied Biosystems/Sciex, Concord, Canada) equipped with a positive electrospray ionization (ESI) interface under full-scan (200-1800 amu) mode.

PHOTOPHYSICS AND PHOSPHORESCENCE LIFETIME MEASUREMENTS

Absorption spectra were recorded on an 8453 UV/Vis diode-array spectrophotometer (Agilent), and luminescence spectra on a LS50B spectrometer (PerkinElmer). Absolute quantum yields of emission were measured on a Horiba FluoroLog3 (www.horiba.com) equipped with a Quanta-phi integrating sphere. Quantum yields in PBS, PBS containing 10% of foetal bovine serum were measured in oxygen free conditions as described in [17].

Phosphorescence lifetimes were assessed on a Cary Eclipse fluorescence spectrometer (Varian-Agilent) using 380 nm excitation, 650 emission and 30 μs delay time. For rapid lifetime determination on Victor2 reader (PerkinElmer), 'time-resolved fluorescence' mode was used, with D340 excitation and D642 emission filters, counting at two delay times 30 μs (t_1) and 40 μs (t_2) with gate time 100 μs and total counting cycle 1 s). Phosphorescence lifetime (τ) was calculated according to the equation: $\tau = (t_2-t_1)/\ln(F_1/F_2)$ where F_1 and F_2 correspond to TR-F readings at delay times t_1 and t_2.

CELL CULTURE

Mouse embryonic fibroblasts (MEFs), african green monkey kidney (COS-7), human epithelial carcinoma (HeLa), human neuroblastoma (SH-SY5Y) and rat pheochromocytoma (PC12) cells from ATCC (Manassas, VA, USA) were cultured as described previously, using DMEM supplemented with 10%FBS (for MEF, COS-7, HeLa and SH-SY5Y cells) or RPMI1640 supplemented with horse serum and FBS (for PC12 cells) media and collagen-poly-D-lysine coated glass bottom minidishes (for microscopy analysis) or collagen IV-coated 96-well plates (for plate reader measurements). Primary neurons from rat brain were kindly provided by Dr. Y. Nolan (Anatomy Department, UCC). Cell viability was assessed by measuring total cellular ATP with a CellTiter-Glo luminescent kit (Promega), according to manufacturer's recommendations.

Live cell microscopy was performed on a fluorescent microscope Axiovert 200 (Carl Zeiss, Goettingen, Germany) equipped with an LED excitation module (LaVision GmbH, Goettingen, Germany). An UV LED (390 nm) and PtCP filter cube (ex. 390/40 nm, em. 655/40 nm) were used for imaging the Ir-porphyrins. Cells were incubated with Ir1 and Ir2, typically for 6-16 h, then washed three times, counter-stained with ER Tracker Green (1 μM, 30 min), washed again and imaged. For ATP depletion experiments, cells were incubated for 1.5 h in glucose-free DMEM, supplemented with 10% FBS, 10 mM galactose, 1 mM sodium pyruvate, 20 mM HEPES, pH 7.2, then with oligomycin (10 μM) for 0.5 h, followed by staining with Ir1 and Ir2 (10 μM concentration) for 6 h in this medium and fluorescence microscopy imaging.

Phosphorescence lifetime measurements were conducted on Victor2 plate reader as described above. For probe calibration and monitoring of oxygenation under graded hypoxia, cells stained with Ir1 (10 μM, 16 h) were exposed to different levels of atmospheric O_2 in a glove box (Coy scientific), with 60 min pre-incubation and 30-60 min of measurement at each O_2 concentration in presence of Antimycin A (10 μM). To achieve 0% O_2, a solution containing glucose (100 mM) and glucose oxidase (50 μg/ml, Sigma G7141) was added to the cells (1/10 of the volume) exposed to 1-2% O_2. For stimulation experiments, 10x stock solutions of effectors were added during the measurement to produce the indicated final concentrations. Relative cell oxygenation was calculated as described before[55] using phosphorescence lifetime data obtained with respiring and non-respiring (Antimycin A-treated) cells under the same ambient O_2 concentrations.

DATA ASSESSMENT

The results of plate reader experiments were processed in Microsoft Excel and Origin 6.0 for fitting the calibration. The data represent average values with standard deviations as error bars. To ensure consistency, all experiments were performed in triplicate.

ACKNOWLEDGEMENTS

This work was supported by the Science Foundation Ireland, grant 07/IN.1/B1804 and the Austrian Science Fund (FWF; Research Project No. P21192-N17). Authors thank Dr. Y. Nolan and I. O'Brien (Anatomy department, UCC) for the help with isolation of rat primary neurons, and Prof. X. Guo, T. Burger, J. Rentner and S. Gamper from TU Graz for technical assistance.

REFERENCES

[1] T. Sanden, G. Persson, P. Thyberg, H. Blom, J. Widengren Anal. Chem. ***2007****, 79, 3330-3341.*

[2] M. D. Brand, D. G. Nicholls Biochem. J. ***2011****, 435, 297-312.*

[3] C.-C. Wu, H.-N. Luk, Y.-T. T. Lin, C.-Y. Yuan Talanta. ***2010****, 81, 228-234.*

[4] K. A. Foster, F. Galeffi, F. J. Gerich, D. A. Turner, M. Müller Prog. Neurobiol. ***2006****, 79, 136-171.*

[5] Y. Liu, F. A. Villamena, J. Sun, T.-y. Wang, J. L. Zweier Free Rad. Biol. Med. ***2009****, 46, 876-883.*

[6] A. A. Bobko, I. Dhimitruka, T. D. Eubank, C. B. Marsh, J. L. Zweier, V. V. Khramtsov Free Rad. Biol. Med. ***2009****, 47, 654-658.*

[7] X.-d. Wang, H.-x. Chen, Y. Zhao, X. Chen, X.-r. Wang Trends Anal.Chem. ***2010****, 29, 319-338.*

[8] D. B. Papkovsky Methods Enzymol. ***2004****, 381, 715-735.*

[9] A. Carreau, B. El Hafny-Rahbi, A. Matejuk, C. Grillon, C. Kieda J. cell. mol. med. ***2011****, 15, 1239-1253.*

[10] E. Takahashi, D. F. Bruley, B. B. Williams, N. Khan, B. Zaki, A. Hartford, M. S. Ernstoff, H. M. Swartz in Clinical Electron Paramagnetic Resonance (EPR) Oximetry Using India Ink, Vol. 662, Springer US, ***2010****, pp.149-156.*

[11] S. Higaki, H. Fujii, M. Nagano, S. Katagiri, Y. Takahashi Biomed. Res. ***2010****, 31, 165-168.*

[12] E. Takahashi, T. Takano, Y. Nomura, S. Okano, O. Nakajima, M. Sato Am. J. Physiol. Cell Physiol. ***2006****, 291, C781-C787.*

[13] E. G. Mik, C. Ince, O. Eerbeek, A. Heinen, J. Stap, B. Hooibrink, C. A. Schumacher, G. M. Balestra, T. Johannes, J. F. Beek, A. F. Nieuwenhuis, P. van Horssen, J. A. Spaan, C. J. Zuurbier J. mol. cell. cardiol. ***2009****, 46, 943-951.*

[14] E. G. Mik, J. Stap, M. Sinaasappel, J. F. Beek, J. A. Aten, T. G. van Leeuwen, C. Ince Nat. Meth. ***2006****, 3, 939-945.*

[15] U. Neugebauer, Y. Pellegrin, M. Devocelle, R. J. Forster, W. Signac, N. Moran, T. E. Keyes Chem. Comm. ***2008****, 5307-5309.*

[16] Y. E. Koo, Y. Cao, R. Kopelman, S. M. Koo, M. Brasuel, M. A. Philbert Anal. Chem. ***2004****, 76, 2498-2505.*

[17] R. I. Dmitriev, H. Ropiak, G. Ponomarev, D. V. Yashunsky, D. B. Papkovsky Bioconjug. chem. ***2011****, 22, 2507-2518.*

[18] R. I. Dmitriev, H. M. Ropiak, D. V. Yashunsky, G. V. Ponomarev, A. V. Zhdanov, D. B. Papkovsky FEBS J. ***2010****, 277, 4651-4661.*

[19] R. I. Dmitriev, A. V. Zhdanov, G. V. Ponomarev, D. V. Yashunski, D. B. Papkovsky Anal. Biochem. ***2010****, 398, 24-33.*

[20] A. Fercher, S. M. Borisov, A. V. Zhdanov, I. Klimant, D. B. Papkovsky A.C.S. Nano. ***2011****, 5, 5499-5508.*

[21] C. Wu, B. Bull, K. Christensen, J. McNeill Angew. Chem. Int. Ed. ***2009****, 48, 2741-2745.*

[22] X.-d. Wang, H. H. Gorris, J. A. Stolwijk, R. J. Meier, D. B. M. Groegel, J. Wegener, O. S. Wolfbeis Chem. Sci. ***2011****, 2, 901-906.*

[23] M. P. Coogan, J. B. Court, V. L. Gray, A. J. Hayes, S. H. Lloyd, C. O. Millet, S. J. A. Pope, D. Lloyd Photochem. Photobiol. Sci. ***2010****, 9, 103-109.*

[24] Y.-E. Koo Lee, E. E. Ulbrich, G. Kim, H. Hah, C. Strollo, W. Fan, R. Gurjar, S. Koo, R. Kopelman Anal. Chem. ***2010****, 82, 8446-8455.*

[25] R. I. Dmitriev, D. B. Papkovsky Cell. Mol. Life Sci. ***2012****. DOI: 10.1007/s00018-011-0914-0*

[26] T. Yoshihara, Y. Yamaguchi, M. Hosaka, T. Takeuchi, S. Tobita Angew. Chem. Int. Ed. ***2011*** *DOI: 10.1002/anie.201107557*

[27] S. Zhang, M. Hosaka, T. Yoshihara, K. Negishi, Y. Iida, S. Tobita, T. Takeuchi Cancer Res. ***2010****, 70, 4490-4498.*

[28] D. B. Papkovsky, T. C. O'Riordan J. Fluoresc. ***2005****, 15, 569-584.*

[29] T. C. O'Riordan, A. V. Zhdanov, G. V. Ponomarev, D. B. Papkovsky Anal. Chem. ***2007****, 79, 9414-9419.*

[30] A. Fercher, T. C. O'Riordan, A. V. Zhdanov, R. I. Dmitriev, D. B. Papkovsky Methods Mol. Biol. ***2010****, 591, 257-273.*

[31] R. N. Pittman, A. S. Golub, H. Carvalho in Measurement of Oxygen in the Microcirculation Using Phosphorescence Quenching Microscopy

Oxygen Transport to Tissue XXXI, Vol. 662 (Eds.: E. Takahashi, D. F. Bruley), Springer US, ***2010****, pp.157-162.*

[32] S. Sakadzic, E. Roussakis, M. A. Yaseen, E. T. Mandeville, V. J. Srinivasan, K. Arai, S. Ruvinskaya, A. Devor, E. H. Lo, S. A. Vinogradov, D. A. Boas Nat. Meth. ***2010****, 7, 755-759.*

[33] K. Kellner, G. Liebsch, I. Klimant, O. S. Wolfbeis, T. Blunk, M. B. Schulz, A. Göpferich Biotechnol. Bioeng. ***2002****, 80, 73-83.*

[34] S. R. Schwarze, A. Ho, A. Vocero-Akbani, S. F. Dowdy Science. ***1999****, 285, 1569-1572.*

[35] S. Futaki, I. Nakase, A. Tadokoro, T. Takeuchi, A. T. Jones Biochem. Soc. Trans. ***2007****, 35, 784-787.*

[36] B. Gupta, T. S. Levchenko, V. P. Torchilin Adv. Drug Deliv. Rev. ***2005****, 57, 637-651.*

[37] Y.-E. Koo Lee, R. Smith, R. Kopelman Ann. Rev. Anal. Chem. ***2009****, 2, 57-76.*

[38] S. M. Borisov, T. Mayr, G. Mistlberger, K. Waich, K. Koren, P. Chojnacki, I. Klimant Talanta. ***2009****, 79, 1322-1330.*

[39] K. Koren, S. M. Borisov, R. Saf, I. Klimant Eur. J. Inorg. Chem. ***2011****, 2011, 1531-1534.*

[40] C. L. Conway, I. Walker, A. Bell, D. J. H. Roberts, S. B. Brown, D. I. Vernon Photochem. Photobiol. Sci. ***2008****, 7, 290-298.*

[41] K. K. Sharman, A. Periasamy, H. Ashworth, J. N. Demas Anal. Chem. ***1999****, 71, 947-952.*

[42] I. Nakase, T. Takeuchi, G. Tanaka, S. Futaki Adv. Drug Deliv. Rev. ***2008****, 60, 598-607.*

[43] G. Ter-Avetisyan, G. Tunnemann, D. Nowak, M. Nitschke, A. Herrmann, M. Drab, M. C. Cardoso J. Biol. Chem. ***2009****, 284, 3370-3378.*

[44] F. Duchardt, M. Fotin-Mleczek, H. Schwarz, R. Fischer, R. Brock Traffic. ***2007****, 8, 848-866.*

[45] G. J. Doherty, H. T. McMahon Ann. Rev. Biochem. ***2009****, 78, 857-902.*

[46] I. M. Kaplan, J. S. Wadia, S. F. Dowdy J. Control Release. ***2005****, 102, 247-253.*

[47] S. Pujals, E. Giralt Adv Drug Deliv Rev. ***2008****, 60, 473-484.*

[48] M. Scocchi, A. Tossi, R. Gennaro Cell. Mol. Life Sci. ***2011****, 68, 2317-2330.*

[49] R. Fischer, K. Kohler, M. Fotin-Mleczek, R. Brock J. Biol. Chem. ***2004****, 279, 12625-12635.*

[50] T. C. O'Riordan, K. Fitzgerald, G. V. Ponomarev, J. Mackrill, J. Hynes, C. Taylor, D. B. Papkovsky Am. J. Physiol. Regul. Integr. Comp. Physiol. ***2007****, 292, R1613-1620.*

[51] J. Hynes, L. D. Marroquin, V. I. Ogurtsov, K. N. Christiansen, G. J. Stevens, D. B. Papkovsky, Y. Will Toxicol. Sci. ***2006****, 92, 186-200.*

[52] E. R. Carraway, J. N. Demas, B. A. DeGraff, J. R. Bacon Anal. Chem. ***1991****, 63, 337-342.*

[53] S. M. Borisov, G. Nuss, I. Klimant Anal. Chem. ***2008****, 80, 9435-9442.*

[54] F. Belleudi, C. Scrofani, M. R. Torrisi, P. Mancini PLoS ONE. ***2011****, 6, e29159.*

[55] R. I. Dmitriev, A. V. Zhdanov, G. Jasionek, D. B. Papkovsky Anal. Chem. ***2012****.* ***DOI:*** *10.1021/ac3000144*

SUPPLEMENTARY DATA

Complexes of Ir(III)-octaethylporphyrin with peptides as probes for sensing cellular O2

KLAUS KOREN, RUSLAN I. DMITRIEV, SERGEY M. BORISOV, DMITRI B. PAPKOVSKY AND INGO KLIMANT

FIG. S1. ^{1}H NMR SPECTRUM OF IR1.

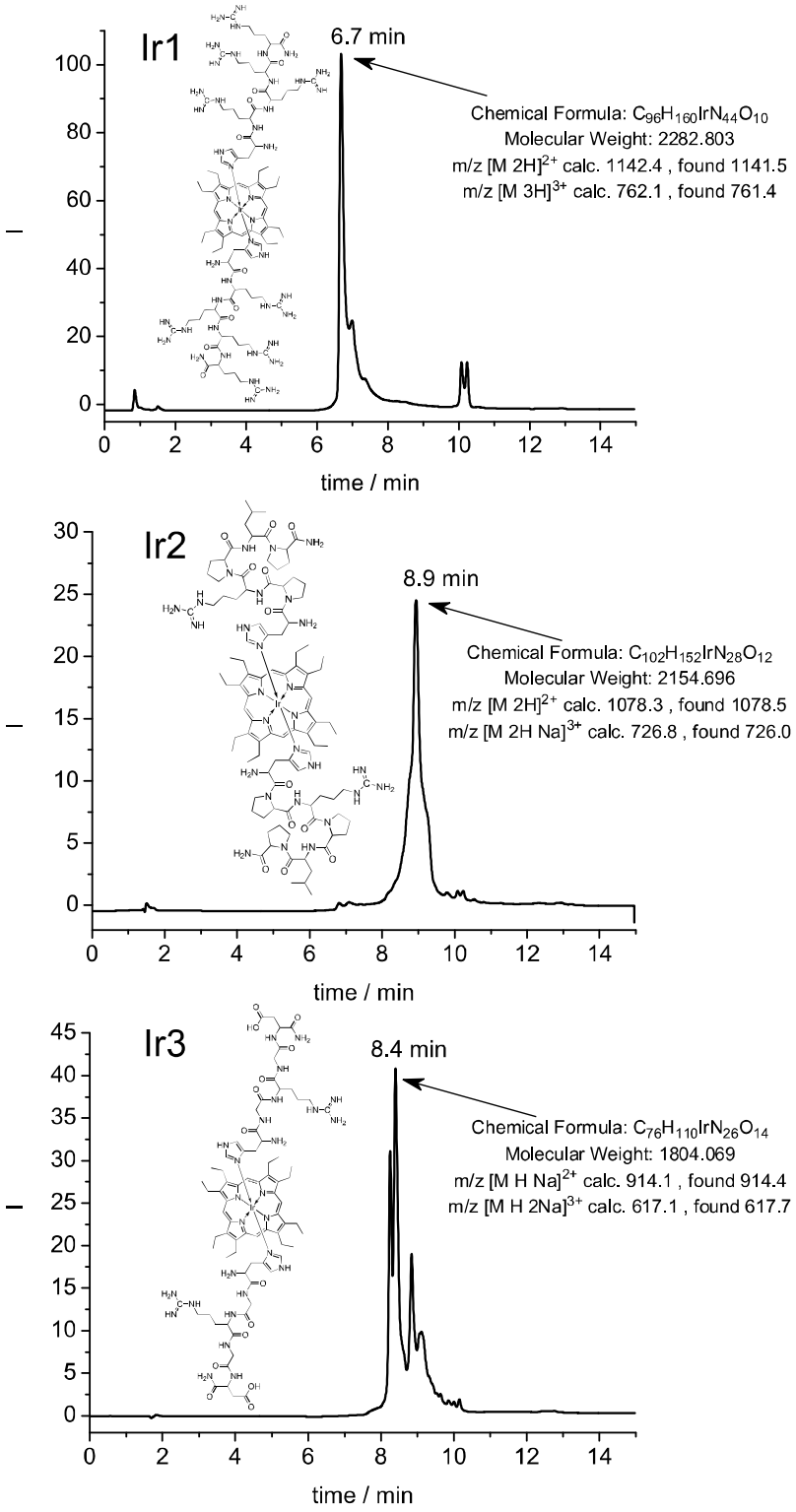

FIG. S2. RP-HPLC CHROMATOGRAMS OF IR1, IR2 AND IR3, WITH STRUCTURAL M/S DATA EVALUATED ON A TRIPLE QUADRUPOLE SPECTROMETER.

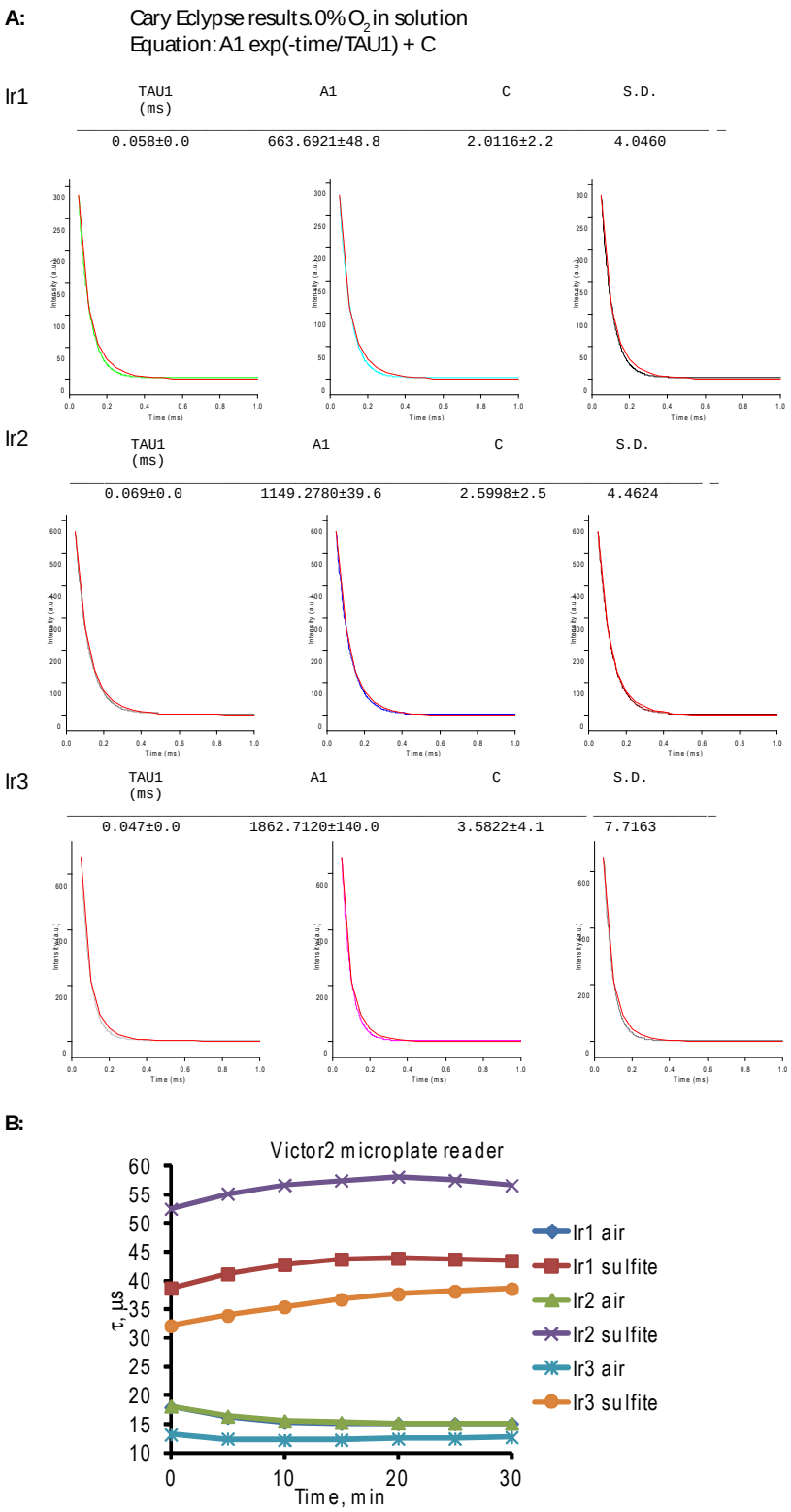

FIG. S3. PHOSPHORESCENCE DECAY CURVES AND LIFETIME VALUES FOR THE IR CONJUGATES IN AQUEOUS SOLUTIONS (PBS).

TABLE S4. PHOSPHORESCENCE INTENSITIES (F1, T = 30 μS) FOR VARIOUS CONCENTRATIONS OF CONJUGATE IR1 OBTAINED IN PBS/1% FBS ON VICTOR2 MICROPLATE READER.

	Air		Sulfite (deoxygenated)	
Ir1 μM	average	stdev	average	stdev
10	151445.0	49388.15	3316721	770843.6
1	67389.6	22185.56	483681	75986.63
0.1	16504.3	4254.608	52404.33	9896.208
0.01	1985.3	1012.473	9293.667	9091.802
0.001	626.2	92.65363	841.8889	30.21359
0	407.7	43.48563	418.7778	17.03509

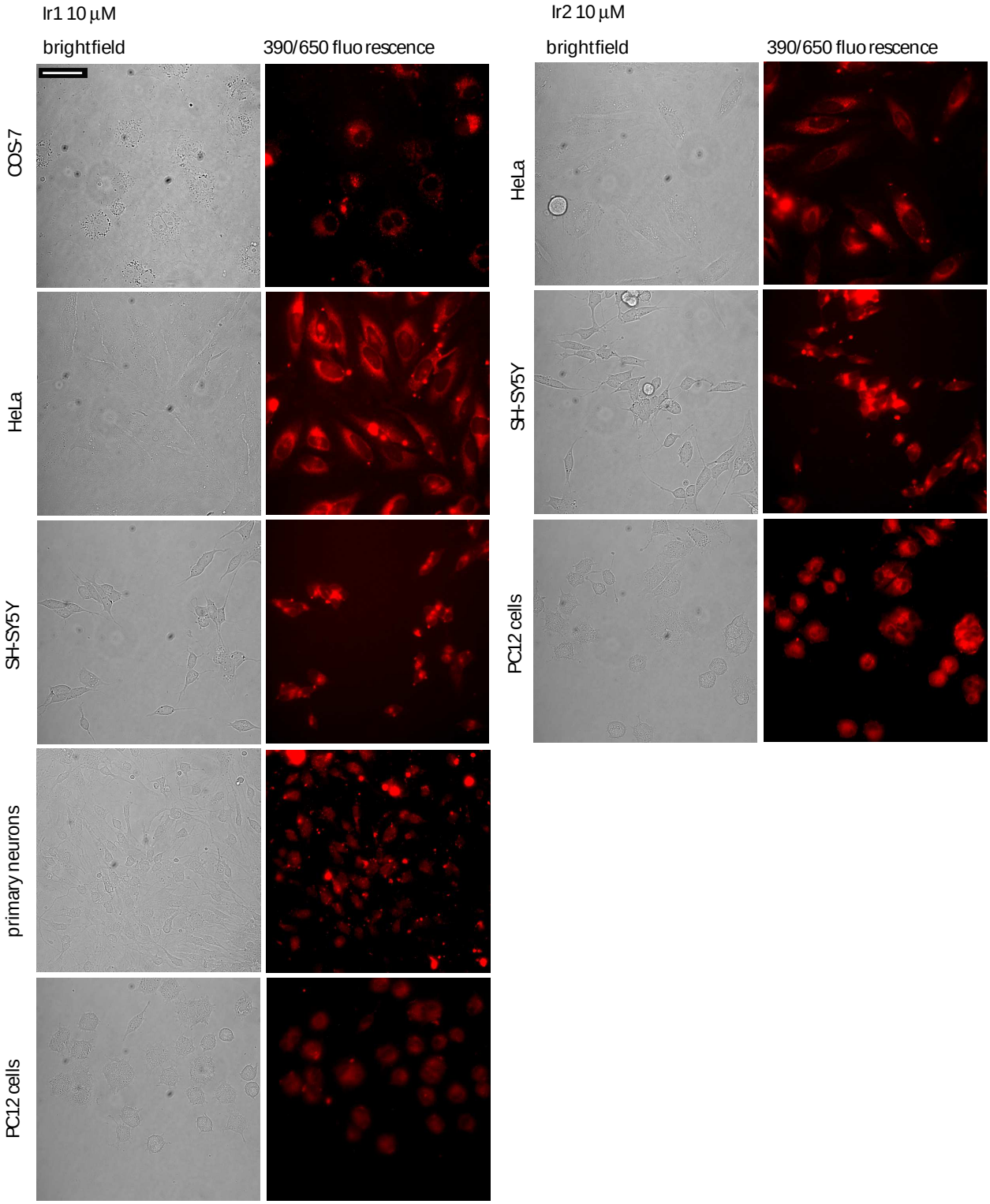

FIG. S5. BRIGHTFIELD AND FLUORESCENT IMAGES OF OTHER CELL LINES STAINED WITH IR1 AND IR2 PROBES. SCALE BAR 50 µM.

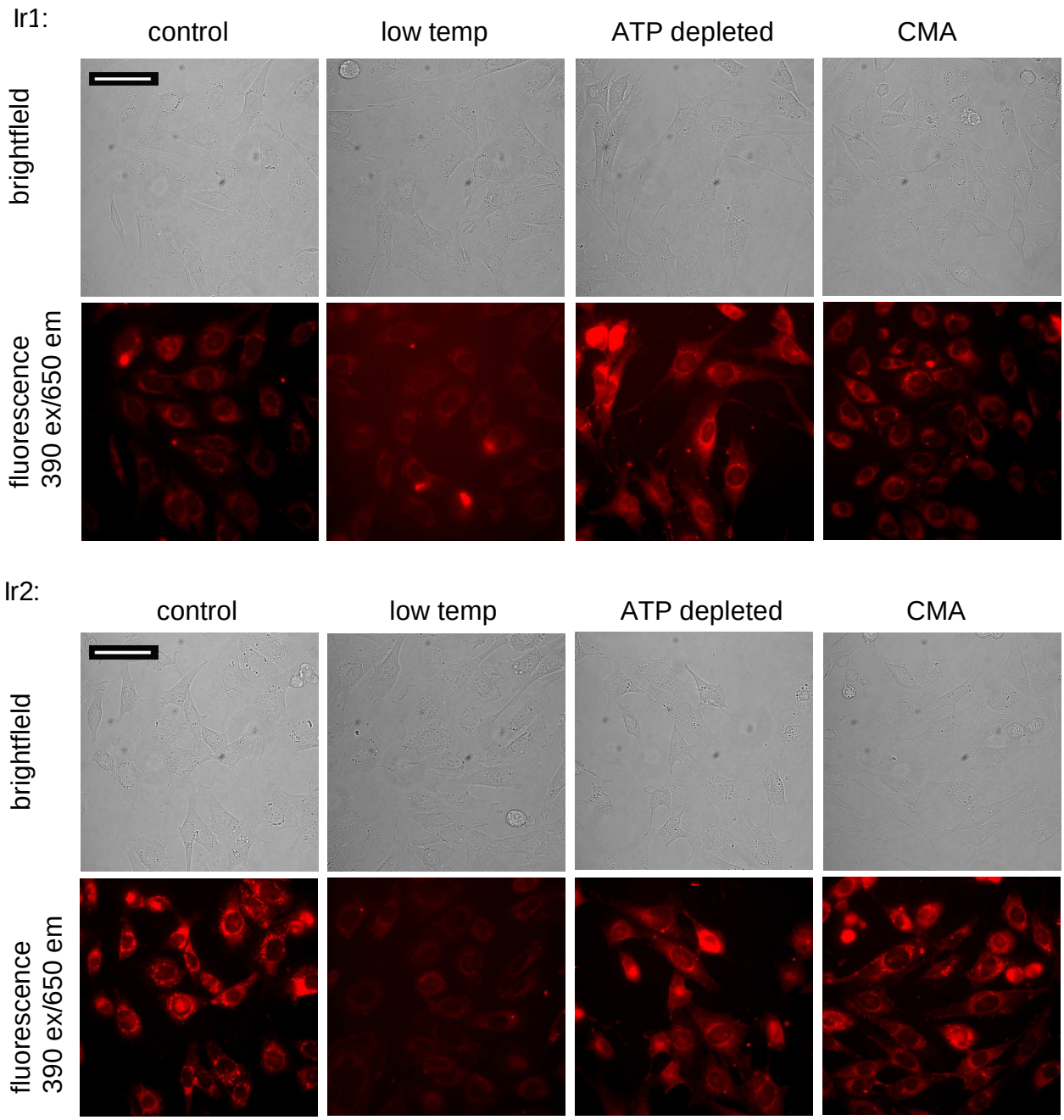

FIG. S6. EFFECTS OF TEMPERATURE, ATP DEPLETION AND INHIBITION OF LYSOSOMAL FUNCTION ON INTRACELLULAR ACCUMULATION OF THE PROBES IN MEF CELLS. IR1 AND IR2 WERE LOADED (AT 10 μM FOR 6 H) IN CELLS EXPOSED TO ATP DEPLETION, CONCANAMYCIN A (CMA) TREATMENT OR LOW TEMPERATURE (4 ^{0}C), THEN WASHED AND INVESTIGATED BY FLUORESCENCE MICROSCOPY (BRIGHTFIELD AND FLUORESCENCE IMAGES). SCALE BAR 50 μM.

Based on the work previously done with Ir(III) porphyrins it was seen that the direct coupling to the central atom is an interesting synthetic approach. Additionally, the biological work showed that the porphyrins can be used inside cells and show moderate to low toxicity while conserving their good photophysical properties.

In order to make a step further in intracellular oxygen measurements, directed localization within the cell would be desirable. In particular, localization of the probe inside the mitochondria would be favorable. As oxygen is predominantly consumed in the mitochondria, it would be best to locate the probe directly there.

Previous work [1,2] states that the lipophilic cation, triphenylphosphonium ion, localizes inside the mitochondria due to the negative inside transmembrane potential. For the Ir(III) porphyrines this means that linking them to triphenylphosphonium ions could lead to the desired localization pattern.

In a first step Ir-OEP-CO-Cl was reacted with (2-Dimethylaminoethyl)triphenylphosphonium bromide, a tertiary amine bearing the needed triphenylphosphonium. A spectral shift and changed solubility are first evidences that this reaction is possible. Detailed photophysical and biological studies will show if it will be possible to use this probe for mitochondria staining.

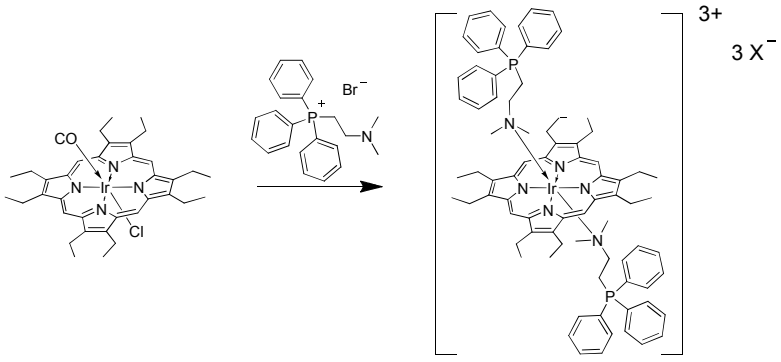

FIGURE 1: POSSIBLE REACTION SCHEME TOWARDS MITOCHONDRIA TARGETING IR(III) PORPHYRIN

REFERENCES

[1] T. Murase, T. Yoshihara, S. Tobita, Mitochondria-specific Oxygen Probe Based on Iridium Complexes Bearing Triphenylphosphonium Cation, Chemistry Letters. 41 (2012) 262–263.

[2] N. Kolevzon, U. Kuflik, M. Shmuel, S. Benhamron, I. Ringel, E. Yavin, Multiple Triphenylphosphonium Cations as a Platform for the Delivery of a Pro-Apoptotic Peptide, Pharmaceutical Research. 28 (2011) 2780–2789.

Within the group of metalloporphyrins used in optical sensor applications platinum(II) and palladium(II) 5,10,15,20-meso-tetrakis-(2,3,4,5,6-pentafluorophenyl)-porphyrin (TFPP) are especially interesting. In contrast to other porphyrins those are highly photostable. Unfortunately, synthetic modifications of porphyrin macrocycles can be synthetically laborious and often influence the photophysical properties.

Click-reactions could be a way to overcome these limitations. The concept of click-reactions was put into focus by Sharpless et. all [1]. According to his view click reactions are reactions that can be used to effectively link small units with each other. This concept is based on processes that occur in nature where also small subunits are linked to produce bigger complex molecules. Nature actually only needs a small set of reactions to create a huge variety of molecules. So what characteristics have to be fulfilled by a reaction to be classified as a click reaction? In general, click reactions should be fast, have a high yield, be selective and stereospecific, stable at physiological condition and should work at mild reaction conditions with no or simplex purification [2]. So from a practical point of view click reactions are a class of well working reactions.

In the last years a variety of reactions were classified as click reactions and demonstrated to be synthetically interesting. A few classic click reactions will be described here (figure 1). The classic click reaction is the so called azide-alkyne cycloaddition. This reaction normally employs a Cu(I) salt as catalyst. Notably this reaction even made it into undergrad labs all over the world [3]. Aside from the huge success of this reaction the needed metal catalyst is not favorable for biological systems due to potential toxicity. Therefore, several additions and improvements to the reaction are reported [2].

The second click reaction often used is the so-called thiol-en reaction. In this reaction a thiol reacts with a double bond. The reaction can be classified as a radical reaction and can be triggered either by light or with an initiator [4]. Additionally to the radical based thiol-en reaction, these functional groups can also be used in the Michael addition, another click reaction [5]. The nucleophilic ring opening of an epoxide is a further example of an effective reaction.

Azide-alkyne cycloaddition (CuAAC)

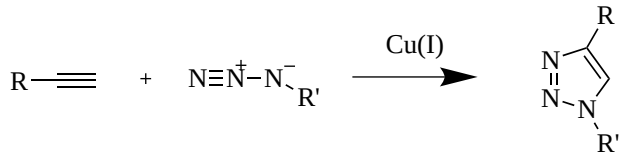

Thiol-en radical addition

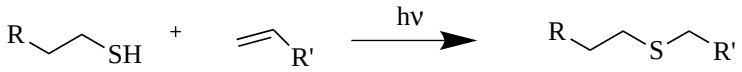

Ring-opening reaction of epoxides

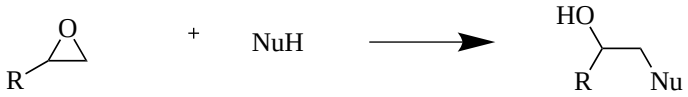

para-fluoro nucleophile substitution

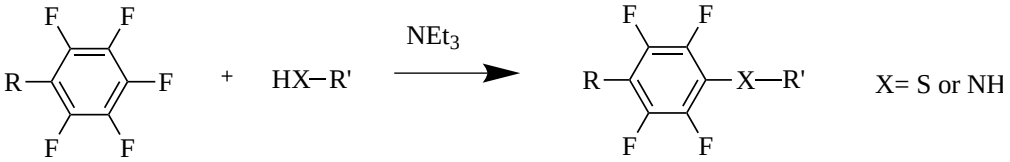

FIGURE 1: SELECTED CLICK-REACTIONS

Regarding nucleophilic reactions the following is of special interest. The nucleophilic substitution of the labile para-fluorine atoms of 2,3,4,5,6-pentafluorophenyl groups is also classified as a click-reaction [6]. Nucleophiles like thiols or amines can be used to substitute the para-fluoro atom. The reaction works well with polar aprotic solvents like DMF or acetonitrile in the presence of a base (e.g. triethylamine).

The Pt- and Pd-TFPP indicators mentioned above possess four of the pentafluorophenyl groups needed. Therefore, those indicators are accessible to click based functionalization [7–9]. Thiols are common groups in biological material and can also be introduced to polymers or other materials. In order to improve the performance of Pt- and Pd-TFPP in optical oxygen sensors, it seems reasonable to use this chemistry. In a first step the stability of optical oxygen sensors will

be improved by linking the indicator directly to the matrix material. This covalent linking will minimize unfavored processes like dye migration or leaching.

REFERNCES

[1] H.C. Kolb, M.G. Finn, K.B. Sharpless, Click Chemistry: Diverse Chemical Function from a Few Good Reactions, Angew. Chem. Int. Ed. Engl. 40 (2001) 2004–2021.

[2] C.R. Becer, R. Hoogenboom, U.S. Schubert, Click Chemistry beyond Metal-Catalyzed Cycloaddition, Angew. Chem. Int. Ed. 48 (2009) 4900–4908.

[3] T.V. Hansen, P. Wu, W.D. Sharpless, J.G. Lindberg, Just Click It: Undergraduate Procedures for the Copper(I)-Catalyzed Formation of 1,2,3-Triazoles from Azides and Terminal Acetylenes, J. Chem. Educ. 82 (2005) 1833.

[4] K.L. Killops, L.M. Campos, C.J. Hawker, Robust, Efficient, and Orthogonal Synthesis of Dendrimers via Thiol-ene "Click" Chemistry, J. Am. Chem. Soc. 130 (2008) 5062–5064.

[5] U. Mansfeld, C. Pietsch, R. Hoogenboom, C.R. Becer, U.S. Schubert, Clickable initiators, monomers and polymers in controlled radical polymerizations – a prospective combination in polymer science, Polym. Chem. 1 (2010) 1560.

[6] C.R. Becer, K. Babiuch, D. Pilz, S. Hornig, T. Heinze, M. Gottschaldt, u. a., Clicking Pentafluorostyrene Copolymers: Synthesis, Nanoprecipitation, and Glycosylation, Macromolecules. 42 (2009) 2387–2394.

[7] D. Samaroo, C.E. Soll, L.J. Todaro, C.M. Drain, Efficient microwave-assisted synthesis of amine-substituted tetrakis(pentafluorophenyl)porphyrin, Org. Lett. 8 (2006) 4985–4988.

[8] S.M. Borisov, P. Lehner, I. Klimant, Novel optical trace oxygen sensors based on platinum(II) and palladium(II) complexes with 5,10,15,20-meso-tetrakis-(2,3,4,5,6-pentafluorphenyl)-porphyrin covalently immobilized on silica-gel particles, Analytica Chimica Acta. 690 (2011) 108–115.

[9] P. Battioni, O. Brigaud, H. Desvaux, D. Mansuy, T.G. Traylor, Preparation of functionalized polyhalogenated tetraaryl-porphyrins by selective substitution of the p-Fluorines of meso-tetra-(pentafluorophenyl)porphyrins, Tetrahedron Letters. 32 (1991) 2893–2896.

STABLE OPTICAL OXYGEN SENSING MATERIALS BASED ON CLICK-COUPLING OF FLUORINATED PLATINUM(II) AND PALLADIUM(II) PORPHYRINS - A CONVENIENT WAY TO ELIMINATE DYE MIGRATION AND LEACHING

THIS CHAPTER WAS ACCEPTED FOR PUBLICATION AS A FULL PAPER IN

SENSORS AND ACCTUATORS B 2012, VOLUME 169, 173-181

DOI: 10.1016/J.BBR.2011.03.031

AUTHORS: KLAUS KOREN, SERGEY M. BORISOV AND INGO KLIMANT

ABSTRACT

Nucleophilic substitution of the labile para-fluorine atoms of 2,3,4,5,6-pentafluorophenyl groups enables a click-based covalent linkage of an oxygen indicator (platinum(II) or palladium(II) 5,10,15,20-meso-tetrakis-(2,3,4,5,6-pentafluorophenyl)-porphyrin) to the sensor matrix. Copolymers of styrene and pentafluorostyrene were chosen as polymeric materials. Depending on the reaction conditions either soluble sensor materials or crosslinked microparticles were obtained. Additionally, we were able to prepare ormosil-based sensors with linked indicator, which showed high sensitivity towards oxygen. The effect of covalent coupling on sensor characteristics, sensor stability and photophysical properties were studied.

1. INTRODUCTION:

Optical oxygen sensors are among the most important sensor systems and are widely applied in industry and academia alike [1,2]. Applications of optical oxygen sensors include pressure sensitive paints [3–5], food packaging [1] and biological applications [6,7] to mention only a few. Numerous optical oxygen sensors were reported during the last decades and the materials employed are now fairly established [8,9]. Most state-of-the art sensing materials rely on oxygen

indicators physically entrapped in a polymer matrix or in an organically modified silica (ormosil) [10]. For this reason they present several major shortcomings, which originate from the fact that dye molecules can freely migrate within the matrix. First, aggregation of the dye can occur with time. Second, calibration plots can be affected due to redistribution of the dye between different environments within the matrix which are known to have different polarity and oxygen permeability [11]. Third, diffusion of the dye molecules into adjusting materials such as polymeric support is thermodynamically favored and readily occurs with time. Evidently, this affects storage stability of the sensor. Since migration processes are accelerated at higher temperatures even short treatment (e.g. during sterilization) may affect the calibration. Moreover, many oxygen sensing materials rely on the use of nano- and microparticles [12,13] dispersed in a polymer matrix [14] where the migration processes can be even more critical due to large contact surface. Finally, simple entrapment of the dye does not completely prevent it from leaching particularly if organic solvents, lipophilic samples or surfactants are present [15].

Obviously, the above mentioned shortcomings can be overcome by covalently linking the indicator dye to the polymer. This approach is rather common for other indicators (e.g. pH indicators) but is not state-of-the art in case of oxygen sensors. Possible explanations are increasing production costs and significant synthetic effort required for both: the preparation of functionalized indicators and the coupling step. A possible route towards such sensing materials could include click chemistry [16,17] which enables functionalization of polymers [18–20] and dyes alike [21] using very mild and straightforward reaction conditions. Within the arsenal of common click reactions [22] the nucleophilic substitution of the labile para-fluorine atoms of a 2,3,4,5,6-pentafluorophenyl groups seems to be a quite promising method[23,24]. Fortunately, highly photostable oxygen indicators such as Pt(II) and Pd(II) complexes of meso-tetra(pentafluorophenyl)porphyrin (TFPP) [25–28] and tetra(pentafluorophenyl)porphyrin lactones [29,30] possess such functionality. Additional positive features of these dyes are commercial availability, excellent photostability and good quantum yields. Although other porphyin based indicators with near infrared (NIR) emission were recently employed [31,32], PtTFPP and PdTFPP are still widely used. Also, nucleophilic substitution reactions have been widely used for derivatization/covalent coupling of TFPP and its complexes [33,34].

In oxygen sensors polymers and ormosil are doubtless the most common materials used. Important parameters for a good sensor matrix are adequate gas permeability, excellent

chemical and photochemical stability, good processability of the sensing materials and commercial availability [9]. Within the set of different polymers, polystyrene (PS) is the most frequently used matrix. For ormosil based sensors a variety of different materials with varying composition were reported [35–37].

In this contribution we will present a click chemistry based approach to covalently link the indicator to two different sensor matrixes and investigate the influence of the covalent attachment on sensor characteristics, photophysical properties and sensor stability.

2. EXPERIMENTAL

2.1. REAGENTS:

Styrene (St) and tetraethoxysilane (TEOS) were purchased from Fluka (www.sigmaaldrich.com) and pentafluorostyrene (PFS), phenyltrimethoxysilane (PTMS) and 3-mercaptopropyltrimethoxysilane (MPS) from ABCR (www.abcr.de). For St and PFS the stabilizer was removed by filtration over Al_2O_3. The radical initiator azo-bis-(isobutyronitril) (AIBN) and 1,3-propanedithiol were obtained from ACROS (acros.com), triethylamine (NEt_3) from Sigma-Aldrich, platinum(II)- and palladium(II)-meso-tetra(2,3,4,5,6-pentafluorophenyl)porphyrin (PtTFPP and PdTFPP, respectively) and platinum(II) octaethylporphyrin (PtOEP) from Frontier Scientific (www.frontiersci.com), polystyrene (MW. 250000) from Fisher Scientific (www.fishersci.com) and poly(ethylene glycol terephthalate) support (Mylar®) from Goodfellow (www.goodfellow.com). Anhydrous DMF was obtained from Sigma-Aldrich, all other solvents were purchased from Roth (www.carl-roth.de) and used without further purification. Synthetic air and nitrogen were of 99.999% purity and were purchased from Linde gas (www.linde-gas.at).

2.2. CHARACTERIZATION AND MEASUREMENT SETUP:

^{19}F NMR spectra were recorded on Varian Mercury 300 spectrometer (282.46 MHz) in deuterated chloroform and referenced against Me_4Si for ^{1}H and ^{13}C. Weight and number average molecular weights (Mw and Mn), as well as the polydispersity index PDI=Mw/Mn, were determined by size exclusion chromatography (SEC) with the following set-up: Merck Hitachi

L6000 pump, separation columns from Polymer Standards Service (8mm*300 mm, STV 5 µm grade size; 106, 104 and 103 Å pore size), refractive index detector (model Optilab DSP InterferometricRefractometer) from Wyatt Technology. Polystyrene standards from Polymer Standard Service were used for calibration. All SEC runs were performed with THF as the eluent. Pt content in the sensor material was determined by ICP-OES after microwave assisted digestion. SEM images were recorded on a Zeiss Ultra 55 scanning electron microscope equipped with a field-emission gun (FEG). The particles were fixed on a double-stick carbon tape on a conventional specimen holder and sputtercoated by using a Pt/Pd (50:50) target.

Absorption spectra were measured at a Cary 50 UV–VIS spectrophotometer (www.lzs-concept.com). Emission spectra were acquired on a Hitachi F-7000 fluorescence spectrometer (www.inula.at) equipped with a red-sensitive photo-multiplier R 9876 from Hamamatsu (www.hamamatsu.com). The emission spectra were corrected for the sensitivity of the PMT which was calibrated using a halogen lamp. Relative luminescence quantum yields were determined using a solution of PtOEP in toluene as a standard [38](quantum yield = 41.5%). The solutions of the dyes were thoroughly deoxygenated by bubbling argon through.

Luminescence phase shifts were measured with a two-phase lock-in-amplifier (SR830, Stanford Research Inc., www.thinksrs.com). Excitation was performed with the light of a 405 nm LED which was sinusoidally modulated at a frequency of 5 kHz for PtTFPP or 500 Hz for PdTFPP. A bifurcated fiber bundle was used to guide the excitation-light to the sensor film and to guide back the luminescence. A BG12 excitation glass filter and an OG630 emission filter (both from Schott, www.schott.com) were used. The luminescence was detected with a photo-multiplier tube (H5701-02, Hamamatsu, www.sales.hamamatsu.com). Temperature was controlled by a cryostat ThermoHaake DC50. Gas calibration mixtures were obtained using a gas mixing device (MKS, www.mksinst.com). For low oxygen concentrations measurements were performed using the same two-phase lock-in-amplifier and a home-made calibration chamber as described earlier[34].

2.3. POLYMERIZATION OF PS-CO-PFS:

Within this work two copolymers of St and PFS were polymerized in a solvent free manner, one with a high PFS content (PS-PFS-1) and one with a low PFS content (PS-PFS-2). In case of, PS-PFS-1 2 ml of St and 1 ml of PFS were used, while for PS -PFS-2 5.5 ml of St and 35 µl of PFS. Both

mixtures were deoxygenated for 30 minutes, then 1 mol% of AIBN was added. The reactions were carried out at 85 °C in a N_2 atmosphere for 20 h. In both cases the solid polymerization product was dissolved in CH_2Cl_2 and precipitated with MeOH, this procedure was repeated three times. The fluoride content in the polymers was determined with a fluoride-sensitive electrode after microwave assisted combustion[39].

2.4. POLYMER-COUPLING:

As demonstrated in scheme 1, two routes towards sensor polymers were chosen. Route a) PS-PFS-1 and Pt- or PdTFPP were cross-linked using a less than equimolar amount of propanedithiol. In a typical procedure 105 mg of PS-co-PFS-1 were dissolved in 1 ml DMF, then1 to 5 mg of PtTFPP or PdTFPP were added. Subsequently 14 µl of propandithiol and 100 µl of TEA were added. The mixture was stirred at 75 °C for 10 to 20 minutes, until it turned into a "jelly". To ensure complete reaction the "jelly" was left stirring at 75 °C for another 2 hours. Finally the "jelly" was washed three times with EtOH and acetone to remove DMF, TEA as well as the unreacted propanedithiol and indicator. After drying the polymer was crushed in a mortar yielding crosslinked sensor particles. Route b) PS-PFS-2 was used and propanedithiol was added in excess to prevent cross-linking. In a typical procedure 100 mg of PS-PFS-2 were dissolved in 2 ml of DMF and reacted with 30 µl of propandithiol (60 equivalents) and 50 µl of TEA (35 equivalents) at 75 °C for 5 to 6 hours. After precipitation and subsequent washing with MeOH the thiol-saturated polymer (TSP) was dried at 60 °C. Subsequently PtTFPP or PdTFPP were introduced: 10 mg of the dye were dissolved in 5 ml of DMF, 50 µl of TEA were added and the mixture was heated to 75 °C, then 100 mg of TSP, dissolved in 3 ml of DMF, were added drop wise. After 5 h the soluble sensor polymers were obtained by precipitation and washing with MeOH.

2.5. ORMOSIL-COUPLING:

15 mg of PtTFPP or PdTFPP were dissolved in 100 µl of anhydrous DMF, 20 µl of TEA were added as well as 3.2 molar equivalents of MPS. The reaction was carried out for 1 hour in a closed vial at 75 °C. Reaction progress was monitored using TLC (silica gel): in contrast to the unreacted dye which is hydrophobic, the modified dye binds to the TLC plate. Since the functional dye is hydrolysis sensitive it was used without further isolation. To the above mixture 2 ml of EtOH, 1 ml of TEOS, 1 ml of PTMS and 630 µl of water were added. After 15 minutes at 65

°C the mixture turned into a porous solid and was left at this temperature for another 2 hours. Finally the mixture was dried at 200 °C in drying chamber (3 hours). After washing with acetone and CH_2Cl_2 the dry product was crushed in a mortar to yield ormosil sensor microparticles (OSP).

2.6. SENSOR PREPARATION:

The „cocktails“ for coating the reference sensors were prepared by dissolving 1 to 5 mg PtTFPP or PdTFPP and 100 mg of polystyrene in 1000 mg of $CHCl_3$. Sensor films containing cross-linked sensor particles were prepared as follows. 20 mg of the CLSPs or the OSP were dispersed in 50 mg of silicon E4 (www.wacker.com) and 150 mg of hexane. In case of the soluble sensor polymer 100 mg of the material were dissolved in 1000 mg of $CHCl_3$. All cocktails were knife-coated on either a glass slide or a PET-foil to give, after solvent evaporation, phosphorescent sensor films.

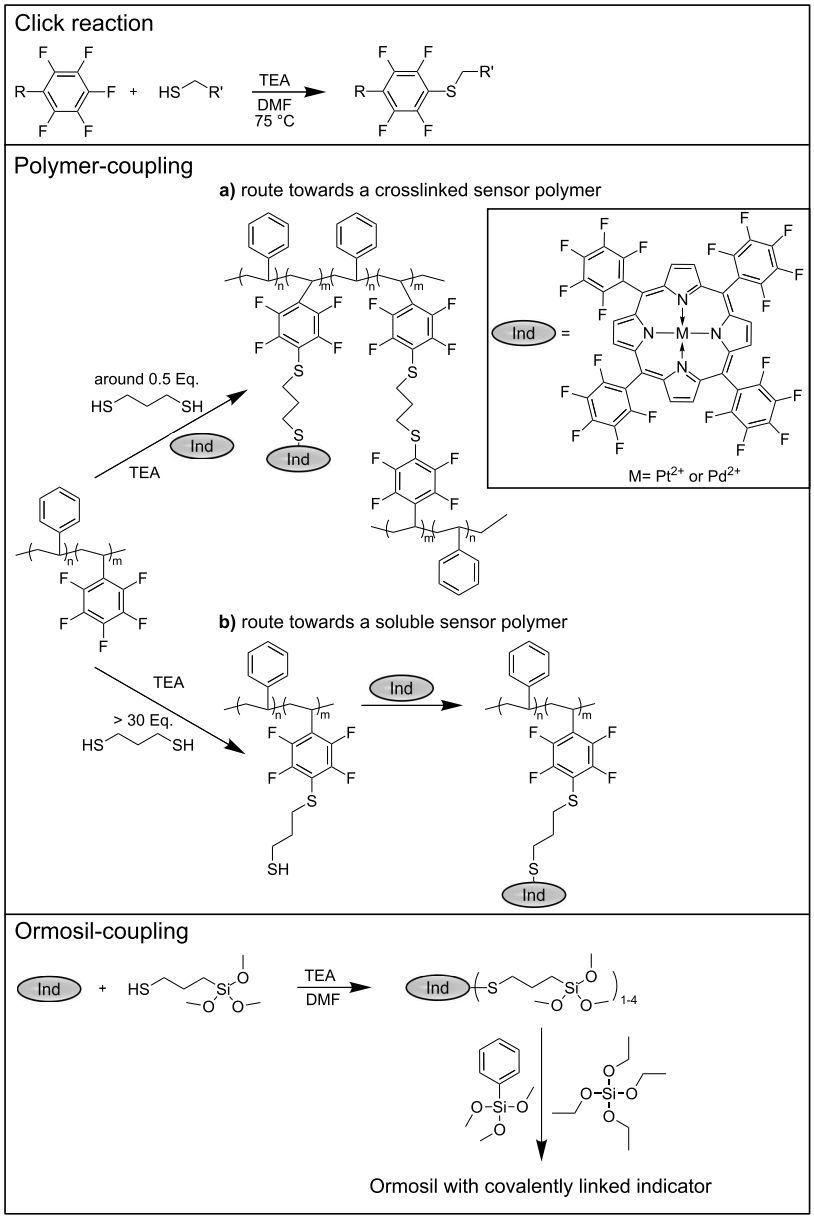

SCHEME 1: CLICK BASED SYNTHESIS OF OXYGEN-SENSITIVE MATERIALS BY GRAFTING INDICATORS ONTO POLY(STYRENE-CO-PENTAFLUROSTYRENE) OR BY INTRODUCING FUNCTIONALIZED INDICATOR TO ORMOSIL BASED MATERIALS. FOR THE POLYMER BASED MATERIALS TWO ROUTES CAN BE DISTINGUISHED: ROUTE A) LEADS TO CROSS-LINKED SENSOR POLYMERS; ROUTE B) YIELDS A SOLUBLE SENSOR POLYMERS WITH COVALENTLY COUPLED INDICATOR.

3.1. CHOICE OF MATERIALS

PtTFPP and PdTFPP are doubtless among the most commonly used indicators in optical oxygen sensors. Although recently other indicators (e.g. NIR emitting benzoporphyrins[31,40,41]) were synthesized, the TFPP based indicators satisfy with commercial availability, excellent photostability and red emission that can easily be visualized. Synthetic modification of such an important indicator seems therefore worthwhile. Due to the presence of pentafluorophenyl groups such a modification or better functionalization is possible via a click chemistry pathway. The nuceleophilic substitution of the labile para-fluorine atoms of a pentafluorophenyl group with a thiol is the essential step [22], as it yields groups which are suitable for covalent coupling. This approach was used to link the indicators to polymer matrixes as well as to an ormosil.

3.2. POLYMER-COUPLING

3.2.1. POLYMER SYNTHESIS AND CLICK MODIFICATION

High molecular weight styrene-pentaflurostyrene-copolymers were synthesized via radical polymerization of the monomers similarly to the literature procedure [42]. This method was chosen as it yields polymers with high molecular weight which generally improves the mechanical stability of the sensor film. Other polymerization methods like nitroxide-mediated radical polymerization (NMP) can of course be used and may have better controllability [43], however high molecular weight polymers are not always easily accessible [44,45]. The properties of the obtained polymers are summarized in table 1.

TABLE 1: PROPERTIES OF POLY(STYRENE-CO-PENTAFLUROSTYRENE)

Polymer	PFS / mol%	Mw / g/mol	Mw/Mn
PS-PFS-1	23.5	418000	2.3
PS-PFS-2	0.5	494000	2.5

In order to graft the indicator dye to the polymer via click chemistry, a dithiol was chosen for the nucleophilic substitution of the labile para-fluorine atoms of the pentafluorophenyl residues. The reaction progress for the soluble sensor polymer with coupled indicator was monitored via ^{19}F NMR. At first, PS-PFS-2 was reacted with a large excess (60 times) of propanedithiol. Excess of the dithiol was used to minimize potential cross-linking and to ensure only one binding between the thiol residues and the polymer. After 6 hours nearly every para-fluorine was substituted by a thiol group as seen in the ^{19}F NMR (figure 1b). In the next step the indicator dyes, either PtTFPP or PdTFPP, was grafted onto the polymer. Also in this step the indicator was used slightly in excess (about 2 equivalents) again to prevent cross-linking.

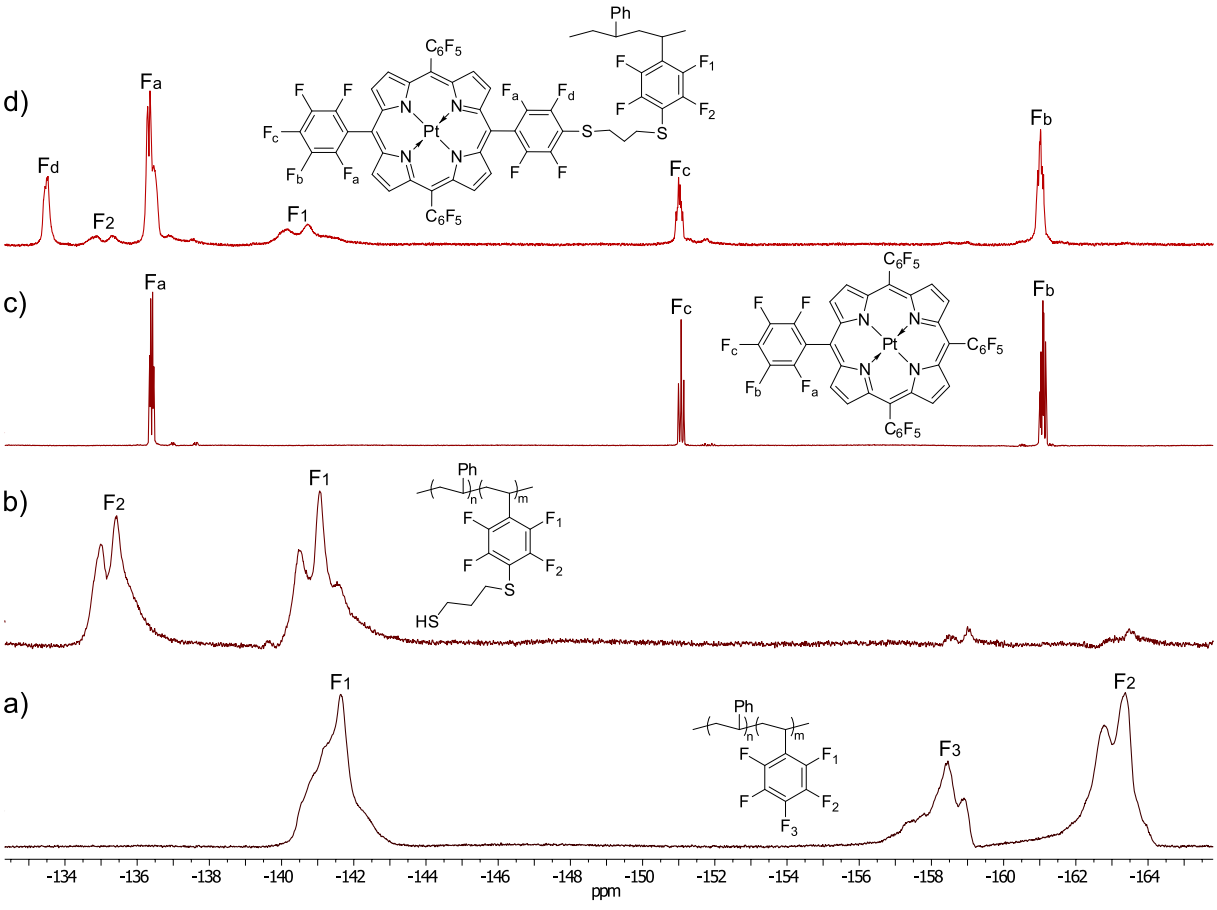

FIGURE 1: ^{19}F NMR SPECTRA OF A) PS-PFS-2 B) PS-PFS-2 AFTER SATURATING WITH PROPANEDITHIOL C) THE FREE INDICATOR DYE PTTFPP AND D) PTTFPP GRAFTED ONTO PS-PFS-2; ALL MEASUREMENTS WERE PERFORMED IN $CDCL_3$

In the final product six different peaks were observed in the ^{19}F NMR and are clearly attributed. The para-flourine peak corresponding to the dye decreased by roughly 25% confirming that the indicator dye is coupled to the polymer, as intended, only once. The platinum content in the final sensing material was determined to be 7.6 mg/g. This indicates that about 82% of the previously introduced pentafluorphenyl groups in the polymer reacted with a PtTFPP via the dithiol linkage. The molecular weight increased to 644000 g per mol.

In order to generate a cross-linked sensing material with covalently linked indicator PS-PFS-1 was reacted with 0.5 equivalents of propanedithiol in the presence of the indicator. Within 10 to 20 minutes a jelly-like product was formed, indicating the spontaneous cross-linking of polymer chains. The product was washed with different organic solvents including CH_2Cl_2 and $CHCl_3$ without being dissolved, indicating that the cross-linking was successful.

3.2.2. PHOTOPHYSICAL PROPERTIES

Covalent bonds between the dye and the matrix are expected to increase sensor stability without negatively affecting the sensor's characteristics especially brightness and sensitivity. As can be seen in Table 2, coupling of the indicator did not affect the position of the absorption and emission bands. Similarly, the phosphorescence quantum yields (Q.Y.) and decay times were only marginally affected.

TABLE 2: COMPARISON OF THE PHOTOPHYSICAL PROPERTIES OF COVALENTLY LINKED PTTFPP (SPP1) AND THE NON-COUPLED INDICATOR

Code	solvent	λmax abs / nm	λmax em / nm	Q.Y.	τ / µs
PtTFPP	Toluene	396, 509, 541	652	0.19	33
PtTFPP coupled to PS-PFS-2	Toluene	397, 509, 542	653	0.16	27
PtTFPP	CHCl3	392, 508, 540	653	0.33	69
PtTFPP coupled to PS-PFS-2	CHCl3	392, 509, 541	654	0.29	58

3.2.3. SENSOR CHARACTERISTICS

Cross-linked sensor polymers were crushed into microparticles and dispersed in silicone rubber. The soluble polymers with the coupled indicators were dissolved in $CHCl_3$ to give homogeneous sensor films after solvent evaporation. Furthermore, the indicator was also simply dissolved (physically entrapped) in the polymer. PS based sensors were chosen as a reference.

TABLE 3: SENSOR CHARACTERISTICS OF NEW SENSOR MATERIALS COMPARED TO ADEQUATE REFERENCE SENSORS.

Code	Matrix	Type	Dye (amount in w%)	$\tau 0$ / µs	$\tau 0/\tau - 1^{\dagger}$	$I0/I - 1^{\dagger}$
S1*	PS-PFS-1	coupled + crosslinked	PtTFPP (1w%)	59.3 ± 0.2	2.74	3.57
S2*	PS-PFS-1	coupled + crosslinked	PtTFPP (5w%)	49.9 ± 0.1	2.66	3,20
S3	PS-PFS-1	dissolved	PtTFPP (1w%)	61.5 ± 0.1	3.02	4.27
S4	PS-PFS-2	coupled	PtTFPP (5w%)	56,4 ± 0.1	2.04	3.06
S5	PS-PFS-2	coupled	PdTFPP (5w%)	951 ± 7	4.54‡	6.74‡
Ref 1	PS	dissolved	PtTFPP (1w%)	58.8 ± 0.1	2.02	2.88
Ref 2	PS	dissolved	PtTFPP (5w%)	49.8 ± 0.1	1.78	2.18
Ref 3	PS	dissolved	PdTFPP (1w%)	964 ± 4	3.97‡	5.97‡

*** Crosslinked sensor particles of PtTFPP on PS-PFS-1 dispersed in silicone rubber † at 100% synthetic air ‡ calibration from 0 to 42 hPa (τ_0/τ -1 at 42 hPa)**

Figure 2 shows the calibration plots obtained for the new materials and Table 3 summarizes the respective sensor properties. Non-linear Stern-Volmer calibration plots are quite common for optical oxygen sensors [11]. Such a calibration behavior can be adequately described by the two-site model (eq. 1) [10,11], where K_{SV1} and K_{SV2} are the two different Stern-Volmer constants, and

F is the distribution coefficient. Although this model is not physically meaningful, for the decay time measurements fitting with high correlation coefficients ($r^2 > 0.999$) is possible.

$$\frac{\tau}{\tau_0} = \frac{F}{1 + K_{SV1} * pO_2} + \frac{1 - F}{1 + K_{SV2} * pO_2}$$

EQUATION 1

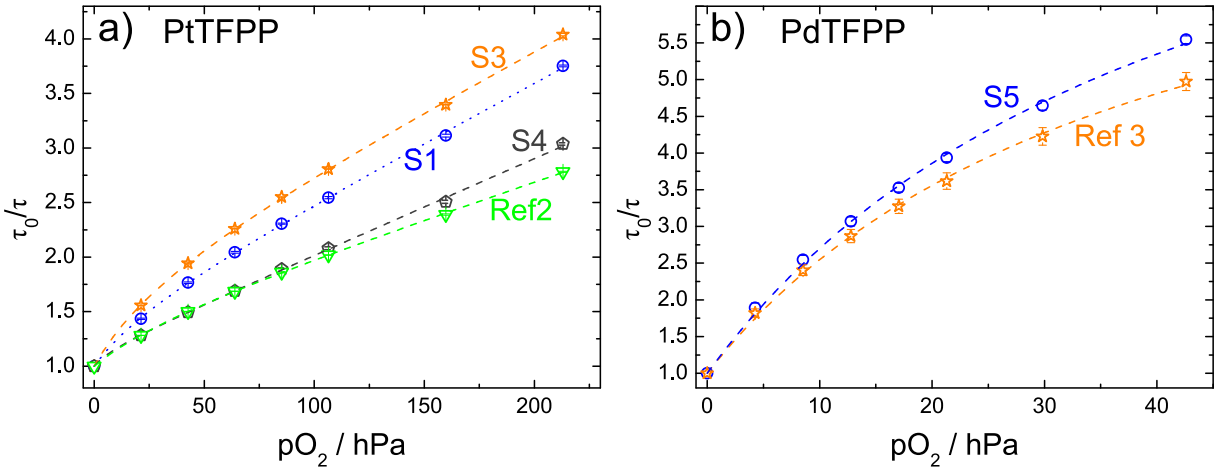

FIGURE 2: A) STERN-VOLMER PLOTS FOR THE PTTFPP BASED OXYGEN SENSING MATERIALS. THE SENSOR MATERIALS WITH PS-PFS-1 AS MATRIX (S1 AND S3) HAVE A HIGHER SENSITIVITY THAN THOSE BASED ON PS OR PS-PFS-2. B) STERN-VOLMER PLOTS FOR THE PDTFPP BASED OXYGEN SENSING MATERIALS.

Sensors S1 and S2 differ only by the amount of loaded indicator, their calibration curves are nearly similar, even though the decay time of S2 is significantly reduced. Usually a higher dye loading increases brightness, but often aggregation or insolubility are limiting factors. For S2 the decreased decay time (and decreased $I_0/I-1$) can indicate that PS and PFS tend to form block-like structures, if the PFS content is high due to the difference in polymerization rate of the two monomers. Within the blocks the indicator dyes are closer to each other leading to a decreased decay time. When PtTFPP is only dissolved in PS-PFS-1 (S3) the resulting sensor is more sensitive then when the indicator is coupled to the same polymer (S1). This might be due to a decrease in the free volume upon crosslinking which affects gas permeability.

S1 and S2 are insoluble in organic solvents, but the beads can easily be dispersed in common matrixes (such as hydrogels or silicones) also along with other components (e.g. temperature-sensitive beads, titanium dioxide beads or other additives). On the other hand, if the indicator is only coupled to the polymer without crosslinking the chains the resulting material is still soluble (S4 and S5) and can easily be applied on polymeric or inorganic substrates. Compared to PtTFPP the palladium analogue (PdTFPP) has a roughly 15 times longer decay time, which results in higher sensitivity of the sensors using this indicator. All optical sensors including oxygen sensors show cross-sensitivity to temperature and this is of course valid for the materials presented here. This cross-sensitivity results from two components, namely the thermal quenching of the indicator (which lowers τ_0 with increasing temperature) and the change in oxygen diffusion and solubility within the polymer (which normally increases the sensitivity). In this respect the investigated materials show similar behavior to the reference sensors and other reported oxygen sensors [31]. For example in case of S4 the decay time decreased by 0.3 % per K and the sensitivity increased by roughly 0.6 % per K.

3.2.4. SENSOR STABILITY

Immobilizing the indicator in the sensor matrix is expected to have positive effects on sensor stability. As known, dye migration and aggregation are factors that limit long term stability, and can be caused by high indicator concentrations which can alter the characteristics of the sensor [46]. Notably, dye molecules can also migrate into the support [47] especially when polymeric fibers or polymeric sensor supports are used. The migration of the dye into other polymers is accelerated by heat or by the presence of organic solvents that swell either the matrix or the polymeric support. Evidently, this effect is suppressed by covalently coupling the dye to the sensor matrix.

Poly(methyl methacrylate) (PMMA) plastic optical fibers are commonly used, as cheap alternatives to glass fibers, for optical signal transduction. PMMA fibers were coated with PtTFPP coupled to PS-PFS-2 as well as with PtTFPP in PS (both materials dissolved in chloroform). The coated fibers were dried at 60 °C for 6 hours and then compared to a corresponding sensor spot (PtTFPP/PS on PET support). The results are presented in Fig. 3. As it can be observed, sensitivity decreases dramatically (by about 2-fold) when the indicator is not

linked to the polymer. This indicates that the migration of the indicator into the PMMA (which has lower gas permeability than PS) is very efficient. Similar effects were observed by Badocco et al. who characterized the sensors prepared by coating of PMMA fibers with a Pt(II) porphyrin in polysulfon [48]. In fact, the authors documented decrease in the sensitivity over time and observed very long dynamic response times for the sensors. It is evident (Fig. 3) that when the dye is coupled to the polymer, the negative effects are dramatically reduced. In fact, the sensitivity decreases only by about 4%. Thus, minimized risk of dye migration enables simple coating procedures for polymeric fibers and increases long-term stability of optical sensors.

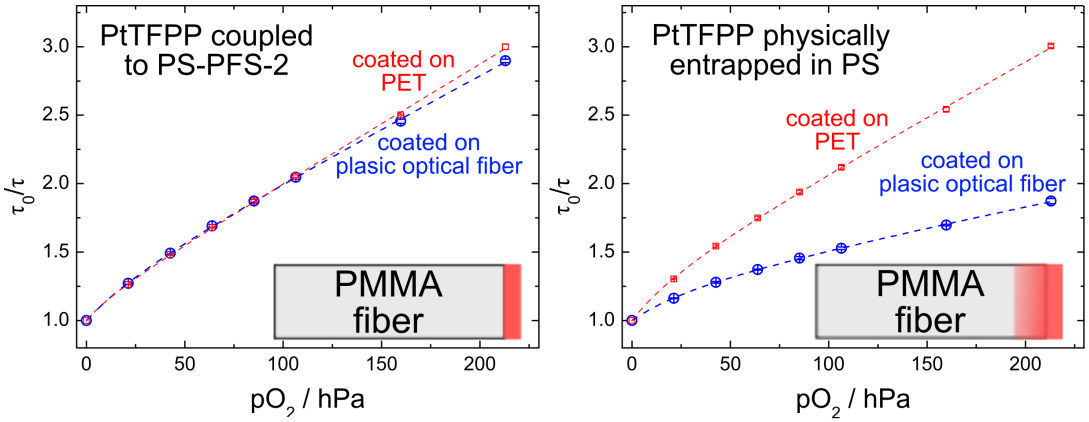

FIGURE 3: BLUE CIRCLES REPRESENT STERN-VOLMER PLOTS OF PTTFPP EITHER COUPLED TO PS-PFS-2 (LEFT) OR PHYSICALLY ENTRAPPED IN PS (RIGHT); BOTH COATED ON A PMMA FIBER. RED SQUARES REPRESENT A REFERENCE SENSOR SPOT ON PET SUPPORT. THE SENSITIVITY OF THE PTTFPP/PS COATED FIBER DROPS DRAMATICALLY DUE TO MIGRATION OF THE INDICATOR INTO THE FIBER. COVALENT COUPLING REDUCES MIGRATION TO A MINIMUM.

A further stability problem of optical oxygen sensors arises from dye leaching. This issue can be solved by covalently coupling the dye to the matrix. For example, crosslinked sensor particles can be easily incorporated into a gas permeable membrane (e.g. silicone or hydrogel). Even when exposed to organic solvents, which are known to swell the particles, leaching of the dye was not observed. Not surprisingly, in case of the indicator coupled to the polymer (S4 and S5) the exposure to pure organic solvents like $CHCl_3$ leads to dissolving of the sensor, as the polymer itself is soluble. Exposure of the film to solvents that do not the dissolve but swell the polymer (e.g. acetone) is possible. This is of particular interest as sensor films are sometimes, for example during cleaning, exposed to such solvents or mixtures of solvents with water. As shown in Fig. 4, dye leaching occurred rapidly when sensors with entrapped indicator are dipped or exposed to

such solvents or solvent mixtures. When the dye is linked to the polymer the dye will not be released from the sensor layer even when stored in the solvent for several days.

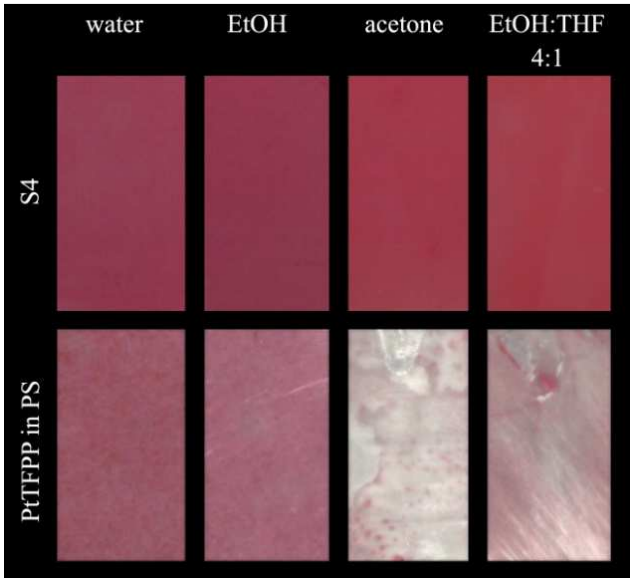

FIGURE 4: SENSOR FILMS AFTER DIPPING INTO DIFFERENT ORGANIC SOLVENTS. IF PTTFPP IS COUPLED TO PS-PFS-2 THE SENSOR FILMS REMAIN COLORED AFTER DIPPING AND EVEN LONG TIME EXPOSURE, SEVERAL DAYS, (TOP). WHEN THE INDICATOR IS ONLY PHYSICALLY ENTRAPPED IN PS SEVERAL SOLVENTS REMOVE THE INDICATOR FROM THE SENSOR WHICH IN A FEW SECONDS (BOTTOM).

Short time exposure of sensor films to organic solvents like acetone can change the sensor signal and sometimes which is even more critical can extract the dye into the environment. When exposing S4 to acetone or THF/EtOH mixtures τ_0 does not change, while the sensitivity of the sensor is slightly increased (slope increased by 3-4%). On the other hand, when a sensor with a non coupled indicator (Ref1) is exposed to those solvents the sensor signal will drop immediately and the indicator will be fully extracted.

The previously discussed stability problems arise from the mobility of the indicator in the matrix itself or from the exposure of the sensor to certain solvents. An additional factor, which plays an important role in determining the stability, is photostability. In general, photostability is mostly determined by the indicator rather than by the sensor matrix. To check the effect of covalent linkage of the indicator to the matrix a reference sensor (Ref 1) and S4 were both continuously illuminated. After 5.5 hours the intensity of S4 dropped by 3.5% while the reference sensor lost 1.4% of its initial intensity (Fig. 5). Although the photostability slightly decreased due to

covalent coupling, this is not crucial, as normally only short light pulses are needed for measuring. Additionally, decay time measurements are possible for which the effect of photo bleaching is negligible.

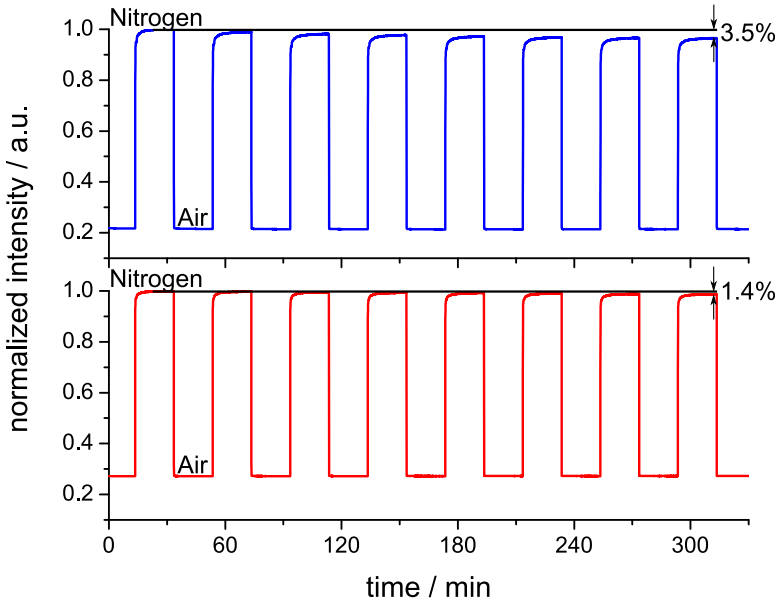

FIGURE 5: COMPARISON OF THE PHOTOSTABILITY OF S4 (TOP) AND REF 1 (BOTTOM). AFTER COVALENT COUPLING OF THE INDICATOR THE PHOTOSTABILITY SLIGHTLY DECREASES.

3.3. ORMOSIL-COUPLING

A second highly important sensor matrix is organically modified silica (ormosil). These materials can be synthesized from a variety of alkoxysilanes by condensation. Depending on the reaction conditions and the precursors used quite different sensor materials can be obtained including, for example, ormosil films[49], soluble ormosils[10], xerogels[50] or aerogels[51]. Ormosil based materials are rather versatile sensor matrixes, and as such they are an interesting addition to polymers.

Mercaptopropyltrimethoxysilane was used to modify the indicator to enable covalent coupling to the ormosil. Following the click reaction scheme (scheme 1) PtTFPP or PdTFPP were reacted in anhydrous DMF in the presence of TEA. The reaction process was monitored via TLC.

Since the silane modified dye is sensitive to hydrolysis, it is important to use the functionalized dye immediately.

For the proof of principle the functionalized dye was reacted with tetraethoxysilane (TEOS) and phenyltrimethoxysilane (PTMS). The resulting ormosil was dried, crushed and afterwards exposed to organic solvents like acetone or CH_2Cl_2. The resulting ormosil, either containing PtTFPP or PdTFPP, did not present any leaching of the dye. A similar ormosil containing non covalently coupled PtTFPP was synthesized for comparison. When this ormosil was exposed to the same organic solvents instantaneous dye leaching was observed and within a few seconds the particles turned essentially colorless.

The ormosil particles with the linked indicator were dispersed in a silicone matrix. Surprisingly, the prepared materials were found to be highly sensitive to oxygen therefore they could be used as trace oxygen sensors (Figure 6). Again the calibration plots are not linear, so the two-site-model was used to fit the calibration plots. The K_{SV} values given in Figure 6 represent the values obtained for the better quenchable fraction (K_{SV2} is more then 10 times smaller). The quenching constant ($k_q = K_{SV}/\tau_0$) was calculated to be 120 and 116 $Pa^{-1}s^{-1}$ for PdTFPP and PtTFPP, respectively. A comparison with a recently published sensor material [34], in which the indicator is immobilized on the surface of porous silica particles, shows that the sensitivity (K_{SV}) is comparable (≈ 0.4 hPa^{-1} for PtTFPP and ≈ 6.8 hPa^{-1} for PdTFPP). On the other hand, k_q of the published sensor is only half as big as reported here. The quenching constant (k_q) is also significantly smaller for other sensitive ormosils [35] (k_q = 30 to 40 $Pa^{-1}s^{-1}$ using PtOEP) or xerogels [50] (k_q = 54 $Pa^{-1}s^{-1}$ using $[Ru(dpp)_3]^{2+}$).

FIGURE 6: A) STERN-VOLMER PLOTS FOR ORMOSIL BASED SENSOR MATERIAL. B) LOW MAGNIFICATION SEM PICTURE OF AN ORMOSIL PARTICLE SHOWING THE MACRO POROSITY OF THE PARTICLE. C) MAGNIFICATION OF THE SQUARE SHOWN IN B) INDICATING THE NANO POROSITY OF THE MATERIAL.

The high sensitivity towards oxygen showed by the material presented here can be correlated to the highly porous structure, which was verified via SEM measurements. The obtained ormosil particles display both a macro porous structure (Figure 6b) and an additionally nano porous substructure (Figure 6c). Therefore, oxygen can easily diffuse towards the linked indicator dye.

The chosen example shows that ormosils are highly interesting materials as the structure and composition can have a strong influence on the sensors performance. As mentioned above a variety of different ormosil based materials exist and are used, therefore the concept presented here may also be applied for those materials.

4. CONCLUSION

In this article we presented a convenient and quite versatile way to covalently immobilize two frequently used indicators (PtTFPP and PdTFPP) to polymer and ormosil-based sensor materials. The presented way is based on a single step click reaction involving the nucleophilic substitution of the labile para-fluorine atom of the indicator with a thiol. The impact of covalent coupling on sensitivity, photophysical properties and sensor stability was studied. It was found that covalent coupling increases the sensor stability in terms of dye leaching and migration, while conserving the good photophysical properties. The concept was proved to be useful for two important sensor matrixes; but it can possibly be extended to other materials as well. Notably, the same strategy can be adapted for other luminescent dyes bearing pentafluorophenyl group, as for example NIR emitting phosphorescent porphyrin-lactones [29,30].

ACKNOWLEDGEMENT

Financial support by the Austrian ScienceFund (FWF; Research Project No. P21192-N17) is gratefully acknowledged. The authors would like to thank H. Motter, Dr. H. Wiltsche, B. Müller, Dr. M. Quaranta and P. Lehner from the Institute of Analytical Chemistry and Food Chemistry for technical support. Dr. B. Rupp from the Institute for Chemistry and Technology of Materials is thanked for helping with the GPC measurements also Dr. Kathrin Schittelkopf from the Institute for Inorganic Chemistry is thanked for helping with NMR measurements. SEM pictures were recorded with the help of A. Zankel from the Institute of Electron Microscopy and Fine Structure Research.

REFERENCES:

[1] A. Mills, Oxygen indicators and intelligent inks for packaging food, Chem. Soc. Rev. 34 (2005) 1003-1011.

[2] O.S. Wolfbeis, Fiber-Optic Chemical Sensors and Biosensors, Anal. Chem. 80 (2008) 4269–4283.

[3] J.H. Bell, E.T. Schairer, L.A. Hand, R.D. Mehta, Surface Pressure Measurements Using Luminescent Coatings1, Annual Review of Fluid Mechanics. 33 (2001) 155–206.

[4] G.E. Khalil, C. Costin, J. Crafton, G. Jones, S. Grenoble, M. Gouterman, u. a., Dual-luminophor pressure-sensitive paint: I. Ratio of reference to sensor giving a small temperature dependency, Sens. Actuators, B. 97 (2004) 13–21.

[5] J. Hradil, C. Davis, K. Mongey, C. McDonagh, B.D. MacCraith, Temperature-corrected pressure-sensitive paint measurements using a single camera and a dual-lifetime approach, Meas. Sci. Technol. 13 (2002) 1552–1557.

[6] R.I. Dmitriev, A.V. Zhdanov, G.V. Ponomarev, D.V. Yashunski, D.B. Papkovsky, Intracellular oxygen-sensitive phosphorescent probes based on cell-penetrating peptides, Anal. Biochem. 398 (2010) 24–33.

[7] I. Klimant, V. Meyer, M. Kuhl, Fiber-optic oxygen microsensors, a new tool in aquatic biology, Limnology and Oceanography. 40 (1995) 1159–1165.

[8] O.S. Wolfbeis, Materials for fluorescence-based optical chemical sensors., J. Mater. Chem. 15 (2005) 2657–2669.

[9] Y. Amao, Probes and Polymers for Optical Sensing of Oxygen, Microchim. Acta. 143 (2003) 1–12.

[10] I. Klimant, F. Ruckruh, G. Liebsch, A. Stangelmayer, O.S. Wolfbeis, Fast response oxygen micro-optodes based on novel soluble ormosil glasses, Mikrochim. Acta. 131 (1999) 35–46.

[11] E.R. Carraway, J.N. Demas, B.A. DeGraff, J.R. Bacon, Photophysics and photochemistry of oxygen sensors based on luminescent transition-metal complexes., Anal. Chem. 63 (1991) 337–42.

[12] G. Mistlberger, K. Koren, E. Scheucher, D. Aigner, S.M. Borisov, A. Zankel, P. Pölt, I. Klimant, Multifunctional Magnetic Optical Sensor Particles with Tunable Sizes for Monitoring Metabolic Parameters and as a Basis for Nanotherapeutics, Adv. Funct. Mater. 20 (2010) 1842–1851.

[13] K. Koren, G. Mistlberger, D. Aigner, S. Borisov, A. Zankel, P. Pölt, I. Klimant, Characterization of micrometer-sized magnetic optical sensor particles produced via spray-drying, Monatsh. Chem., 141 (2010) 691-697

[14] S.M. Borisov, T. Mayr, G. Mistlberger, I. Klimant, Dye-Doped Polymeric Particles for Sensing and Imaging, in: A.P. Demchenko (Hrsg.), Advanced Fluorescence Reporters in Chemistry and Biology II, Berlin, Heidelberg, Springer Berlin Heidelberg, 2010: S. 193-228.

[15] T.C. O'Riordan, H. Voraberger, J.P. Kerry, D.B. Papkovsky, Study of migration of active components of phosphorescent oxygen sensors for food packaging applications, Anal. Chim. Acta. 530 (2005) 135–141.

[16] J.E. Moses, A.D. Moorhouse, The growing applications of click chemistry, Chem Soc Rev. 36 (2007) 1249–1262.

[17] H.C. Kolb, M.G. Finn, K.B. Sharpless, Click Chemistry: Diverse Chemical Function from a Few Good Reactions, Angew. Chem. Int. Ed. 40 (2001) 2004–2021.

[18] C. Ott, R. Hoogenboom, U.S. Schubert, Post-modification of poly(pentafluorostyrene): a versatile "click" method to create well-defined multifunctional graft copolymers, Chem. Commun. (2008) 3516.

[19] C.R. Becer, K. Babiuch, D. Pilz, S. Hornig, T. Heinze, M. Gottschaldt, u. a., Clicking Pentafluorostyrene Copolymers: Synthesis, Nanoprecipitation, and Glycosylation, Macromolecules. 42 (2009) 2387–2394.

[20] C. Barner-Kowollik, F.E. Du Prez, P. Espeel, C.J. Hawker, T. Junkers, H. Schlaad, u. a., "Clicking" Polymers or Just Efficient Linking: What Is the Difference?, Angew. Chem. Int. Ed. 50 (2011) 60–62.

[21] L.K. Tsou, M.M. Zhang, H.C. Hang, Clickable fluorescent dyes for multimodal bioorthogonal imaging, Org. Biomol. Chem. 7 (2009) 5055-5058.

[22] C.R. Becer, R. Hoogenboom, U.S. Schubert, Click Chemistry beyond Metal-Catalyzed Cycloaddition, Angew. Chem. Int. Ed. 48 (2009) 4900–4908.

[23] P. Battioni, O. Brigaud, H. Desvaux, D. Mansuy, T.G. Traylor, Preparation of functionalized polyhalogenated tetraaryl-porphyrins by selective substitution of the p-Fluorines of meso-tetra-(pentafluorophenyl)porphyrins, Tetrahedron Lett. 32 (1991) 2893–2896.

[24] D. Samaroo, C.E. Soll, L.J. Todaro, C.M. Drain, Efficient Microwave-Assisted Synthesis of Amine-Substituted Tetrakis(pentafluorophenyl)porphyrin, Org. Lett. 8 (2006) 4985–4988.

[25] S.-K. Lee, I. Okura, Photostable Optical Oxygen Sensing Material: Platinum Tetrakis(pentafluorophenyl)porphyrin Immobilized in Polystyrene, Anal. Commun. 34 (1997) 185–188.

[26] L.H. Fischer, S.M. Borisov, M. Schaeferling, I. Klimant, O.S. Wolfbeis, Dual sensing of pO2 and temperature using a water-based and sprayable fluorescent paint, Analyst. 135 (2010) 1224.

[27] T. Mayr, S.M. Borisov, T. Abel, B. Enko, K. Waich, G. Mistlberger, u. a., Light Harvesting as a Simple and Versatile Way to Enhance Brightness of Luminescent Sensors, Anal. Chem. 81 (2009) 6541–6545.

[28] C. McDonagh, C.S. Burke, B.D. MacCraith, Optical Chemical Sensors, Chem. Rev. 108 (2008) 400–422.

[29] G.E. Khalil, C. Costin, J. Crafton, G. Jones, S. Grenoble, M. Gouterman, u. a., Dual-luminophor pressure-sensitive paint: I. Ratio of reference to sensor giving a small temperature dependency, Sens. Actuators, B. 97 (2004) 13–21.

[30] G. Khalil, M. Gouterman, S. Ching, C. Costin, L. Coyle, S. Gouin, u. a., Synthesis and spectroscopic characterization of Ni, Zn, Pd and Pt tetra(pentafluorophenyl)porpholactone with comparisons to Mg, Zn, Y, Pd and Pt metal complexes of tetra(pentafluorophenyl)porphine, J. Porphyrins Phthalocyanines. 06 (2002) 135.

[31] S.M. Borisov, G. Nuss, I. Klimant, Red Light-Excitable Oxygen Sensing Materials Based on Platinum(II) and Palladium(II) Benzoporphyrins, Anal. Chem. 80 (2008) 9435–9442.

[32] O.S. Finikova, A.V. Cheprakov, S.A. Vinogradov, Synthesis and Luminescence of Soluble meso-Unsubstituted Tetrabenzo- and Tetranaphtho[2,3]porphyrins, J. Org. Chem. 70 (2005) 9562–9572.

[33] Y. Tian, B.R. Shumway, D.R. Meldrum, A New Cross-Linkable Oxygen Sensor Covalently Bonded into Poly(2-hydroxyethyl methacrylate)-co-Polyacrylamide Thin Film for Dissolved Oxygen Sensing, Chem Mater. 22 (2010) 2069–2078.

[34] S.M. Borisov, P. Lehner, I. Klimant, Novel optical trace oxygen sensors based on platinum(II) and palladium(II) complexes with 5,10,15,20-meso-tetrakis-(2,3,4,5,6-pentafluorphenyl)-porphyrin covalently immobilized on silica-gel particles, Anal Chim. Acta. 690 (2011) 108–115.

[35] V.S. Tripathi, G. Lakshminarayana, M. Nogami, Optical oxygen sensors based on platinum porphyrin dyes encapsulated in ORMOSILS, Sens Actuators, B. 147 (2010) 741–747.

[36] Z. Tao, E.C. Tehan, Y. Tang, F.V. Bright, Stable Sensors with Tunable Sensitivities Based on Class II Xerogels, Anal. Chem. 78 (2006) 1939–1945.

[37] C. McDonagh, B.D. MacCraith, A.K. McEvoy, Tailoring of Sol–Gel Films for Optical Sensing of Oxygen in Gas and Aqueous Phase, Anal. Chem. 70 (1998) 45–50.

[38] A.K. Bansal, W. Holzer, A. Penzkofer, T. Tsuboi, Absorption and emission spectroscopic characterization of platinum-octaethyl-porphyrin (PtOEP), Chem. Phys. 330 (2006) 118–129.

[39] E.M.M. Flores, M.F. Mesko, D.P. Moraes, J.S.F. Pereira, P.A. Mello, J.S. Barin, u. a., Determination of Halogens in Coal after Digestion Using the Microwave-Induced Combustion Technique, Anal. Chem. 80 (2008) 1865–1870.

[40] F. Niedermair, S.M. Borisov, G. Zenkl, O.T. Hofmann, H. Weber, R. Saf, u. a., Tunable phosphorescent NIR oxygen indicators based on mixed benzo- and naphthoporphyrin complexes, Inorg. Chem. 49 (2010) 9333–9342.

[41] S.M. Borisov, G. Zenkl, I. Klimant, Phosphorescent platinum(II) and palladium(II) complexes with azatetrabenzoporphyrins-new red laser diode-compatible indicators for optical oxygen sensing, ACS Appl. Mater. Interfaces. 2 (2010) 366–374.

[42] W.A. Pryor, T.-L. Huang, Reactions of radicals. XVIII. Kinetics of the polymerization of pentafluorostyrene., Macromolecules. 2 (1969) 70–7.

[43] C.R. Becer, K. Kokado, C. Weber, A. Can, Y. Chujo, U.S. Schubert, Metal-free synthesis of responsive polymers: Cloud point tuning by controlled "click" reaction, J. Polym. Sci. A Polym. Chem. 48 (2010) 1278–1286.

[44] C.J. Hawker, A.W. Bosman, E. Harth, New Polymer Synthesis by Nitroxide Mediated Living Radical Polymerizations, Chem. Rev. 101 (2001) 3661–3688.

[45] R.B. Grubbs, Nitroxide-Mediated Radical Polymerization: Limitations and Versatility, Polym. Rev. 51 (2011) 104–137.

[46] D.B. Papkovsky, J. Olah, I.V. Troyanovsky, N.A. Sadovsky, V.D. Rumyantseva, A.F. Mironov, u. a., Phosphorescent polymer films for optical oxygen sensors, Biosens. Bioelectron. 7 (1992) 199–206.

[47] X.Q. Zhang, C.H. Wang, Physical aging and dye diffusion in polysulfone below the glass transition temperature, J. Polym. Sci. B Polym. Phys. 32 (1994) 569–572.

[48] D. Badocco, A. Mondin, P. Pastore, Determination of thermodynamic parameters from light intensity signals obtained from oxygen optical sensors, Sens. Actuators,. 163 (2012) 165–170.

[49] C. McDonagh, B.D. MacCraith, A.K. McEvoy, Tailoring of Sol–Gel Films for Optical Sensing of Oxygen in Gas and Aqueous Phase, Anal. Chem. 70 (1998) 45–50.

[50] R.M. Bukowski, R. Ciriminna, M. Pagliaro, F.V. Bright, High-Performance Quenchometric Oxygen Sensors Based on Fluorinated Xerogels Doped with [Ru(dpp)3]2+, Anal. Chem. 77 (2005) 2670–2672.

[51] D.L. Plata, Y.J. Briones, R.L. Wolfe, M.K. Carroll, S.D. Bakrania, S.G. Mandel, u. a., Aerogel-platform optical sensors for oxygen gas, J. Non-Cryst. Solids. 350 (2004) 326–335.

It can be seen that the nucleophilic substitution of the labile para-fluorine atoms of a 2,3,4,5,6-pentafluorophenyl group can be used to effectively link the indicator to a thiol and therefore to the matrix. Based on those results further applications of this and similar click reactions occurred for sensor material and biological purposes.

SENSOR MATERIALS AND CLICK-CHEMISTRY

Sensor materials with thiol groups can be employed to link indicators. Besides the para-fluorine substitution also the thiol-en reaction is promising in this respect.

ORMOSIL BASED MATERIALS FOR TRACE OXYGEN MEASUREMENTS

Based on the ormosil material we prepared, we tried to further improve the structure and characteristics of this material. Different precursors and porogens were tested in order to increase the porosity of the ormosil. By increasing the size of the poragen from ethanol to isopropanol or the amount of porogen the sensitivity of the ormosilbased sensor increased. A further improvement was made when allowing the polymerization to take place at static conditions (no stirring). This yields an ormosil monolith with very uniform particles.

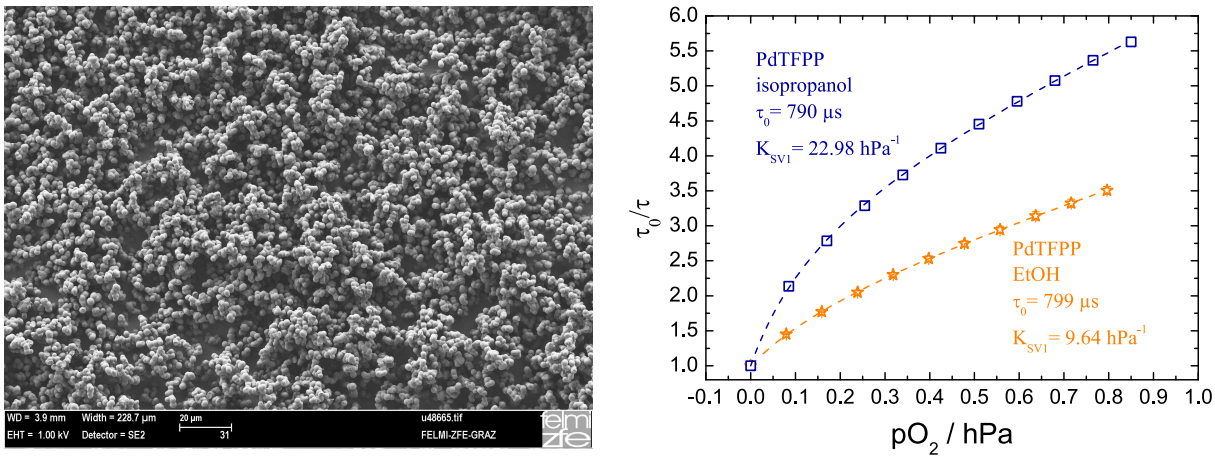

FIGURE 1: LEFT: UNIFORM PARTICLES WITHIN A ORMOSIL MONOLITH; RIGHT: STER-VOLMER PLOTS OF ORMOSIL BASED SENSORS WITH DIFFERENT POROGENS

A further optimization of the ormosil synthesis and evaluation of possible grafting onto the ormosil surface are the next steps.

SYNTHESIS OF FLUORINATED POLYMERS VIA CLICK CHEMISTRY

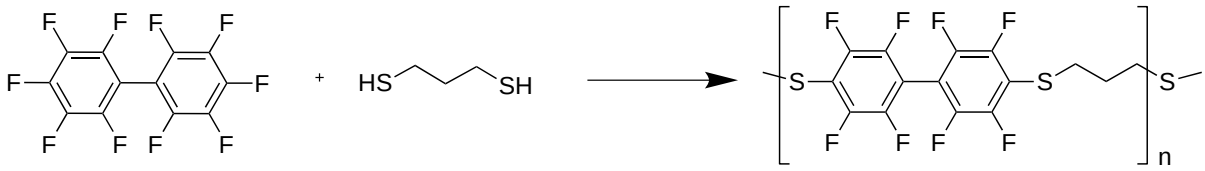

FIGURE 2: SCHEME OF THE CLICK BASED POLYMERIZATION REACTION

The click reaction studied can not only be used to functionalize indicators or to link them to polymers. It may also be used to prepare polymers via polycondensation. Like in all polycondensations the molecular weight of the polymer is determined by molecular ratio of the components and the yield of the reaction. As the yield of the reaction is high, polymerization is possible.

The proposed scheme was tested and succeeded in preparing polymers within a few hours of reaction time. The polymer prepared is soluble in organic solvents and can be applied as a film on different support materials. In terms of oxygen sensing the polymer prepared is not the optimal choice, as it consumes oxygen. Conditioning of the material via previous illumination or oxidation could solve this problem, but was not successful yet.

MOLECULAR PROBES FOR INTRACELLULAR OXYGEN PRODUCED BY CLICK CHEMISTRY

Based on the presented click chemistry, molecular probes for intracellular measurements can be synthetized. Based on Pt-TFPP and Pd-TFPP, we hope to prepare highly photostable molecular probes. The nucleophilic substitution of the labile para-fluorine atoms of a 2,3,4,5,6-

pentafluorophenyl group can be used to introduce a variety of hydrophilic and even cell permeable residues.

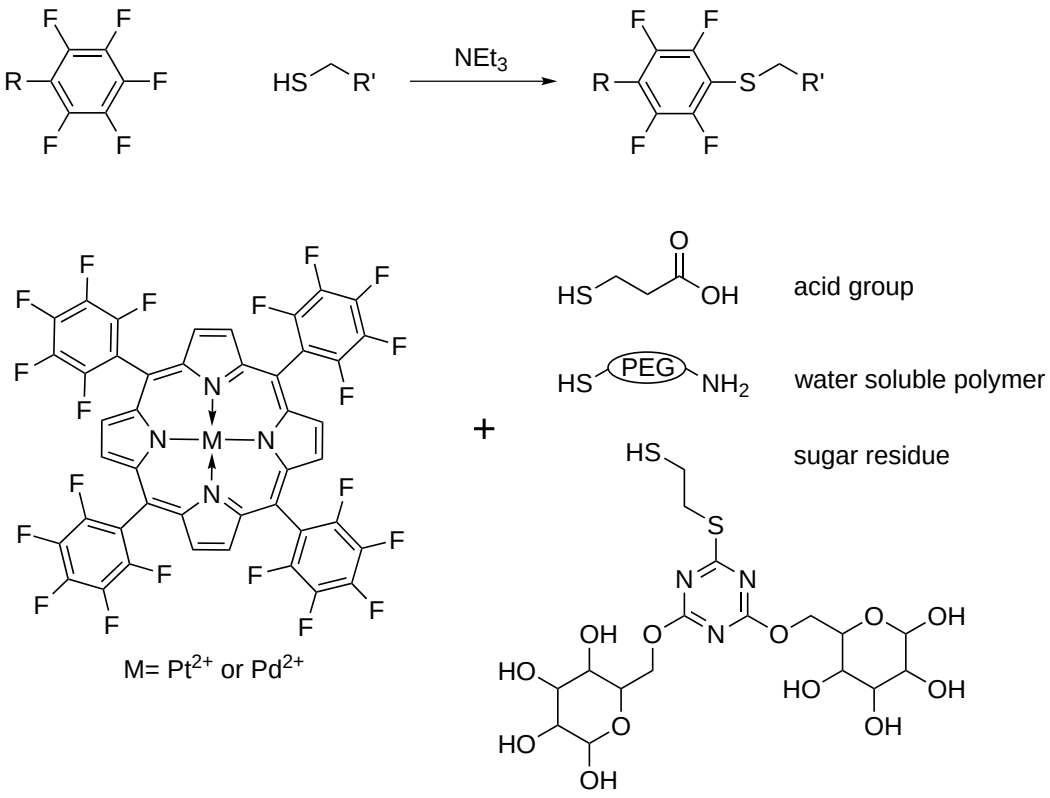

FIGURE 3: DIFFERENT RESIDUES THAT CAN BE LINKED TO PT- AND PD-TFPP VIA CLICK CHEMISTRY

The direct coupling of short peptides via the amino acid cysteine was rather inefficient. Therefore, a short thiol with an acid group was introduced. This enables the coupling with membrane permeable peptides and consequently intracellular oxygen measurements. This concept was tested and showed that cell staining can be observed. Unfortunately, the decay time of the PtTFPP derivate is quite short. Consequently, further studies will be carried out using PdTFPP.

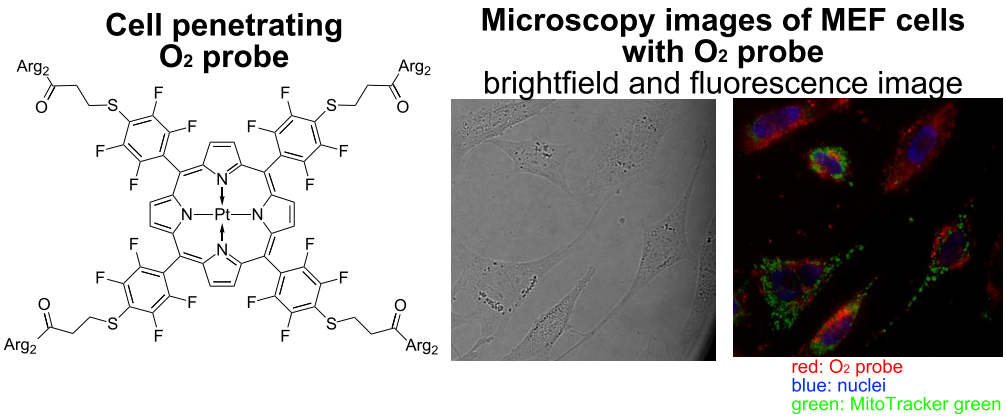

FIGURE 4: PTTFPP MODIFIED WITH EIGHT ARGININE MOLECULES; INTRACELLULAR LOCALIZATION OF THE PROBE COMPARED TO MITOTRACKER GREEN

To increase the solubility of the conjugates in water polyethylene glycol (PEG) residues were introduced on the porphyrine core. The synthesis worked very well and highly water soluble probes were obtained. The additional amino group on the polymer enables further functionalization.

Also probes containing up to eight galactose units were prepared. The galactose residues should increase cell permeability. Unfortunately, the solubility in water was rather low and so far only weak staining could be observed.

The use of click chemistry in biological science is highly favored as low synthetic effort is needed. We demonstrated that functional groups can easily be introduced to two highly photostable indicators. Cell membrane permeability and good water solubility were demonstrated.

The last publication does not focus on the indicator, but rather on the second important component in an optical oxygen sensor – the matrix. As mentioned in the theoretical background, the matrix influences the dynamic range and sensitivity of the sensor. Often the same matrix is used and those influences are neglected.

In the last contribution the same indicator is used in a variety of polystyrene-derivatives. Those polymers have a similar, but still different chemical structure. So it can be ensured that the matrix is still a good environment for the indicator. Using this approach the following questions will be addressed; *Can the matrix influence on sensitivity be predicted? Does the matrix influence the sensor stability?*

TUNING THE DYNAMIC RANGE AND SENSITIVITY OF OPTICAL O_2-SENSORS BY EMPLOYING DIFFERENTLY SUBSTITUTED POLYSTYRENE-DERIVATIVES

THIS CHAPTER WAS SUBMITTED TO SENSORS AND ACCTUATORS B

AUTHORS: KLAUS KOREN, LUKAS HUTTER, BARBARA ENKO, ANDREAS PEIN SERGEY M. BORISOV AND INGO KLIMANT

ABSTRACT

Ten different polystyrene-derivatives were tested with respect to their potential use as matrix materials for optical oxygen sensors. Either halogen atoms or bulky residues were introduced as substituents on the phenyl ring. A fine-tuning of the sensor sensitivity was achieved, without compromising solubility of the indicator in the matrix by providing a chemical environment very similar to polystyrene (PS), a standard matrix in optical O_2 sensors. To put the results into perspective, the studied materials were compared to PS regarding sensitivity of the sensor, molecular weight and glass-transition temperature. The materials promise to be viable alternatives to PS with respect to the requirements posed in various sensor application fields. Some of the polymers (e.g. poly(2,6-dichlorostyrene)) promise to be of use in applications requiring measurements from 0 to 100% oxygen due to linearity across this range. Poly(4-tert-butylstyrene) and poly(2,6-fluorostyrene), on the other hand, yield sensors with increased sensitivity. Sensor stability was evaluated as a function of the matrix, a topic which has not received a lot of interest so far.

Optical oxygen sensors based on phosphorescent dyes are state-of-the-art measurement devices in industry and academia alike [1]. High accuracy achieved over a large range of analyte concentrations and simple instrumentation are the major advantages of such sensors. Additionally contactless measurements are possible through any transparent media.

The basic components of an optical oxygen sensor are a luminescent indicator and a sensor matrix which serves as a solvent for the indicator [2]. Luminescent transition metals complexes [3, 4], especially metaloporphyrins [5–9], are frequently used as indicator dyes. Polymers or organically modified silica (ormosils) are mainly employed as matrix materials [10, 11]. Usually, the indicator dye is entrapped in the matrix and the resulting sensor is deposited onto an optical fibre or a support.

Indicator and matrix affect sensor performance, most importantly dynamic range, sensitivity, robustness and all other parameters. In detail the important parameters regarding the indicator are the decay time, influencing the dynamic range and sensitivity, the molar absorption coefficient and the quantum yield, both influencing brightness, and the spectral properties, determining requirements with respect to needed filters and light sources. Additionally its photophysical and chemical stability has an impact on the lifetime of the sensor.

The sensor matrix is of similar importance regarding the sensor performance. By choosing the right matrix the dynamic range, sensitivity and even long-term stability of the sensor can be influenced. The question of the potential usability of a matrix material can be addressed by considering several key parameters.

For optical oxygen sensors the matrix has to be permeable to oxygen, while being impermeable to other potential quenchers (mainly ions). This requirement is among the key considerations regarding the use of a polymer as an optical oxygen sensor matrix. Additional requirements for matrix materials include their availability - either commercial or simple large scale synthesis, chemical stability, solubility in organic solvents as well as its suitability as a chemical environment for the indicator dye.

As the permeability of the matrix influences the sensitivity and dynamic range several different matrix materials are generally used. Those materials include common polymers like polystyrene (PS), polymethylmethacrylate (PMMA) and cellulose derivatives [12, 10, 13], but also less common polymers [14, 15], ormosils [16, 17] and other materials [18]. These materials are generally chosen for their intrinsic permeability towards oxygen. Their varying permeabilities towards oxygen arises from varying degrees of free volume present in the materials.

Tuning the sensitivity by changing the polymer may pose too big an intervention for an established sensor system given that the matrix has to provide a suitable environment for the indicator. A possible solution may be the use of polymers with similar structure, but varying permeability and copolymers of such. Surprisingly, this possibility has rarely been considered so far and has not been studied in detail.

In this contribution, ten different styrene-derivatives and copolymers of two of the styrene-derivative monomers were produced and studied with respect to their potential use as oxygen sensor matrices. The oxygen permeability of the set of materials, as well as the possibility of fine tuning sensor sensitivity and its dynamic range via copolymerisation were evaluated. For a few selected materials, the photostability of the indicator in the matrix was evaluated and the effects of the matrix on this parameter were assessed.

EXPERIMENTAL

The indicators $PtTPTBPF_4$ or $PdTPTBPF_4$ were synthetized in our lab [5], all solvents were purchased from Carl Roth (www.carlroth.de) and used as received.

2-Fluorostyrene, 2,4-difluorostyrene, 2-chlorostyrene and 2,6-dichlorostyrene were purchased from ABCR (www.abcr.de). 2,6-Difluorostyrene, 4-phenylstyrene and 2,2'-azobis(2-methylpropionitrile) (AIBN) were obtained from Sigma (www.sigmaaldrich.com).

Polystyrene (www.acros.com), poly(4-chlorostyrene), poly(α-methylstyrene) (both from Scientific polymer, www.scientificpolymer.com) and poly(4-tert-butylstyrene) (Sigma) were purchased, the other polymers were synthesised using the following procedure.

SYNTHESIS:

The monomers were filtered through a column packed with aluminium oxide, to remove the contained inhibitor (4-tert-butylcatechol). An appropriately-sized Schlenk-flask was charged with one equivalent of monomer. The liquid was stirred at room temperature under heavy flow of argon for 20 min. 1 mol% of AIBN was added under argon. The flask was sealed and the solution was allowed to react at 75 °C for up to four hours while stirring. Upon complete solidification due to polymerisation, the polymer was allowed to cool.

Then, the polymer was dissolved in dichloromethane to give a roughly 10 wt% solution. The solution was added dropwise to a five-fold volume of methanol, resulting in the precipitation of a white, powder-like precipitate. The suspension was filtered through a paper filter and redissolved in dichloromethane to give a solution containing about 10 wt% of polymer. This step of dissolving and precipitation was repeated three to five times. The polymer was dried in the oven at 60 °C to yield a white, powder-like solid.

POLYMER CHARACTERISATION:

Weight and number average molecular weights (Mw and Mn), as well as the polydispersity index PDI=Mw/Mn, were determined by size exclusion chromatography (SEC) with the following set-up: Merck Hitachi L6000 pump, separation columns from Polymer Standards Service (8 mm*300 mm, STV 5 µm grade size; 106, 104 and 103 Å pore size), refractive index detector (model Optilab DSP Interferometric Refractometer) from Wyatt Technology. Polystyrene standards from Polymer Standard Service were used for calibration. All SEC runs were performed with THF as the eluent.

DSC measurements were made with a Perkin Elmer Pyris Diamond Differential Scanning Calorimeter equipped with a Perkin Elmer CCA7 cooling system using liquid nitrogen. A nitrogen flow of 20 mL min^{-1} and different heating rates varying between 10 and 40 °C per minute were used. The described transitions were taken from the second heating run with a heating rate of 20 °C/min.

PREPARATION OF SENSOR FILMS:

Sensor foils of defined thickness were prepared by knife coating cocktails of comparable viscosity onto poly(ethylene glycol terephthalate) support (Mylar®) from Goodfellow (www.goodfellow.com) using a 25 µm spaced Gardner coating knife. Cocktails typically contained 10 wt% of polymer in chloroform (HPLC-grade) and 1 wt% of $PtTPTBPF_4$ or $PdTPTBPF_4$ with respect to the amount of polymer employed. After casting, the sensor foils were carefully dried for 24 h at 60 °C to ensure complete removal of solvent before characterisation.

CALIBRATION CURVES:

Luminescence phase shifts were measured with a two-phase lock-in-amplifier (SR830, Stanford Research Inc., www.thinksrs.com). Excitation was performed with the light of a 435 nm LED which was sinusoidally modulated at a frequency of 5 kHz for PtTPTBPF4 or 500 Hz for PdTPTBPF4. A bifurcated fiber bundle was used to guide the excitation-light to the sensor film and to guide back the luminescence. A BG12 excitation glass filter and an RG9 emission filter (both from Schott, www.schott.com) were used. The luminescence was detected with a photo-multiplier tube (H5701-02, Hamamatsu, www.sales.hamamatsu.com). Temperature was controlled by a cryostat ThermoHaake DC50. Gas calibration mixtures were obtained using a gas mixing device (MKS, www.mksinst.com).

PHOTOSTABILITY:

Photostability was assessed by exposing sensor films to prolonged irradiation, by focusing the light emitted by a 458 nm high-power 10W LED array (11.12V, 0.699A, 7.8W) (www.led-tech.de) through a lens purchased from Edmund optics (www.edmundoptics.de). Absorption spectra between 350 nm and 800 nm and luminescence lifetimes upon de-oxygenation were measured every 15 min.

OXYGEN CONSUMPTION:

The sensor films were coated with 10% poly(vinyl alcohol) (PVOH), Mw= 86,000 (Scientific polymer) in water to give a 7.5 µm thick blocking layer. The film was dried at 60 °C. Measurements were performed under continuous illumination.

POLYMER SYNTHESIS AND CHARACTERISATION

The effects on sensor parameters, caused by the introduction of various substituents in a PS based sensor matrix were studied for a set of PS-derivatives (scheme 1). Some of the polymers used in this study were purchased, while others where easily prepared via radical polymerisation. In all cases the polymerization was carried out in a solvent-free manner. The polymerizations were stopped after a solid had formed. The polymers were precipitated several times and washed in order to remove oligomers, the remaining initiator and other low molecular weight components. Molecular weight and PDI were determined for all polymers and are listed in table 1. Although the obtained polymers show a partly rather broad size distribution, they are perfectly suitable as matrix material for optical oxygen sensors.

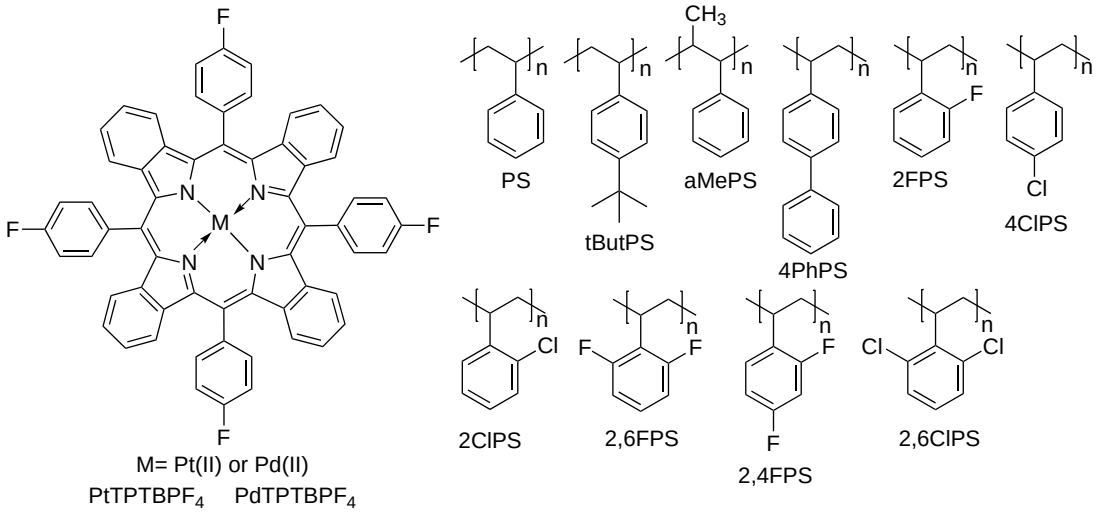

SCHEME 1: STRUCTURES OF THE STUDIED DIFFERENTLY SUBSTITUTED POLYSTYRENE-DERIVATIVES AND THE INCORPORATED INDICATORS.

TABLE 1: MOLECULAR WEIGHT, POLYDISPERSITY INDEX AND GLASS-TRANSITION TEMPERATURE OF THE POLYMERS:

Polymer	Mw / g/mol	PDI	Tg / °C
PS	250,000	n.d.	100 [19]
tButPS	50,000-100,000	n.d.	n.d
aMePS	186,300	1.04	167-169 [19]
4PhPS	25,210	1.7	132.8
2FPS	38,540	2.0	91.9
4ClPS	69,700	2.8	122.2
2ClPS	82,480	2.8	129.2
2,6FPS	138,240	2.7	107.5
2,4FPS	38,150	1.8	88.3
2,6ClPS	106,320	1.9	157.0
2,6ClPS +4ClPS (1+1)	379,500	2.8	138.6
2,6ClPS +4ClPS (2+1)	381,800	4.4	136.6
2,6ClPS +4ClPS (1+2)	759,000	3.5	123.1

Except for the fluorinated polymers the materials were generally characterised by glass-transition temperatures (T_g) higher than the corresponding value for PS. This may be beneficial considering steam sterilization, generally performed at 120 °C. A T_g lower than the temperature applied during sterilization may lead to migration processes and thus compromises sensor calibration and usability. The higher T_g values found for some of the substituted polystyrenes (table 1) may have a beneficial impact on this problem.

As outlined in the introduction the sensitivity of an optical oxygen sensor is determined by both the indicator dye used and the polymer the dye is embedded in. While for some applications highly sensitive materials are needed, other applications demand sensors with linear calibration plots up to 100 % oxygen. Potential fields of interest could be sensors in diving-technology or the study of photosynthesis with optical O_2 sensors. In both cases oxygen partial pressures (pO_2) can exceed 200 hPa. In this range ($pO_2 > 200$ hPa), conventional sensors employing PS as matrix show a low signal to noise ratio and are characterised by unfavourable dynamics.

The sensitivity of an optical oxygen sensor can be tuned by changing the sensor matrix, as its oxygen-permeability directly influences the sensitivity. When adapting a sensor system to requirements posed by a new application, this effect has often been made use of, by swapping one class of polymer for a totally different one. For example PAN (polyacrylonitril) polymers are generally used as virtually gas-impermeable materials [20] whereas Teflon AF or silicones are employed in applications demanding high permeability. Solubility of the indicator in the matrix is highly important, yet Teflon AF and silicones are very bad solvents and unsuitable environments for most oxygen indicators. Furthermore, swapping the matrix may cause changes in sensitivity by several orders of magnitude, and compromises the processability of the sensor material. Due to the drastic changes in sensitivity interchanging between very different matrixes may not be considered as “fine-tuning”

By only slightly modifying the polymer with respect to their chemical nature the limitations regarding suitability as chemical environment for the indicator and the lack of possibilities for fine-tuning can be overcome and the sensitivity could be adjusted. In this study, we introduced halogen atoms or bulky substituents at different positions of the phenyl ring of polystyrene. In one case, the effect of a methyl group introduced on the polymer backbone was also investigated. By introducing those substituents we want to change the free volume inside the polymer. $PtTPTBPF_4$, was used as an indicator, and the sensors were calibrated from 0 to 1000 hPa O_2 (table 2). It is important to note that the chosen indicator is well soluble in all of the polymers investigated. Furthermore, all polymers can easily be dissolved in organic solvents such as CH_2Cl_2, $CHCl_3$ or toluene which facilitates preparation of sensor foils.

TABLE 2: SENSOR CHARACTERISTICS OF THE POLYMERS CONTAINING $PTTPTBPF_4$ AS OXYGEN SENSITIVE DYE:

Polymer	τ_0 / µsec	τ_0/τ-1[a]	τ_0/τ-1[b]	I_0/I-1[a]	I_0/I-1[b]	KSV / hPa^{-1} [c]
PS	52.55	3.13	9.98	3.92	17.35	0.0174
tButPS	51.15	7.09	9.79	13.10	48.12	0.0477
aMePS	51.25	2.52	8.30	3.23	16.04	0.0157
4PhPS	49.26	2.88	9.95	3.37	15.28	0.0153
2FPS	54.48	1.87	6.44	2.16	9.57	0.0096
4ClPS	52.79	2.72	8.82	3.27	14.59	0.0147
2ClPS	53.60	1.69	6.30	1.96	9.42	0.0093
2,6FPS	54.54	4.30	11.30	5.68	24.80	0.0245
2,4FPS	57.78	2.36	7.66	2.82	12.25	0.0124
2,6ClPS	50.90	1.38	5.24	1.63	8.25	0.0080
2,6ClPS +4ClPS (1+1)	53.20	2.38	8.08	2.97	14.14	0.0139
2,6ClPS +4ClPS (2+1)	53.53	2.22	7.69	2.76	13.29	0.0131
2,6ClPS +4ClPS (1+2)	54.31	2.92	9.56	3.63	16.87	0.0168

a: at 210 hPa oxygen

b: at 1000 hPa oxygen

c: determined from I_0/I via linear fit

All prepared sensors showed a fairly fast response to a change in oxygen concentration. Generally, all roughly 2.5µm thick sensors films had a response time (t_{90}) of less than 10 sec, so changing the polymer had no significant effect on the response of the sensor. Regarding the measured decay times some variations were observed. Except for 2,6ClPS all other halogenated polymers yielded an increase in the observed decay time (compared to the one measured in PS).

Contrary to this trend the introduction of alkyl groups or an additional aromatic ring resulted in a slightly decreased τ_0. This indicates a reduction in the nonradiative deactivation of the indicator inside most of the halogenated polymers.

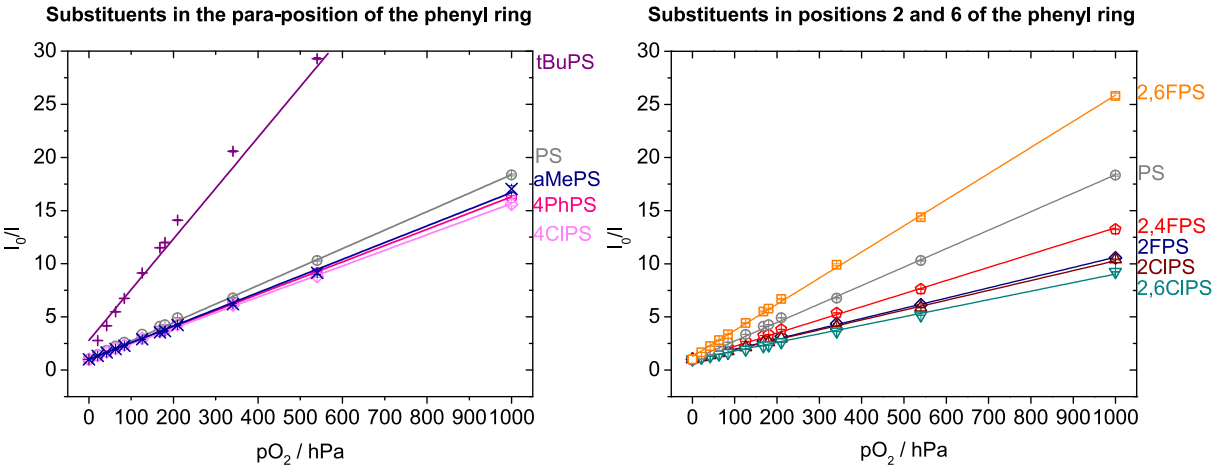

FIGURE 1: STERN-VOLMER PLOTS OF THE INVESTIGATED POLYMERS INCORPORATING PTTPTBPF$_4$ AS OXYGEN INDICATOR. EXCEPT FOR TBUPS ALL OTHER MATERIALS GAVE HIGHLY LINEAR CALIBRATION PLOTS UP TO A PO_2 OF 1000 HPA.

Introducing halogen atoms on the phenyl ring had a significant impact on the sensitivity. The biggest change was observed in the case of 2,6ClPS, where the sensitivity was reduced by more than 50% (compared to K_{SV} in PS). Also the other chlorinated polymers showed lower permeability. Fluorinated polymers on the other hand, were more difficult to classify. Two of the polymers, 2FPS and 2,4FPS, lowered the sensitivity, while 2,6FPS had the opposite effect. It is interesting to note, that 2,6FPS is around three times more sensitive than 2,6ClPS. Introducing a methyl group on the backbone or extending the phenyl ring by adding an additional one had only a small impact on the permeability (lowered by roughly 10%). This is surprising as we hoped to increase the permeability by introducing those groups. The biggest effect was observed for tButPS. In this polymer the sensitivity increased dramatically, which is in agreement with the literature [21]. The difference in sensitivity measured in the polymers corresponds to a change in permeability for oxygen, which is in turn related to the free volume in the polymer. The introduction of a tert-butyl group increases the spacing between the polymer strands and creates free volume. Other substituents lead to a denser packing inside the polymer and restrain oxygen permeability.

Interestingly, the Stern-Volmer plots obtained from the intensity signals were highly linear for nearly all of the sensors while the decay time-based Stern-Volmer plots (supplementary information) showed a high degree of non-linearity. Especially tButPS gives a highly non-linear calibration plots (I_0/I and τ_0/τ) at high O_2 concentrations. On one hand tButPS is very suitable for measuring low and even trace oxygen concentrations. On the other hand this material as well as 2,6FPS and even PS (especially decay time-based) are not well suitable for measuring high oxygen partial pressures. For applications involving oxygen partial pressures higher than 200 hPa sensors based on 2,6ClPS, 2ClPS or 2FPS seem very promising. Sensors based on those polymers show desirable dynamics from 0 to 1000 hPa pO_2 in intensity- as well as decay time-based calibrations. The possibility of fine tuning the sensor sensitivity was assessed by studying products of the co-polymerisation of 2,6ClPS and 4ClPS, whose respective bulk-polymers are characterised by very different oxygen permeabilities. The prepared co-polymers showed different sensitivity than the respective bulk-polymers. However, no linear correlation between the monomer ratio and the sensitivity was observed. The respective calibration curves closely resemble the one obtained for 4ClPS and the influence of varying amounts of 2,6ClPS is rather weak (supplementary information).

Although it was not possible to predict the sensitivity by employing co-polymerisation-products of different styrene derivatives, the possibility of tuning the sensor sensitivity over a broad range of oxygen concentrations by using a set of chemically very similar matrix materials is demonstrated. The sensor matrices presented herein constitute promising alternatives to polystyrene as a sensor matrix, especially in sensor applications, where lower or higher sensitivity is required.

SENSOR STABILITY

Singlet oxygen produced in the quenching process is a potential source of dye and polymer degradation, and compromises sensor stability. Sensor stability is commonly believed to be dependent on the indicator dye. Yet the impact of the matrix on the stability of a sensor should not be underestimated. Apart from acting as a chemical barrier, that protects the sensor from chemical degradation processes such as hydrolysis, the matrix also plays a role in reducing potential photo-degradatory reactions affecting the dye. It is thus essential for sensor stability.

This influence is highly dependent on the chemical nature of the sensor matrix and is demonstrated in this work for a selected set of different, yet comparable, polystyrene-based polymers

For this purpose sensors were prepared containing $PdTPTBPF_4$ as indicator. This indicator was chosen as it is nearly fully quenched by oxygen at ambient conditions [5]. Consequently the production of singlet oxygen is increased and photo-degradation processes can be observed on a shorter timescale.

The stability of the indicator was assessed by monitoring the decrease in the absorption bands (figure 2a). Additionally the stability of the sensor was monitored via measuring the change in decay time (τ_0) in absence of oxygen (figure 2b).

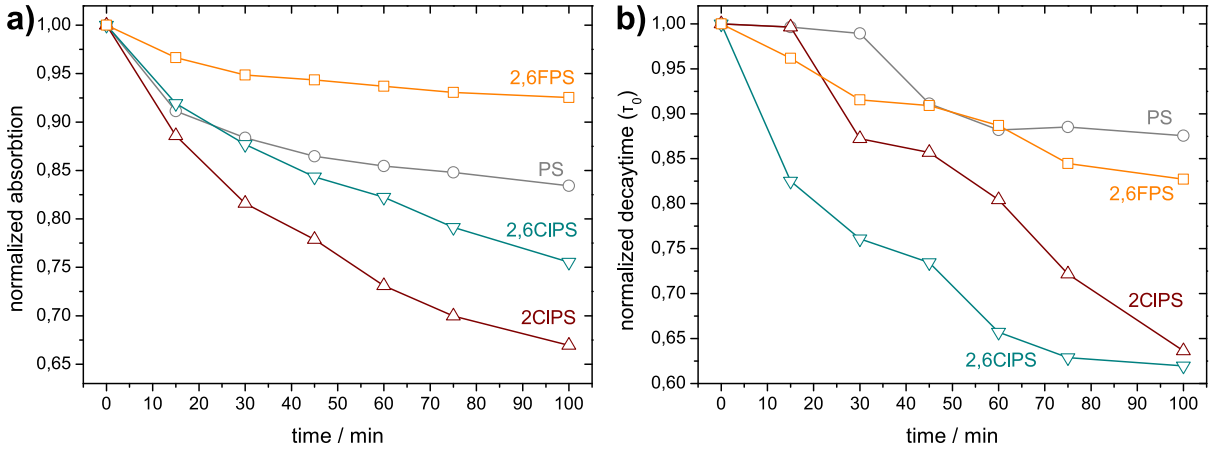

FIGURE 2: SENSOR PHOTOSTABILITY; A: MEASURED PHOTOBLEACHING OF PDTPTBPF4 AT 445 NM, B: CHANGE IN DECAY TIME IN FOR DIFFERENT POLYMERS UPON CONTINUOUS ILLUMINATION.

It is important to state that bleaching was only observed after continuous irradiation with a high power LED array. In typical sensor applications, where the sensor is only illuminated by short light pulses, bleaching is not so critical.

Compared to the standard PS based sensor only introducing fluoride increased the stability, while chloride had an opposite effect. Furthermore, the measured decay time changed in all polymers after light exposure. Such a change may be explained by the formation of quenchers in the sensor material - a realistic assumption, as the produced singlet oxygen is known to form peroxides or similar structures upon reacting with the matrix [22, 23]. In order to validate this

theory the photo induced oxygen consumption within the sensor material was measured using a new approach.

OXYGEN CONSUMPTION

Some of the prepared sensors were covered with an oxygen impermeable poly(vinyl alcohol) (PVOH) layer and continuously illuminated while measuring the decay time. As shown in figure 3a the oxygen concentration within all the sensors decreased over time. Despite the predominant opinion, that the underlying quenching process in optical oxygen sensors is fully reversible and does not consume any oxygen [24], our data suggests a different view on this topic. As illustrated in figure 3b the singlet oxygen formed upon quenching of the dye in the excited state can react with the matrix or the indicator and can therefore be consumed. By introducing a blocking layer an exchange with the environment is no longer possible, the produced singlet oxygen reacts within the sensor material and oxygen depletion can be measured. This rate of reaction is relatively low and therefore such behaviour can only be observed under continuous illumination in the absence of diffusional exchange with surrounding. Our experimental results are in agreement with the measurements regarding sensor stability and lead to the conclusion that oxidation of the matrix occurs within optical O_2 sensors. Due to its high relevance for optical oxygen sensors, a detailed study on this phenomenon is planned.

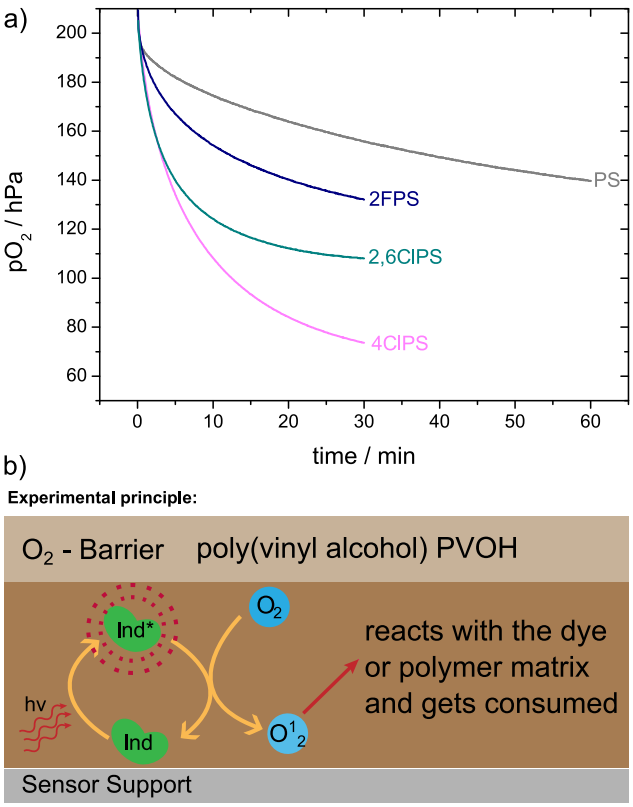

FIGURE 3: PHOTO INDUCED OXYGEN CONSUMPTION IN THE SENSOR MATERIAL. A: MEASURED DECREASE IN OXYGEN CONCENTRATION INSIDE THE SENSOR UPON CONTINUOUS ILLUMINATION INDICATING THE CONSUMPTION OF OXYGEN; B: EXPERIMENTAL SETUP – AN OXYGEN BARRIER IS COATED ON TOP OF THE SENSOR MEMBRANE. THE PRODUCED SINGLET OXYGEN REACTS WITH THE SENSOR COMPONENTS AND GETS CONSUMED

CONCLUSION

In this study, we demonstrated that different polystyrene-derivatives can be obtained in a fairly simple polymerisation and be used as sensor matrices in optical oxygen sensors. The materials studied herein can be used to tune the sensitivity of the sensor without compromising the favourable characteristics of polystyrene as a sensor matrix, since a high degree of similarity in chemical nature is conserved. For applications demanding high sensitivity and low oxygen levels tButPS can be used. In applications involving high concentrations of oxygen 2,6ClPS and 2ClPS may prove to be of special interest, due to their favourable dynamics in higher concentration ranges. Furthermore, we also gained some insight into photoreactions inside sensor membranes, a topic that has been under-estimated so far.

ACKNOWLEDGEMENT

The authors would like to thank the Institute for Chemistry and Technology of Materials for helping with the GPC measurements. Financial support by the Austrian Science Fund (FWF; Research Project No. P21192-N17) is gratefully acknowledged.

REFERENCES

1. *Wolfbeis OS (2008) Anal Chem 80(12):4269–4283*
2. *Wolfbeis OS (2005) J Mater Chem 15:2657–2669*
3. *Borisov SM, Klimant I (2007) Anal Chem 79(19):7501–7509*
4. *Vos JG, Kelly JM (2006) Dalton Trans 4869–4883*
5. *Borisov SM, Nuss G, Klimant I (2008) Anal Chem 80(24):9435–9442*
6. *Niedermair F, Borisov SM, Zenkl G, Hofmann OT, Weber H, Saf R, Klimant I (2010) Inorg Chem 49(20):9333–9342*
7. *Koren K, Borisov SM, Saf R, Klimant I (2011) Eur J Inorg Chem 2011(10):1531–1534*
8. *Amao Y, Okura I (2009) J Porphyrins and Phthalocyanines 13(11):1111*
9. *Finikova OS, Cheprakov AV, Vinogradov SA (2005) J Org Chem 70(23):9562–9572*
10. *Douglas P, Eaton K (2002) Sens Actuators B 82(2–3):200–208*
11. *Tripathi VS, Lakshminarayana G, Nogami M (2010) O Sens Actuators B 147(2):741–747*
12. *Draxler S, Lippitsch ME, Klimant I, Kraus H, Wolfbeis OS (1995) J Phys Chem 99(10):3162–3167*
13. *Lu X, Winnik MA (2001) Chem Mater 13(10):3449–3463*
14. *Stubenrauch K, Sandholzer M, Niedermair F, Waich K, Mayr T, Klimant I, Trimmel G, Slugovc C (2008) Eur Polym J 44(8):2558–2566*
15. *Amao Y, Miyashita T, Okura I (2001) React Funct Polym 47(1):49–54*
16. *Klimant I, Ruckruh F, Liebsch G, Stangelmayer A, Wolfbeis OS (1999) Mikrochim Acta 131(1-2):35–46*
17. *Estella J, Wencel D, Moore JP, Sourdaine M, McDonagh C (2010) Anal Chim Acta 666(1-2):83–90*
18. *Scheicher SR, Kainz B, Köstler S, Suppan M, Bizzarri A, Pum D, Sleytr UB, Ribitsch V (2009) Biosens Bioelectron 25(4):797–802*
19. *Mark JE (2009) Polymer Data Handbook, 2nd ed. Oxford University Press, USA*
20. *Liebsch G, Klimant I, Wolfbeis OS (1999) Adv Mater 11(15):1296–1299*
21. *Apostolidis A, Klimant I, Andrzejewski D, Wolfbeis OS (2004) J Comb Chem 6(3):325–331*
22. *Pospíšil J, Nešpůrek S, Pilař J (2008) Polym Degrad Stab 93(9):1681–1688*
23. *Wu H, Song Q, Ran G, Lu X, Xu B (2011) TrAC Trends Anal Chem 30(1):133–141*
24. *Demas JN, DeGraff BA, Coleman PB (1999) Anal Chem 71(23):793A–800A*

TUNING THE DYNAMIC RANGE AND SENSITIVITY OF OPTICAL O2-SENSORS BY EMPLOYING DIFFERENTLY SUBSTITUTED POLYSTYRENE-DERIVATIVES

KLAUS KOREN, LUKAS HUTTER, BARBARA ENKO, ANDREAS PEIN SERGEY M. BORISOV AND INGO KLIMANT

In this supplementary information additional Stern-Volmer plots of the studied materials are shown. Nonlinear Stern-Volmer calibration plots are quite common for optical oxygen sensors [1]. Such a calibration behavior can be adequately described by the two-site model (eq. 1), where K_{SV1} and K_{SV2} are the two different Stern-Volmer constants, and F is the distribution coefficient.

$$\frac{\tau}{\tau_0} = \frac{F}{1 + K_{SV1} * pO_2} + \frac{1 - F}{1 + K_{SV2} * pO_2} \qquad \text{EQUATION 1}$$

[1] E.R. Carraway, J.N. Demas, B.A. DeGraff, J.R. Bacon, Photophysics and photochemistry of oxygen sensors based on luminescent transition-metal complexes., Analytical Chemistry. 63 (1991) 337-42

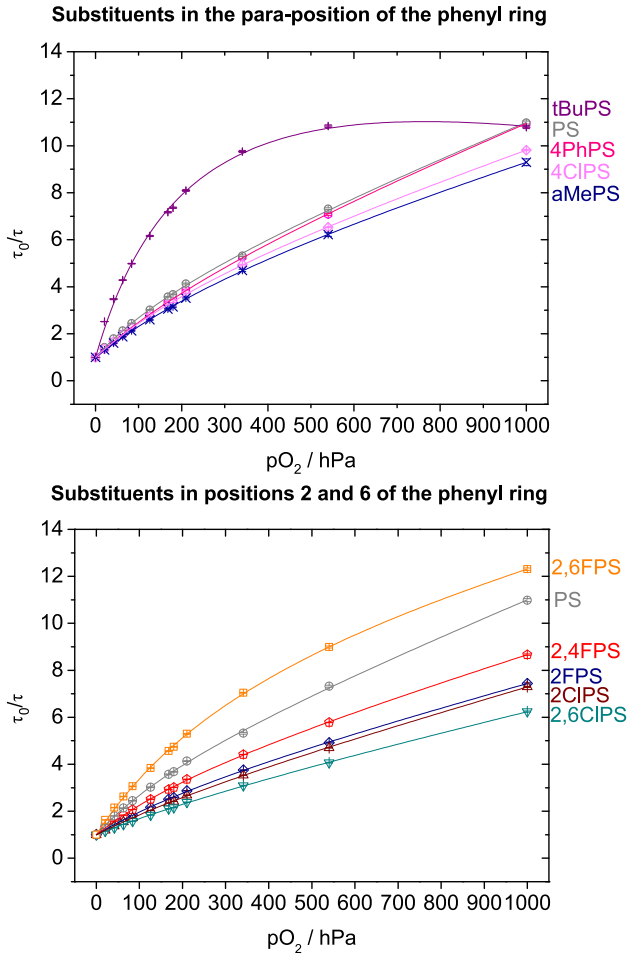

FIGURE S1: DECAY TIME BASED STERN-VOLMER PLOTS OF THE CHARACTERIZED SENSORS. IN CONTRAST TO THE INTENSITY BASED CURVES THOSE PLOTS ARE HIGHLY NON-LINEAR.

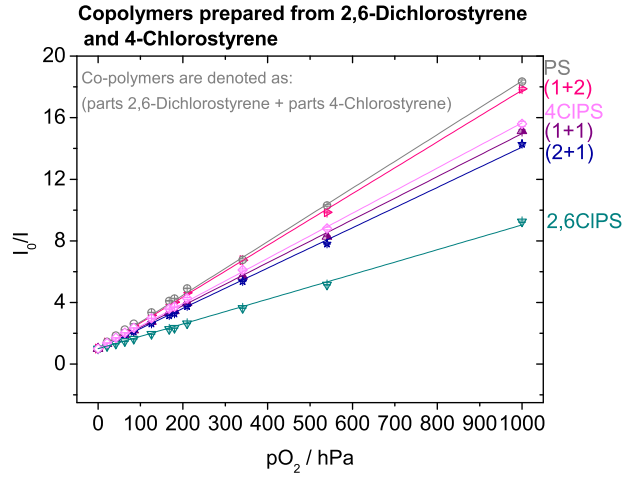

FIGURE S2: STERN-VOLMER PLOTS OF THE PREPARED COPOLYMERS AND THE RESPECTIVE BULK POLYMERS.

CONCLUSION

Throughout this thesis oxygen was the analyte of choice; a highly important small molecule that enables life on this plant. So measuring the concentration of this gas is of great importance.

In this work optical oxygen sensors were studied in many aspects, from synthesis of a new class of indicators, preparation of improved sensor materials up to linking both indicator and matrix with each other. All those attempts had the idea of improving or tuning current optical oxygen sensors and making them more accessible to a variety of applications. Those applications include intracellular oxygen measurements where special probes were designed and demonstrated to be cell penetrating and oxygen sensitive. Additional applications include trace oxygen sensors for applications in almost anaerobic regions like deep oceans. Also industrial processes were analyzed using oxygen sensors; in particular, O_2 sensors were used to measure the hardening of coatings.

From the chemical point of view reactions for the fast and efficient modification and functionalization of indicators were developed and used. Based on Ir(III)-porphyrins a method was developed that enabled changing the axial ligands in a single step. For the commonly used indicators PtTFPP and PdTFPP click chemistry was used to couple or functionalize them. Those straight-forward reaction schemes enable the production of custom-made sensors.

The matrix, this mostly underestimated part of a sensor, was put into focus and it was demonstrated that via changing the matrix the sensor can be tuned. Additionally the effects of the matrix on sensor stability were studied and it was shown that the matrix has an impact on this as well.

A lot is still unknown about the role of oxygen on evolution, growth, development and death of organisms. Optical oxygen sensors can be a valuable tool to solve those questions of life and can reveal interesting information.

During this thesis I became more and more attracted by the importance of oxygen especially in biology and the development of life. Life has built up a very complex machinery to ensure that oxygen can be used as energy source. Therefore, this molecule triggers so many reactions in organisms and decides if an organism survives or not. With the help of optical oxygen sensors I want to further investigate the importance of this molecule and try to put some further pieces in the puzzle of life.